Order Number 9108586

Skeletal growth and chemistry of the sea urchin *Strongylocentrotus* (Echinodermata:Echinoidea)

Scancar, Sonja Marguerite, Ph.D.

University of Cincinnati, 1990

U·M·I
300 N. Zeeb Rd.
Ann Arbor, MI 48106

SKELETAL GROWTH AND CHEMISTRY OF THE SEA URCHIN *Strongylocentrotus* (ECHINODERMATA: ECHINOIDEA)

A dissertation submitted to the
Division of Graduate Studies and Research
of the University of Cincinnati

in partial fulfillment of the
requirements for the degree of

Doctor of Philosophy

in the Department of Geology
of the College of Arts and Sciences

1987

by

Sonja M. Scancar

B. A., Case Western Reserve University, 1972

M. S., State University of New York at Stony Brook, 1976

UNIVERSITY OF CINCINNATI

April 26 19 85

I hereby recommend that the thesis prepared under my supervision by Sonja M. Šcančar

entitled Skeletal Chemistry and Growth of the Sea Urchin, Stronylocentrotus (Echinodermata: Echinoidea)

be accepted as fulfilling this part of the requirements for the degree of Doctor of Philosophy

Approved by:

David L. Meyer

John E. Grover

Composite photograph showing an interambulacral column observed through a luminoscope. See text for discussion.

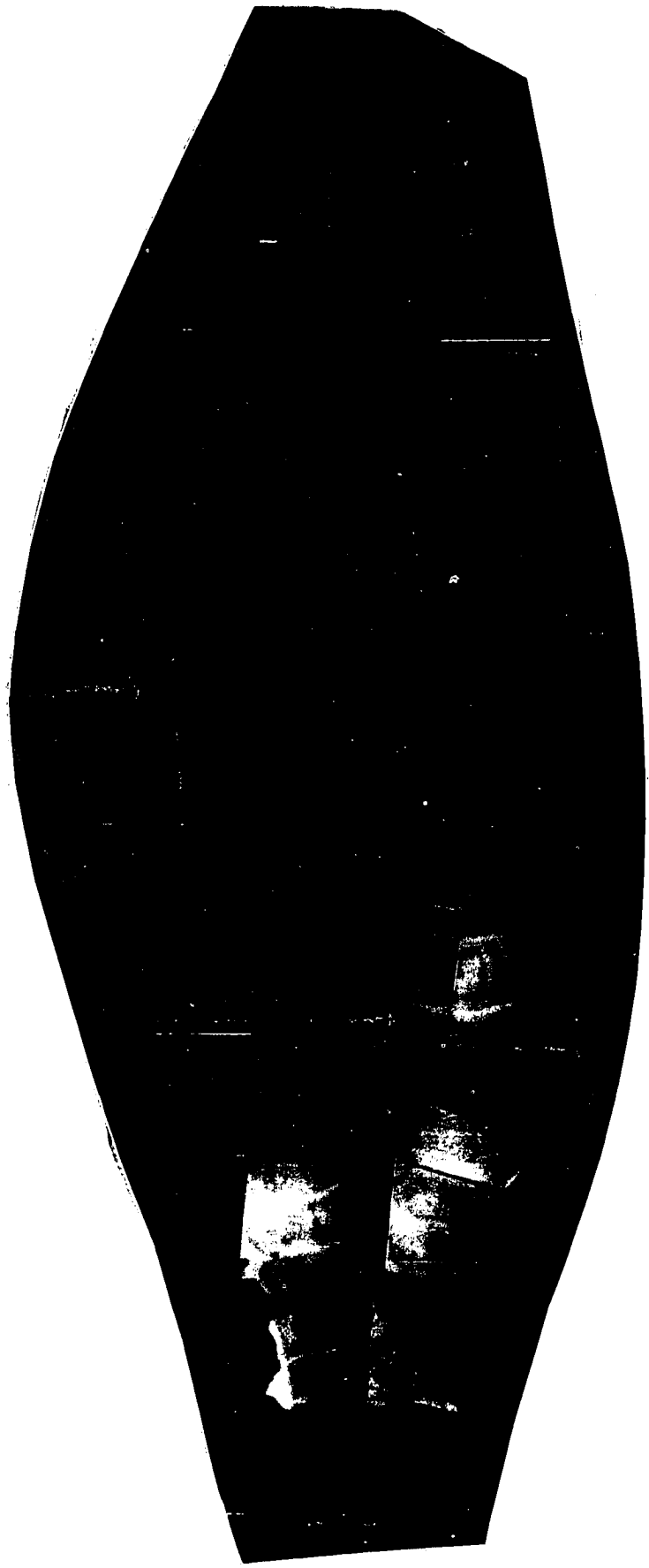

ABSTRACT

Investigation of the coronal plates of the regular echinoid *Strongylocentrotus* (Echinodermata: Echinoidea) shows that skeletal growth and chemistry may be interrelated.

Microstructural zonation can be observed in the middle layers of interambulacral plates and is best seen with scanning electron microscopy (SEM). Stereom formed during spring/summer skeletal growth is more porous (thinner trabeculae, larger intertrabecular channels) compared to stereom formed during fall/winter skeletal growth. This zonation may be correlated with variations in growth rates and may be influenced by an interaction of environmental factors (temperature, salinity and so on) with biological factors (physiological cycles, reproductive cycles).

While growth zonation may be correlated with microstructural zonation, growth zonation is best recorded with X-radiography, or autoradiography. Analysis of the accretionary growth of several interambulacrals reveals that synchronous zones can be correlated within and between interambulacral columns of the same individual. Correlated, synchronous zones are used to reconstruct a growth series of the interambulacrum, which demonstrates that the addition of new plates and their subsequent accretionary growth are both important in the overall anisometric growth of the test.

Compositional variation can be seen in the middle skeletal layer of the individual interambulacral plates with cathodoluminescence and electron microprobe analysis. Luminescent (manganese-rich, iron-poor) zones

are associated with high rates of skeletal accretion while non-luminescent (manganese-poor, iron-rich) bands are associated with low rates of skeletal accretion. Electron microprobe analysis reveals cyclical variation in the calcium carbonate and magnesium carbonate composition of interambulacral plates. These variations in skeletal chemistry may reflect cyclical changes in water chemistry or nutrient content.

Analysis of coronal plates by atomic absorption spectrophotometry shows that the bulk composition of the entire plate varies with its relative position within the test. Ambulacral plates contain more magnesium and less calcium than their interambulacral counterparts; this may be related to differences in porosity, tubercularity or mode of growth. Compositional differences also occur between older, adoral plates and younger, adapical plates. Magnesium and iron levels increase in progressively older plates while calcium levels decrease. Strontium is fairly constant throughout the interambulacrum.

ACKNOWLEDGEMENTS

The writer would like to thank many persons whose assistance facilitated this project. She is particularly grateful to Dr. David Meyer, Principal Advisor, for his encouragement and guidance throughout this study. Dr. John Grover and Dr. J. Barry Maynard of the Advisory Committee shared their expertise and provided many insights throughout the research. Their editorial comments, and those of Dr. Meyer, were truly appreciated.

Special thanks is given to Richard Spohn and Judy Moore of the U.C. Geology Library for their help with library research efforts; to Gini Edwards and Andy Janiak (A.J.) of the Geology Department for their ready technical assistance; to Robin Frank, Joan Cullen, Mark Miller, Peter Purazella, Sally Sutton and Barbara Rassman, fellow graduate students, who shared their knowledge and expertise.

Special appreciation is due to Dr. Ian Steele for his help with electron microprobe analyses at the University of Chicago; to Dr. Michael Fowler and Dr. J. Robert Dodd for their help in discussing the analysis of skeletal materials.

The writer also thanks the Tenneco Fund for a summer grant used at the Oregon Institute of Marine Biology; the Lerner-Gray Fund for Marine Research for a grant to defray photography-related expenses; the U.C. Graduate School for funding of electron microprobe work.

A special thanks is due to the Department of Geology for support in the form of supplies, equipment and so on.

Last, but not least, a sincere thanks to Mrs. Martin Scancar for her patience, encouragement and proofreading.

TABLE OF CONTENTS

ABSTRACT.....iii

ACKNOWLEDGEMENTS.....v

PREFACE.....1

REVIEW OF THE ECHINOID SKELETON.....2
Skeletal formation and growth.....4
The larval skeleton.....4
Post larval skeletal growth: addition of plates.....7
Post larval skeletal growth: accretionary growth.....8
Skeletal microstructure.....11
Crystallographic features of the echinoderm skeleton.....12
Monocrystalline nature of skeletal elements.....12
Crystallographic orientation of echinoid calcite.....13
Skeletal chemistry.....14
Major elements.....14
Minor and trace elements.....16
Isotopic composition.....18

OVERVIEW OF THE STUDY.....20
Statement of purpose.....20
Selection of an appropriate genus for study.....22
Suitability of *Strongylocentrotus*.....22
Ecology of *Strongylocentrotus*.....23
General materials and methods.....26

MICROSTRUCTURAL ZONATION WITHIN INTERAMBULACRAL COMPONENTS.....28
Sample preparation methods.....28
Observations with scanning electron microscopy.....30
Microstructural zonation in *Strongylocentrotus*.....35

SKELETAL GROWTH.....38
Major features of test growth.....38
Addition and growth of coronal plates.....42
Addition of coronal plates.....42
Accretionary growth of coronal plates.....44
Correlation of growth zones in interambulacral plates.....47
Correlation of zones throughout an interambulacrum.....49

CHEMICAL HETEROGENEITY WITHIN CORONAL PLATES.....56
Methods used in cathodoluminescence.....57
General background of cathodoluminescence.....57
Sample preparation methods.....58
Observations with cathodoluminescence.....60
Methods used in electron microprobe analysis.....65
Observations with electron microprobe analysis.....66
Chemical heterogeneity within interambulacral components.....71

CHEMICAL VARIATION OF CORONAL PLATES.....73
Sample preparation and methods used for atomic absorption.....74
Results of chemical analyses.....77
Compositional differences between ambulacrals and interambulacrals.....77
Compositional variation within interambulacral series.....81
Variation of skeletal chemistry within the individual.....88

CONCLUSIONS.....91
Summary.....91

BIBLIOGRAPHY.....93

LIST OF TABLES

Table 1: General skeletal characteristics of some major faunal groups.....3
Table 2: Growth zone characteristics.....10

LIST OF FIGURES

Figure 1: Schematic diagram of *Echinus*.....5
Figure 2: Geographic distribution of (A) *S. franciscanus*; (B) *purpuratus*; and (C) *S. droebachiensis*.....24
Figure 3: Bathymetric range of *Strongylocentrotus*, by species.....25
Figure 4: Vertical, apical and peristomial diameters relative to horizontal diameter of *S. droebachiensis*.....40
Figure 5: Number of coronal plates relative to (A) horizontal diameter and (B) vertical diameter in *S. droebachiensis*.....43
Figure 6: Reconstructed growth series of an interambulacrum: *S. franciscanus*.....52
Figure 7: Growth of individual interambulacral plates relative to position of plate.....54
Figure 8: $CaCO_3$ and $MgCO_3$ variation (mole percent) along adradial-interradial axis of an ambital interambulacral of *S. droebachiensis*.....67
Figure 9: $CaCO_3$ and $MgCO_3$ variation (mole percent) along adoral-adapical axis of an ambital interambulacral of *S. droebachiensis*.....69
Figure 10: $CaCO_3$, $MgCO_3$ and $SrCO_3$ variation (mole percent) of ambital plates of *S. droebachiensis*.....80
Figure 11: $CaCO_3$, $MgCO_3$, $SrCO_3$, $FeCO_3$ and $MnCO_3$ variation of an interambulacral series: *S. franciscanus*.....82
Figure 12: $CaCO_3$, $MgCO_3$ and $SrCO_3$ variation of an interambulacral series: *S. droebachiensis*.....84
Figure 13: $CaCO_3$, $MgCO_3$ and $SrCO_3$ variation of an interambulacral series: *S. purpuratus*.....85

Figure 14: Mg:Ca ratios relative to position of the interambulacral in *Strongylocentrotus* species.....87
Figure 15: Mg:Sr ratios relative to position of the interambulacral in *Strongylocentrotus* species.....89

LIST OF PLATES

Plate 1: Scanning electron photograph of etched interambulacral.....31
Plate 2: Scanning electron photograph of adoral interambulacral.....32
Plate 3: Scanning electron photograph of ambital interambulacral.....34
Plate 4: Radiographs of (A) interambulacrals with tubercles; (B)same interambulacrals with tubercles removed; (C) ambulacrals....46
Plate 5: Radiographs of (A) homologous interambulacrals of same individual and (B) adjacent interambulacrals of same column.....48
Plate 6: Radiograph of entire interambulacrum.....50
Plate 7: Luminoscope photographs of (A) unpolished interambulacral and (B) polished interambulacrals.....61
Plate 8: Composite photograph combining radiograph and luminscope photograph.....63

LIST OF APPENDICES

Appendix A: Supplement to REVIEW OF THE ECHINOID SKELETON.....104
Appendix B: Supplement to SKELETAL GROWTH.....105
Appendix C: Supplement to CHEMICAL HETEROGENEITY WITHIN CORONAL PLATES.....108
Appendix D: Supplement to CHEMICAL VARIATION OF CORONAL PLATES.....114

PREFACE

Echinoderms are an interesting faunal group that draw the attention of biologists and paleontologists. They form an integral part of many marine ecosystems (see Moore, 1966, for a general review) and are popular among naturalists. The echinoderm skeleton also draws the interest of medical researchers and materials scientists seeking a precursor for synthetic bone tissue (e.g. White et al., 1972; Weber and White, 1973).

Echinoderms, moreover, are important in many geological studies. Their skeletal fragments can be primary constituents of ancient carbonate environments (e.g., Meyers, 1974, p. 838). In some cases, their activity produces trace fossils such as borings and burrows (see McLean, 1967; Bromley and Asgaard, 1975). Particularly interesting is the use of skeletal elements from echinoderms in studies of carbonate geochemistry and diagenesis (Schroeder, 1969; Wollast and Reinhard-Derie, 1972; Grover and Kubanek, 1983).

The general purpose of this study is to examine the skeletal growth and chemistry of the regular echinoid *Strongylocentrotus* and to see if skeletal growth and chemistry are correlated in some way. In this manner, it may be possible to underscore the importance of echinodermal material in the geological record.

REVIEW OF THE ECHINOID SKELETON

The echinoderm skeleton is composed of several discrete, calcareous "monocrystalline" elements. Echinoderm calcite commonly has a high magnesium content, ranging from 4 to 16.3 weight percent magnesium (Chave, 1954, p. 270-272). Each element behaves optically as a single crystal, with a few exceptions such as the polycrystalline echinoid teeth. Calcification of these elements is initiated intracellularly or extracellularly (outside and/or between cells). While these elements often show characteristic accretionary growth patterns, the entire skeletal system also grows by the addition of elements.

Many of these features distinguish the echinoderm skeletal system from the hard parts of other animal groups (see Table 1, p. 3). Unlike other invertebrates, echinoderms have an endoskeleton; that is, the echinoderm skeleton is internal, originating from the mesodermal tissue layer. For this reason, modification (i.e., the absorption and redeposition of skeletal material, best known in vertebrates) may be important in the skeletal growth of echinoderms (Ebert, 1967, p. 148; Swan, 1966, p. 405). Accretionary growth, coupled with growth by addition, is also a definitive feature of the echinoderm skeletal system. The most distinctive feature of the echinoderm skeletal system is the monocrystalline character of the skeletal elements. In every other major group of organisms, skeletal elements are polycrystalline. That elements are monocrystalline is especially striking because of the porous microstructure of each element in echinoderms.

Although calcite is widespread throughout all organisms as a skeletal mineral, the occurence of skeletal high magnesium calcite is infrequent.

Table 1: General skeletal characteristics of some major faunal groups

Group	Skeletal type	Dominant mineralogy	Crystallography	Major mode of skeletal growth	Initiation site
Protista Or. Foraminiferida Or. Radiolaria	"endoskeleton"	C,A,S	amorphous to polycrystalline	accretion	intracellular
Porifera		C,A,S	amorphous to polycrystalline	accretion, "addition"	intracellular, extracellular
Cnidaria	exoskeleton	C,A	polycrystalline	accretion	intracellular, epithelial
Mollusca	exoskeleton	C,A	polycrystalline	accretion	intracellular, epithelial
Arthropoda	exoskeleton	C,CP	polycrystalline	addition, molting	intracellular, epithelial
Echinodermata	endoskeleton	C	monocrystalline skeletal units	addition, accretion, modification?	intracellular, epithelial
Chordata	endoskeleton	AP,CP	polycrystalline	accretion, modification	epithelial

Skeletal type: endoskeleton indicates that soft tissue separates skeleton from environment; exoskeleton indicates that skeleton is exposed to environment.

Mineralogy: C - calcite; A - aragonite; S - silica; CP - calcium phosphate; AP - apatite.

Skeletal growth: terms defined in Raup and Stanley (1978).

Initiation site: intracellular refers to within cell formation of crystallites, often in association with vacuoles; extracellular refers to crystallite formation outside of cells, but within organism's body; epithelial is a major type of extracellular crystallite formation in association with epithelial cells.

Table based on information in Boersma (1978), Eanes and Posner (1970), Kling (1978), McAlester (1968), Matthews et al. (1982), Raup and Stanley (1978), (1970), and Wilbur (1980).

These distinctive features make the chemistry, morphology, generation and growth of the echinoderm skeleton worthwhile subjects for investigation.

Generalities regarding the echinoderm skeleton are often based on studies of echinoids, popularly known as sea urchins (regular echinoids), sand dollars and sea biscuits (irregular echinoids). A schematic diagram showing the major skeletal features of the echinoid test (or corona) is provided in Figure 1 on page 5. Details regarding echinoid skeletal morphology are available in a number of sources, including Hyman (1955, p. 414-453) and Melville and Durham (1966, p. U220-U257).

Note that echinoids constitute an important group in the geological record. Although their diversity and abundance are limited during the Paleozoic, echinoids are found in a variety of Paleozoic strata (Kier, 1965, p. 453; Durham, 1966, p. 385). Echinoid diversity increases dramatically during the Jurassic, with the establishment of several new orders (Kier, 1974, p. 82). Nearly nine hundred species of echinoids currently exist in the marine environment (ibid., p. 85) and echinoids are, perhaps, "more successful now than at any time in the past" (Durham, 1966, p. 390). Clearly, the echinoids merit further study.

Skeletal formation and growth

The larval skeleton

Many studies of skeletal formation and growth in echinoids focus on skeletal development during the larval phase, better known as the echinopluteus or pluteus stage. Skeletal formation may begin as early as the blastula phase (Bevelander and Nakahara, 1960, p. 45), but these early

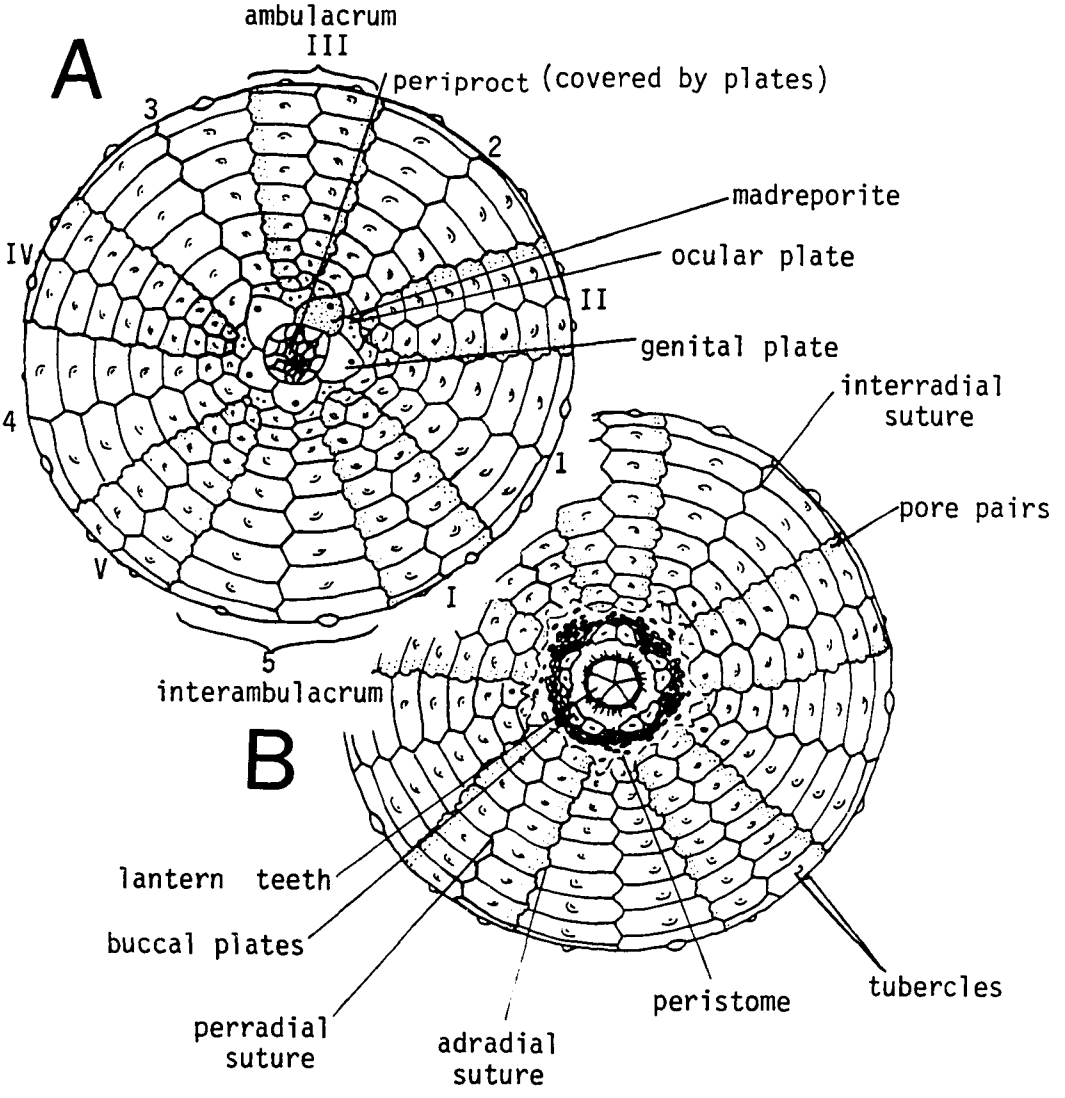

Figure 1. Schematic diagram of *Echinus* test (Recent), spines removed, showing: (A) aboral (adapical) surface; (B) adoral surface, approximately natural size. Redrawn from Melville and Durham (1966, p. U222).

skeletal elements are not important in subsequent skeletal development. Autoradiographic studies show that calcification is an integral part of the gastrulation process which leads to pluteus formation from the blastula (Okazaki, 1975, p. 208).

At the onset of gastrulation, intracellular calcitic granules (the "spicular rudiment" of some workers) appear in association with mesenchymal cell aggregates. Subsequently, the granules become more triangular in form, eventually coalescing into triradiate spicules. Continued branching and coalescence of the spicules leads to the formation of skeletal arm rods (Hyman, 1955, p. 490) and the basket-like skeleton of the four-armed pluteus (Okazaki, 1975, p. 210).

During the late larval (advance pluteus) stage, invagination of the ectodermal wall forms the "echinus rudiment", or imaginal disc. It is in the rudiment that the adult mouth and lantern form, as the young urchin develops within the larval body (ibid., p. 220). In addition to the lantern, a number of test elements, i.e., the coronal plates, first form in the echinus rudiment (Gordon, 1926, p. 263-280; Gordon, 1929, p. 290-298, 308-310). Elements such as the genital plates form in the dorsal surface of the pluteus. When the pluteus is 4 to 6 weeks old, the young urchin escapes through the larval encasing and the skeletal arm rods break off.

A newly metamorphosed juvenile urchin is, on the average, about 1 mm in diameter and has several skeletal elements, including genital and ocular plates, buccal plates, spines, pedicellariae and lantern elements. It also has from three to ten coronal plates per column. At the time of metamorphosis, all existing coronal plates lie on the oral surface and the

apical system covers the entire aboral surface (Hyman, 1955, p. 500). As growth continues, the apical system covers proportionally less of the aboral surface. All the types of skeletal elements observed in adult urchins are present in the newly metamorphosed juvenile such that juvenile urchins are similar to their adult counterparts.

Post larval skeletal growth: addition of plates

Growth continues in juvenile echinoids and it is uncertain whether growth ever ceases entirely in adult echinoids. As the echinoid grows, the test increases in size to accommodate the expansion of soft tissues. Overall, the addition of new coronal plates and the subsequent accretionary growth of these elements generates test growth.

While the addition of new plates appears unending in most regular echinoids, there is an upper limit to the total number of coronal plates in most irregular echinoids. The proportion of ambulacral plates to interambulacral plates, moreover, also changes as the test grows.

During early stages of post-larval growth, the number of ambulacral plates per column is equivalent to the number of interambulacral plates per column (Swan, 1958, p. 510). This proportionality does not continue throughout the life of the regular echinoid.

Coronal plates initially form at the perimeter of the apical system and are dislocated towards the peristome as newer plates form (Markel, 1981, p. 37). Complete reabsorption of coronal plates near the peristome, a common hypothesis among early workers, does not occur in most regular echinoids (ibid., p. 50).

It is surprising that the relationship between the numbers of coronal

plates and test diameter can vary within one species. See, for example, Table A-1 of the appendix which is duplicated from Mortensen (1943, p. 206). Individuals of the same species and with similar horizontal diameters (the ambital diameter of some workers) differ substantially in number of coronal plates (compare specimen 2 with specimen 20 in Table A-1). Conversely, individuals with equal numbers of coronal plates may vary significantly in test diameter (contrast specimen 1 with specimen 13 in Table A-1). The type of data presented in Table A-1 may be useful in examining geographical variation in echinoids.

Post-larval skeletal growth: accretionary growth

Test growth also results from the accretionary growth of coronal plates. In adult irregular echinoids, with fixed numbers of test plates, coronal growth is largely caused by skeletal accretion. How accretionary growth is related to the addition of new coronal plates in regular echinoids is not entirely understood.

Accretionary growth leads to the development of growth zones or lines that have been recognized in several echinoid genera (Moore, 1935, p. 116-121; Durham, 1955, p. 78; Swan, 1966, p. 405). Such zones also occur in other echinoderms, including crinoids (Meyer, 1965, p. 1208) and blastoids (Macurda, 1966, p. 92). In echinoids, growth zones form in coronal plates as well as other skeletal elements, i.e., plates of the apical system (Moore, 1935, p. 116) and spines (Weber, 1969b, p. 452).

Growth zones occuring in coronal plates are actually internal features (Pearse and Pearse, 1975, p. 732) and therefore are not always readily apparent. A variety of preparation techniques such as grinding,

acid etching, charring and oil immersion may be necessary to reveal zones more clearly (Durham, 1955, p. 76; Jensen, 1969, p. 42). Perhaps the most effective means of showing growth zones in coronal plates is through X-radiography (Pearse and Pearse, 1975, p. 733).

Pearse and Pearse (1975, p. 741-742) characterized the growth zones of coronal plates using these methods (see Table 2). In their observations, opaque zones (zones that inhibit the transmission of X-rays) appeared light in reflected light, dark in transmitted light. The properties of translucent zones (zones that allow X-ray transmission) were the converse of those of opaque zones.

Experimentation with laboratory-reared echinoids suggests that opaque zones form during times of increased food supply and decreased temperatures (ibid., p. 742). These conditions normally occur during the fall/winter season in the organism's geographic range. Translucent zones presumably develop under conditions of decreased food supply and increased temperatures (i.e., spring/summer season). Based on these observations, Pearse and Pearse (1975, p. 742) argued that growth zonation in echinoids probably is a seasonal phenomenon.

Growth zones can also be characterized on the basis of microstructural features (ibid., p. 735). Opaque zones, for example, are a denser meshwork with smaller (less than 15 μm diameter) pores and thicker trabeculae relative to translucent zones. These features, moreover, are consistent with the X-ray transmission properties of opaque and translucent zones. Observations of experimentally-induced zones indicate that opaque zones are correlated with high growth rates whereas translucent zones are correlated with low growth rates (ibid., p. 739).

TABLE 2

Characteristics	Zone type	
	OPAQUE	TRANSLUCENT
REFLECTED LIGHT	LIGHT	DARK
TRANSMITTED LIGHT	DARK	LIGHT
INTERTRABECULAR CHANNELS	SMALLER	LARGER
TRABECULAR DIAMETER	LARGER	SMALLER
ORIENTATION	GREATER	LESSER
ETCHING	SLOWER	FASTER
GRINDING/WEATHERING	POSITIVE RELIEF	NEGATIVE RELIEF
GROWTH RATE	FASTER	SLOWER
FOOD SUPPLY	HIGH	LOW
TEMPERATURE	LOW	HIGH
SEASON	FALL/WINTER	SPRING/SUMMER

Appearance: In reflected light, "light" zones reflect more light relative to "dark" zones and hence have a light appearance.
In transmitted light, "dark" zones transmit more light relative to "dark" zones and hence have a light appearance.

Microstructural features: Trabecular diameter, i.e., the thickness of calcitic rods, is "smaller" (15 m and less) in translucent zones, "larger" (20 m and more) in opaque zones.
Intertrabecular channels, i.e., pore spaces, are "smaller" in opaque zones (in association with larger trabecular diameters) and "larger" in translucent zones (in association with smaller trabecular diameters).
Degree of orientation, i.e., morphological organization of the skeletal meshwork, is "greater" in opaque zones, "lesser" in translucent zones.

Structurally related features: Etching, i.e., dissolution of skeletal material in acidic solutions, occurs at a "slower" rate in opaque zones and a "faster" rate in translucent zones.
Grinding/weathering, i.e., abrasion/erosion processes, produces "positive relief" in opaque zones, "negative relief" in translucent zones.

Environmental/seasonal characteristics: These are largely self-explanatory and are based on observations of laboratory-reared urchins. These characteristics may differ in other echinoids.

(MODIFIED FROM PEARSE AND PEARSE, 1975, P. 741)

Questions regarding growth zonation in echinoids still remain. While differential growth rates apparently cause zonation, a satisfactory explanation (reproductive periodicity, environmental fluctuation?) for differential growth rates has not been determined. More importantly, it must be resolved if growth zones can be utilized to examine the ontogenetic history of echinoids. Such information would be particularly useful in paleontological studies.

Skeletal microstructure

Echinoderm skeletal material has a distinctive microstructure best revealed through scanning electron microscopy (SEM). The porous skeleton is a fine meshwork of interconnecting calcitic rods (trabeculae), similar in appearance to commercial plastic foam. This inorganic portion of the skeleton is frequently called the stereom. When the organism is alive, the pore spaces (intertrabecular channels) are filled with soft tissues, termed the stroma by some workers. Whether any of this organic material serves as an organic matrix in skeletal formation is uncertain (see Currey and Nichols, 1969; Travis, 1970; Shimizu and Yamada, 1980; Loeper and Pearse, 1982 for a thorough discussion).

SEM studies of skeletal meterial from echinoids have provided considerable information regarding the function and taxonomic importance of the coronal skeleton. Microstructural features of coronal plate surfaces were described in papers by Oldfield (1976) and Regis (1977). An extensive investigation of coronal pores in ambulacral plates by Smith (1978) related the microstructural details to the function of the associated organic material. In a similar study, Smith (1980) correlated stereomic

patterns with the functions of associated soft tissues. He concluded (1980, p. 76-77) that stereomic microstructure is primarily controlled by the interaction of phylogeny, associated stroma, growth rate and, to a lesser extent, environmental factors.

In SEM studies, microstructural features related to growth are often difficult to distinguish. Microstructural zonation (see Table 2) is in fact characterized from observations of thin sectioned skeletal material using light microscopy (Pearse and Pearse, 1975, p. 734-736). The difficulty of detecting microstructural zonation may be caused by the three-dimensional framework of the skeletal mesh (ibid., p. 734). Alternatively, some characteristic differences in the microstructure of opaque and translucent zones (i.e., trabecular diameter and intertrabecular channel size) may be obscure.

Crystallographic features of the echinoderm skeleton

Monocrystalline nature of skeletal elements

Much of the original work in the area of echinoderm crystallography is based on optical methods developed by German researchers (reviewed by Raup, 1959, p. 661-663). Studies using optical methods and, later, X-ray diffraction studies (e.g., West, 1937, p. 459) indicate that individual skeletal elements typically are monocrystalline, although some elements are polycrystalline (e.g., teeth of the lantern apparatus in echinoids; see Prenant, 1926, p. 36). Despite these studies, there is some disagreement regarding the crystallographic nature of skeletal elements in echinoderms.

Some confusion resulted from the observation that features such as

the tubercles on echinoid plates are polycrystalline, yet occur in crystallographic continuity with the plate (Raup, 1965, p. 935; Towe, 1967, p. 1049). Donnay and Pawson (1969, p. 1149) suggested that the mechanical action of the spine on the tubercle can cause the tubercle to become polycrystalline during growth.

Observations of crystallites on fractured surfaces of echinoderm calcite also suggests that the skeletal calcite of echinoderms may be polycrystalline (O'Neill, 1981, p. 647). Such evidence is not equivocal because the crystallites may instead be artifacts of fracturing (see discussion of microtome-induced artifacts in echinoid larval skeleton by Urakami et al., 1980, p. 181-185). The novel approach of crystal decoration coupled with SEM observations further substantiates that most skeletal elements are monocrystalline (Dillaman and Hart, 1981, p. 316). This method, first developed by Okazaki et al. (1980, p. 161-163), can also detect any variation in the a-axis orientation.

Crystallographic orientation of echinoid calcite

Regardless of the crystallographic nature of skeletal elements, considerable variation in crystallographic orientation occurs, providing a number of generalized patterns. Crystallographic orientation can vary with phylogeny (echinoid vs. asteroid), type of skeletal element (interambulacral vs. ambulacral plate), and/or ontogeny (a young plate vs. an old plate, within a column). Detailed study of c-axis orientation patterns in echinoids (fossil and Recent) indicated that such patterns provide a possible taxonomic criterion at the ordinal level (Raup, 1962, p. 809).

Raup reported changes in the crystallographic orientation (i.e., the c-axis orientation) of coronal plates in the echinoids *Hemicentrotus* and *Lytechinus* (1960, p. 1047). He suggested that this variation along a column may be related to photosensitivity and life habits of these organisms (ibid., p. 1049-1050). Ontogenetic variation in *Hemicentrotus* is particularly striking because this variation is not observed in other genera of the same family. Recall that c-axis orientation patterns are thought to be stable at the ordinal level.

Little is known about the orientation of the a-axes. Okazaki et al. (1981, p. 412 and 414) note that different subplates (compartments) of the same ambulacral plate vary in a-axis orientation. Although subplates vary in a-axis orientation, all subplates of the same ambulacrum share a common c-axis orientation. Additional research in this area would provide substantial insight to the crystallographic nature of the echinoderm skeleton.

Skeletal chemistry

Major elements

Calcium is the major cation present in both biogenic and non-biogenic calcite. Other cations (e.g., magnesium, strontium, trace amounts of iron) may substitute for calcium in the calcite lattice. Magnesium, for example, is often incorporated in the skeletal calcite of echinoids and other echinoderms. The carbonate portion of echinoid calcite does not show variation in elemental composition, although some variation in the isotopic composition does occur.

Studies of echinoid skeletal chemistry often concentrate on the high

concentration of magnesium, first reported by Clarke and Wheeler (1915, p. 193). This aspect of skeletal chemistry has attracted the attention of geologists interested in carbonate diagenesis (e.g., MacQueen and Ghent, 1970) and protodolomite formation (e.g., Schroeder et al., 1969). Like the patterns of crystallographic orientation observed in echinoids, magnesium concentration varies taxonomically and morphologically. Magnesium content is also believed to vary with environmental parameters such as temperature. It is interesting to note that magnesium concentration also varies within an individual skeletal element, i.e., magnesium is distributed heterogeneously within single skeletal elements.

Magnesium concentration is somewhat lower in the echinoid test (an average 12.3 wt percent $MgCO_3$; see Weber, 1969a, p. 551) than in the skeleton of other echinoderms (12.5 wt percent $MgCO_3$ in crinoids; 13.8 wt percent $MgCO_3$ in ophiuroids and holothuroids; 14.0 wt percent $MgCO_3$ in asteroids; ibid., p. 552-553). Early studies also suggest that magnesium content is variable at lower taxonomic levels (e.g., Terentieva, 1932, p. 49-50). Recent evidence, however, implies that the variation noted at lower taxons is actually related to the geographic range and environmental preferences of lower taxon groups (Weber, 1969a, p. 551-555).

There is extensive documentation that different types of skeletal elements from one individual vary in magnesium concentration (Clarke and Wheeler, 1915, p. 192; Terentieva, 1932, p. 49-50). In echinoids, spines are generally lowest in magnesium and test elements are highest (Weber, 1969a. p. 545-546). The spines of *Echinometra lucunter*, for example, contain about 7.4 wt percent $MgCO_3$ whereas the test contains 14.7 wt

percent $MgCO_3$.

Magnesium concentration of skeletal calcite in echinoderms is also related to environmental temperature, as originally observed by Clarke and Wheeler (1915, p. 195). Subsequent work shows that the magnesium content of the test increases with increasing environmental temperature (e.g., Chave, 1954, p. 277; Davies et al., 1972, p. 879). Magnesium "dependence on temperature" varies with species and different skeletal components (Weber, 1969a, p. 550-551).

Electron microprobe analyses of echinoid skeletal elements have shown that magnesium is often distributed heterogeneously within individual skeletal components, varying as much as five mole percent within one skeletal element (Schroeder, 1969, p. 1061; Schroeder et al., 1969, p. 1614; Fowler, 1972, p. 210; MacQueen et al., 1974, p. 67). In a study of echinoid plates and spines, Fowler (1972, p. 81-100) argued that this heterogeneity results from temperature fluctuations during accretionary growth of the skeletal component. Davies et al. (1972, p. 879-882) carried out a series of spine regeneration experiments and found that growth also affects magnesium distribution.

Minor and trace elements

A number of other elements, including strontium and trace amounts of iron and manganese, are often present in the skeletal calcite of echinoids. In echinoids and other echinoderms, the amount of strontium incorporated in skeletal calcite is low, ranging from 0.10 to 0.20 percent dry wt (Thompson and Chow, 1955, p. 35-36). Unlike magnesium, strontium does not vary appreciably in different taxa.

Some evidence suggests that there is an inverse relationship between strontium levels in echinoid calcite and environmental temperature (Pilkey and Hower, 1960, p. 210-211). This is, however, difficult to demonstrate (see Fowler, 1972, p. 170) and requires additional study.

Davies et al. (1972, p. 880) indicated that some growth-related factor may influence strontium distribution within individual skeletal components. In their study of spine regeneration, they found that strontium content was highest at the growing edge of the regenerating spine (ibid., p. 880). They did not observe any systematic variation of strontium concentration with temperature (ibid., p. 879).

Reviews of chemical composition in marine organisms suggested that several trace elements also occur in the echinoid skeleton (e.g., Vinogradov, 1953, p. 252; Eisler, 1981, p. 427-455). An early analysis of an echinoid test by Noddack and Noddack (1939, p. 33) revealed the presence of the following: antimony, arsenic, bismuth, cadmium, chromium, cobalt, copper, gallium, germanium, gold, iron, lead, manganese, molybdenum, nickel, silver, thallium, tin, titanium, vanadium and zinc.

Other elements reported in echinoid calcite include: aluminum (Vinogradov, 1953, p. 252), barium (ibid., p. 265), cerium (Eisler, 1981, p. 433), and cesium (ibid., p. 433). The occurence of barium, iron, lead, manganese and zinc is particularly striking because these elements are known to form carbonate minerals and may substitute for calcium in calcite or aragonite.

Trace elements in general may be related to environmental parameters (see Eisma et al., 1976), although such studies are not entirely conclusive. Potential application of trace element data in echinoids remains

limited because so little is known about how trace element levels vary. Clearly, additional research on minor and trace elements in echinoid skeletal material is needed.

Isotopic composition

Information regarding isotopic composition, particularly stable isotopes, may also be helpful in considering the skeletal chemistry of echinoderms. Our restricted knowledge of isotopic composition in echinoderms is based entirely on studies of echinoid material but nonetheless provides some interesting observations. Unlike the skeletal material of molluscs, brachiopods and foraminifera, that of echinoids is highly fractionated (Dodd and Stanton, 1981, p. 160) and is enriched in carbon-12 (C^{12}) relative to sedimentary carbonate (Weber and Raup, 1966a, p. 682).

Thorough examination of isotopic composition reveals that δC^{13} and δO^{18} values vary significantly within an individual echinoid (Gross, 1964, p. 174; Weber and Raup, 1966a, p. 685-702; Weber and Raup, 1966b, p. 708-709). Spines, for example, are generally enriched in carbon-13 and oxygen-18 (δC^{13} = -0.24, δO^{18} = -0.98 for *Lytechinus* sp.) relative to test components (δC^{13} = -1.42; δO^{18} = -1.12) of the same individual (Weber and Raup, 1966b, p. 708). Despite diagenetic alteration, a similar relationship can be observed in fossil echinoids (Gross, 1964, p. 174; Weber and Raup, 1968, p. 47).

Some variation in isotopic composition within the individual echinoid may be linked to ontogenetic factors. Analyses of coronal plates from an interambulacral series indicated enrichment in C^{13} in older interambulacral plates (δC^{13} = -2.32 in younger interambulacrals, δC^{13} = -1.69

in older interambulacrals; data from Weber and Raup, 1966a; p. 689-692). Similar trends could be observed in the isotopic composition of plates from an ambulacral series.

Results of stable isotope analyses of several echinoid genera may denote that phylogenetic factors also influence isotopic composition (Weber and Raup, 1066b, p. 714-720). In the family Strongylocentrotidae, the average δC^{13} value was -2.63 and the average δO^{18} value was -1.37 (based on analyses of tests of 27 specimens; ibid., p. 714-715). In Cidaridae, average δC^{13} was -3.92 while average δO^{18} was -2.11 (23 specimens analyzed).

It is not clear whether environmental parameters affect isotopic composition. Indications that δC^{13} and δO^{18} are somewhat temperature dependant (ibid., p. 709) should be further investigated.

Weighing the available data, Weber and Raup concluded that variability in isotopic composition of echinoids is primarily controlled by physiological and genetic factors. Environmental factors play a secondary role at most (ibid., p. 720). They also suggest that the underlying physiological mechanisms that control isotopic composition should be examined further.

OVERVIEW OF THE STUDY

Despite the importance of echinoids and growing interest in the skeletal material of these organisms, questions regarding their skeletal growth remain. It is unclear, for example, whether accretionary growth causes or is related to any chemical heterogeneity within skeletal elements. Whether skeletal chemistry varies ontogenetically is also uncertain, despite studies regarding variation in elemental composition. Although growth zonation is well documented in several echinoid genera, it is not entirely understood how growth zonation is related overall test growth. Such information would increase our understanding of echinoid biology as well as provide information useful in studies of paleoecology and carbonate geochemistry. The general purpose of this study, therefore, is to examine skeletal growth and chemistry in echinoids and to determine how growth and skeletal chemistry may be related.

Statement of Purpose

In this study, skeletal growth and chemistry will be examined by pursuing the specific objectives outlined below.

(1) Description of microstructure and features related to growth zonation.

(2) Observation of growth zones in skeletal components.

  (a) correlation of zones from different coronal plates;

  (b) demonstration of the relationship among plates of a single column and homologous plates from different columns;

(c) application of correlated zones to analysis of the ontogeny of the entire test.

(3) Determination of chemical zonation within skeletal components

(4) Examination of chemical compositions of coronal plates and explanation of variability in skeletal chemistry

(a) determination of calcium, magnesium and strontium concentrations in plates from an ambital series;

(b) determination of calcium, magnesium, strontium, and, where possible, iron and manganese concentrations in plates from an interambulacral series.

Limiting the study to one genus is the best means for pursuing these objectives and studying ontogenetic variability. In this way, the variability in skeletal chemistry and growth at subgeneric levels can also be investigated. Documentation of subgeneric variability could provide some insights regarding the importance of skeletal growth and chemistry in the taxonomy and evolution of echinoids. Should this method be successful, it could also be applied to future studies of other echinoids and echinoderms.

Documentation of subgeneric variability may also provide information that could be relevant to ecological and paleoecological studies. It could provide a criterion for recognizing environmental parameters such as temperature and salinity from biogenic calcites.

It is important to select an appropriate genus for this study in order to understand how skeletal growth and chemistry may be related.

Selection of an appropriate genus for study

Suitability of *Strongylocentrotus* for this study

Familiarity with the Recent genus *Strongylocentrotus* (Brandt, 1835) was a primary reason for selecting it as the subject of this investigation. This genus is, in fact, well suited for the purposes of this study for several reasons outlined below.

(1) A sizable body of literature regarding *Strongylocentrotus* indicates that the biology of this genus is well known relative to that of many other echinoid genera. This information may be very helpful and may give insights regarding skeletal growth and composition.

(2) Growth zones in *Strongylocentrotus* are easily shown. This genus is often the subject of studies of echinoid growth (e.g., Pearse and Pearse, 1975; Ebert, 1967;1968).

(3) This genus is familiar to many workers and its taxonomy is well defined (see Jensen, 1974; 1982 for recent reviews).

(4) Many species of this genus occur intertidally and at shallow depths. Specimens for study can therefore be readily collected.

(5) *Strongylocentrotus* has an extensive geographic range in the Northern Hemisphere, over a wide latitudinal and longitudinal range (see Jensen, 1974). This facilitates the availability of specimens and would permit later expansion of this study into ecological and biogeographical areas.

Ecology of *Strongylocentrotus*

Like other echinoderms, *Strongylocentrotus* is strictly marine and occurs in waters of normal salinity. *Strongylocentrotus* is generally considered to be a cool water organism and its distribution ranges from polar to temperate zones (Jensen, 1974, p. 134-135). The range of some species, such as *S. franciscanus* may extend slightly below 30° latitude, perhaps as a result of variations in major ocean currents.

Biogeographical maps in Figure 2 (ibid., p. 134-135) show the distribution of the species investigated here. *S. droebachiensis* has an extensive range and occurs in both the Eastern and Western Hemispheres. *S. purpuratus* and *S. franciscanus*, on the other hand are restricted to the Pacific Ocean.

In general, *Strongylocentrotus* is thought to be a shallow (100 m) water, or littoral, organism. Many species are, in fact, intertidal, living in the lowermost portion of the intertidal zone (Mortensen, 1943, p. 214). Figure 3, from Jensen (1974, p. 135), shows the bathymetric range of each species. The depth at which a species commonly occurs is sometimes narrower than the bathymetric range indicated in Figure 2. *S. droebachiensis*, for example, normally occurs between 0 and 50 m, although its range extends from 0 to 300 m (Jensen, 1974, p. 135).

Strongylocentrotus, like other regular echinoids, is epibenthic or epifaunal and may occur on a variety of substrates. *S. purpuratus* prefers hard-bottom or rocky substrates in coastal waters with high energies (Mortensen, 1943, p. 240; Kozloff, 1973, p. 174). Intertidal populations of *S. droebachiensis* and *S. franciscanus* are also associated with hard

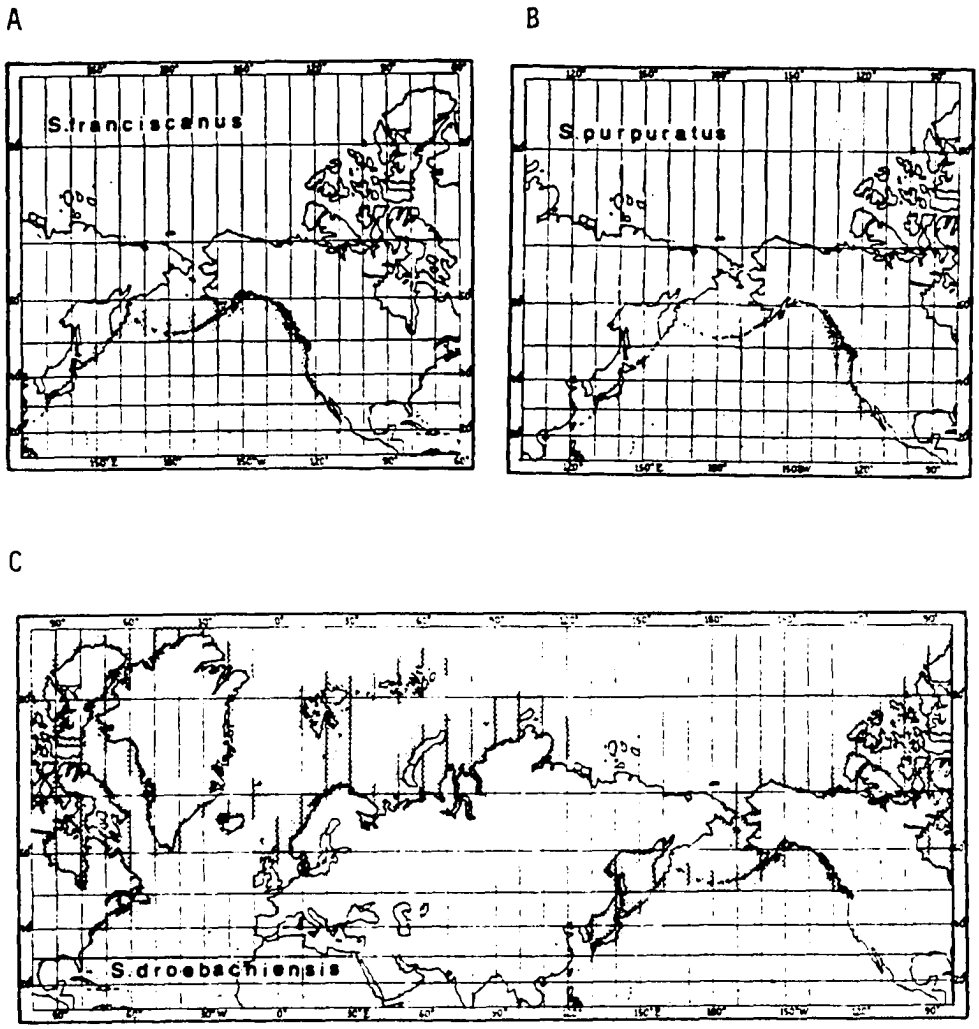

Figure 2. Geographic distribution of (A) *S. franciscanus*; (B) *S. purpuratus*, and (C) *S. droebachiensis*. Reproduced from Jensen, (1974, p. 134-135).

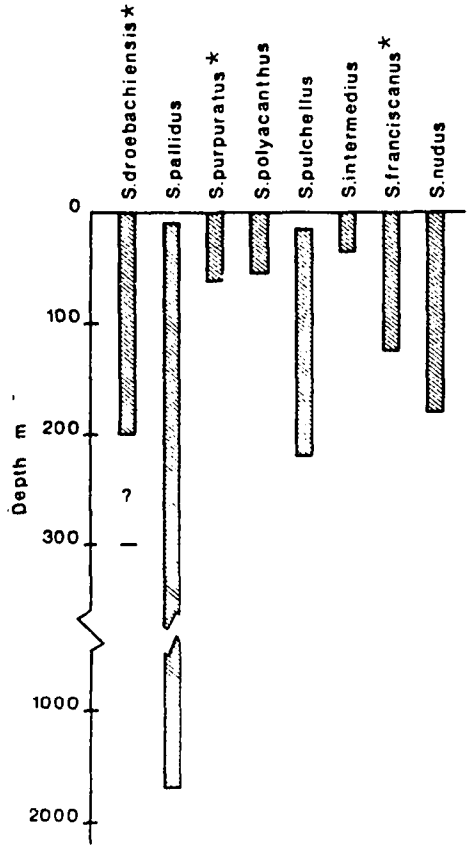

Figure 3. Bathymetric range of *Strongylocentrotus*, by species. Species used in this study are indicated with an asterisk. Reproduced from Jensen (1974, p. 135).

substrates but are not restricted to areas of strong wave action. Subtidal populations of these two species may be found on a variety of substrates, including soft sandy bottoms (Kozloff, 1973, p. 99 and 174).

While *Strongylocentrotus* is an omnivore feeding on whatever is available, algae are its major food source (Mortensen, 1943, p. 190; Johnson and Mann, 1982, p. 278). Its herbivorous activity is particularly important in kelp forest communities (e.g., Duggins, 1981; Tegner and Levin, 1982). Numerous organisms , including sharks, cod and crows, feed on this sea urchin. Perhaps the best known of these predators is the sea-otter which primarily feeds on echinoids (Mortensen, 1943, p. 209).

These generalizations concerning the ecology of *Strongylocentrotus* should be considered in examining skeletal growth and chemistry. Any patterns of skeletal growth and chemistry observed in this study could be related to environmental parameters.

General materials and methods

Three species of *Strongylocentrotus* are actually used in this investigation: *S. droebachiensis*, *S. franciscanus*, and *S. purpuratus*. With its massive (> 0.1 g) coronal plates, *S. franciscanus* is especially well suited for segments of this study requiring large sample sizes, e.g., chemical analyses. Its large plates also facilitate observations of growth zonation. In other portions of the study, however, large coronal plates are troublesome, i.e., it is difficult to mount large elements on stubs used in scanning electron microscopy. Smaller plates from *S. droebachiensis* or *S. purpuratus* were found to be more appropriate.

There is some overlap in the geographic range of these three species (see Figure 2). Differences in geographic distribution should not, therefore, be a major cause of variation in skeletal growth and chemistry observed in this study.

It would be ideal for the purposes of this investigation that all samples be collected at the same location. This was not altogether possible. Specimens of *S. purpuratus* were collected at Sunset Cove in Coos Bay, Oregon (summer, 1979). Specimens of *S. franciscanus* and *S. droebachiensis*, on the other hand, were collected at Friday Harbor Laboratories in the San Juan Islands, Washington (summer, 1981).

After collection, all samples were completely preserved in ethyl alcohol. Sample preparation began with the removal of most organic matter with commercial sodium hypochlorite (household bleach). This process also removed external skeletal elements such as spines. After thorough rinsing and air-drying, individual cleaned tests were stored in plastic bags until required. Tests were disarticulated only as needed because disarticulated material was more difficult to store.

Additional sample preparation was required in many portions of this study. This is discussed in subsequent chapters, where appropriate.

MICROSTRUCTURAL ZONATION WITHIN INTERAMBULACRAL COMPONENTS

Scanning electron microscopy (SEM) furnishes an important means of studying growth zonation in coronal plates. Petrographic microscopy reveals the fenestrate morphology typical of echinoderms and, in some cases, growth zones (see, for example, Weber, 1969b). It is, however, of limited use in examining the finer details of skeletal microstructure. Several studies show that SEM observations are very effective in demonstrating growth zonation in the skeletons of organisms such as bivalves (e.g., Lutz and Rhoads, 1980) and barnacles (e.g., Bourget, 1980). Work on fossil crinoids by Roux (1975, p. 4) suggests that scanning electron microscopy may be equally productive in distinguishing growth-related features in the skeletal material of echinoderms.

Despite such studies and the increasing use of SEM in studies of echinoderms, the microstructural features characteristic of growth zonation in echinoderms are not well known. Only in work by Smith (1980) and Pearse and Pearse (1975) is there any record of growth zonation within the stereom of echinoids. In this study, SEM observations of interambulacral plates are used to describe microstructural features of growth zonation and to determine the capability of SEM work in documenting growth zones. These observations also give a more complete illustration of growth zonation in echinoids.

Sample preparation methods

Zonation is not readily apparent in the surficial skeletal layers of *Strongylocentrotus*. Surface ornamentation obscures any zonation and must

therefore be removed. Interambulacral plates were prepared for SEM study using the same procedure employed in preparing plates for cathodoluminescence (p. 59 of this study). Samples prepared in this manner, however, did not clearly show evidence of growth zonation.

Acid etching, often used to enhance the appearance of skeletal features (e.g., Bourget, 1980, p. 473), was effective in revealing growth zonation with the interambulacrals of *S. droebachiensis* . Interambulacrals were etched in a dilute (0.01M) solution of hydrochloric acid for this portion of the study. Generally, interambulacrals were etched for only a few minutes and were checked during the process to prevent excess dissolution of skeletal material. Small, barely macroscopic zones appearing on the external surface of the interambulacral indicated that the plate was sufficiently etched. Interambulacrals were then rinsed in water to stop further dissolution.

After air-drying, etched interambulacrals were extremely fragile and were therefore handled with great care. Etching removed much of the organic material that remained after bleaching and reduced overall thickness of the plate, thus weakening the interambulacral. Two to three interambulacrals were mounted on each SEM stub with a conductive colloidal silver solution. Mounted samples were reexamined to assure complete cementation.

Mounted samples were then gold-coated using an International Scientific Instruments (ISI) PS-2 Coating Unit. SEM observations were carried out on a Super-II ISI scanning electron microscope and selected features were photographically recorded.

Observations with scanning electron microscopy

Plate 1 is an SEM photograph of the surface of a polished and etched interambulacral plate of *S. droebachiensis* . The fenestrate microstructure common to all echinoderms is readily apparent. Generally, the trabeculae are oriented perpendicular to the growing edges of the interambulacral. Striking changes in trabecular orientation (shown with dark arrows) occur at the intersections of growing edges. These changes in orientation may be significant in strengthening the test overall (see Seilacher, 1979, p. 202-204).

Faint traces of growth zonation (shown with light arrows, Plate 1) also appear within the stereom of the interambulacral. Zones are perpendicular to the general orientation of the trabeculae and are parallel to growing edges of the interambulacral. Note that trabeculae are not as well oriented towards the central portion of the interambulacral, seen in the lower right-hand area of Plate 1.

At somewhat higher magnification, growth zone features in the stereom can be seen more clearly (see Plate 2, a photomicrograph of an adoral interambulacral). Following criteria suggested by Pearse and Pearse (1975, p. 741), smaller intertrabecular channels (or pores) and larger trabecular diameters are indicative of X-ray opaque zones. Larger pores and smaller trabecular diameters of X-ray translucent zones alternate with stereom of the opaque zones.

Both X-ray opaque and X-ray translucent zones occur in galleried stereom, which is largely consistent with Smith's findings regarding zonation in the stereom of the echinoids *Psammechinus* and *Echinus* (1980,

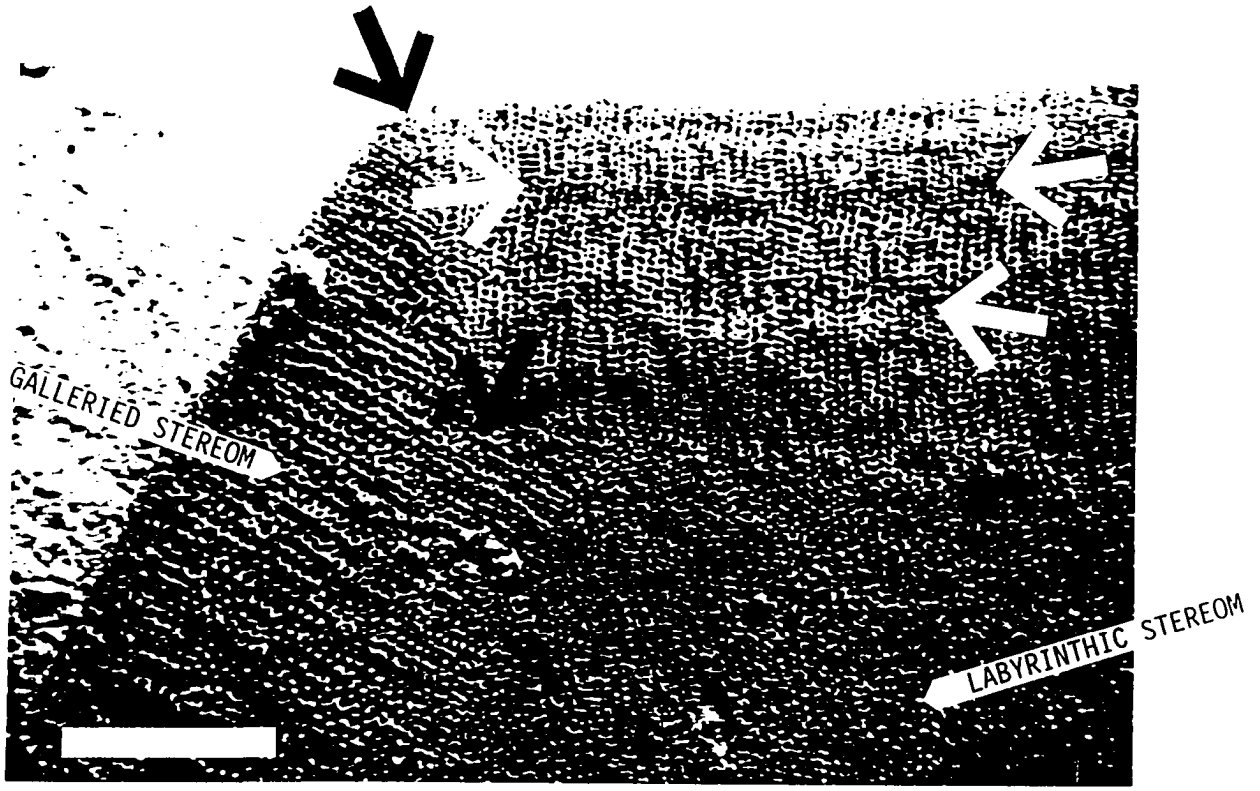

Plate 1. Scanning electron microphotograph of an etched interambulacral plate of *S. droebachiensis* shows fenestrate microstructure of skeleton common to all echinoderms. Changes in trabecular orientation (dark arrows) may be important in strengthening the test. Growth zonation (white arrows) is parallel with plate boundaries (scale bar equals approximately 500 μm).

Plate 2. Scanning electron microphotograph of an adoral interambulacral of *S. droebachiensis* shows growth zones (white arrows). Pores (intertrabecular channels) are smaller and trabecular diameters are larger in opaque zones than in translucent zones. Unoriented stereom in lower left (dark arrow) is labyrinthic stereom of plate nucleus. (scale bar equals 200 μm).

p. 24). Galleried stereom consists of elongated, ordered corridors that are primarily oriented in one direction and usually occurs in association with sutural collagen fibers (ibid., p. 10 and 64). This type of stereom is occassionally termed alpha (α) stereom by some workers (e.g., Roux, 1975, p. 2). Galleries are oriented parallel to the surface and perpendicular to the growing edges in the interambulacral seen in Plate 2.

Variation in pore size and trabecular diameter generates zonation observed within the stereom of the middle skeletal layer. Degree of trabecular orientation (suggested by Pearse and Pearse, 1975, p. 740) and abrupt disruptions in microstructure (suggested by Smith, 1980, p. 24) do not produce zonation within the stereom of *Strongylocentrotus*. There is, however, a rather marked discontinuity between galleried stereom and the central "nucleus" of the interambulacral (shown with dark arrow, Plate 2). This portion of the interambulacral is composed of labyrinthic stereom, a randomly oriented meshwork of trabeculae (see Smith, 1980, p. 12). No zonation is apparent within the labyrinthic stereom of *Strongylocentrotus*. Note that some workers use the term beta (β) stereom to refer to labyrinthic stereom (Roux, 1975, p. 2).

In the SEM microphotograph of an interambulacral near the ambitus (Plate 3), growth zones are parallel with the interradial border. Arrows show the predominant direction of growth. The interradial border is a growing edge or face of the interambulacral and is seen in the bottom area of Plate 3. A translucent zone with large pores and relatively thin trabeculae forms the outermost zone seen in this sample. This translucent zone is, in fact, the youngest zone present in the sample.

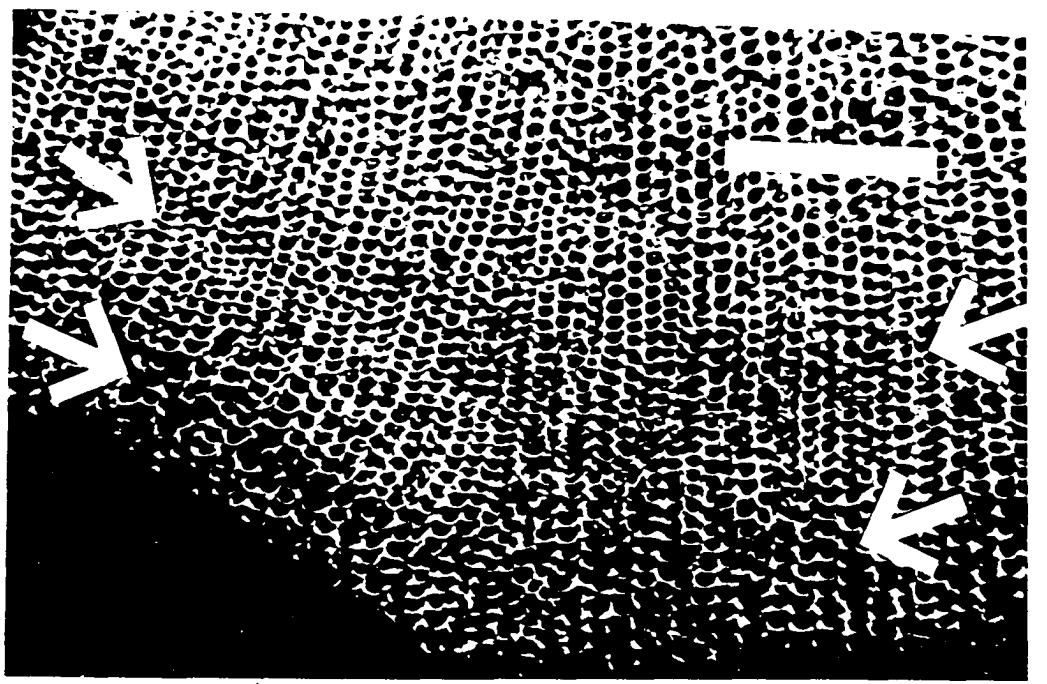

Plate 3. Scanning electron microphotograph of an ambital interambulacral plate. Growth zones (white arrows) occur in well-oriented galleried stereom and are parallel with the interradial margin. Dark arrows show predominant direction of growth (scale bar equals 200 µm).

Microstructural zonation in *Strongylocentrotus*

Scanning electron microscopy gives some insights regarding the nature of growth zonation in *Strongylocentrotus*. Cursory examination of SEM microphotographs shows that growth zonation is absent in some portions of the interambulacral plate. Zonation commonly occurs in galleried (alpha) stereom and is not apparent in labyrinthic (beta) stereom.

Surficial layers of the interambulacral plate also lack any indication of microstructural zonation. While four morphologically distinct, calcareous layers can be seen in the fully developed interambs of *Strongylocentrotus* (Jensen, 1972, p. 41), zonation appears limited to a middle layer of the plate (Jensen's "interior layer of meshwork").

Observations through the course of this study indicate that microstructural zonation is primarily a result of variations in pore size and trabecular diameter. These two variables are inversely correlated, i.e., smaller pore sizes are associated with larger trabecular diameters. This is consistent with conclusions reached by Pearse and Pearse (1975, p. 739-741) and Smith (1980, p. 24) regarding zones within the stereom.

Experimental analysis of growth in *Strongylocentrotus* provides convincing evidence that differential growth rates generate microstructural zonation (Pearse and Pearse, 1975, p. 739-744). By controlling food supply and closely monitoring laboratory-reared urchins, Pearse and Pearse found that translucent zones are associated with slow growth, opaque zones with fast growth. Growth rates, in turn, can be related to environmental conditions. In the case of *Strongylocentrotus*, skeletal growth rate decreases during spring/summer conditions of decreased available nutrients

and increased temperature. Translucent zones therefore develop during the spring/summer season.

This is noteworthy in considering Plate 3. Relatively small trabecular diameters and large channels in the outermost zone indicate that is is a translucent zone, formed during summer skeletal growth. Such an observation is especially striking because the specimen used in this study was, in fact, collected during the summer season. This supports the earlier conclusion of Pearse and Pearse (ibid., p. 744) that translucent zones form in the spring/summer and opaque zones in the fall/winter.

Questions remain regarding zonation within the stereom of echinoids. It is not entirely clear how microstructural zonation is related to chemical zonation observed through electron microprobe analysis and cathodoluminescence. Indirectly, observations in this study indicate that the stereom characteristic of translucent zones should be correlated with non-luminescent (low manganese, high iron) zones. Additional research should clarify if microstructural zones are related to variation of calcium, magnesium and/or strontium within skeletal elements.

Whether microstructural zonation occurs in the stereom of other echinoids and other echinoderms should also be documented in future studies. Coupled with information regarding taxonomic and functional variation in the stereom of echinoids, this type of information would be useful to studies of fossil echinoids.

Scanning electron microscopy is not the best means of documenting growth zones in echinoids. Sample preparation is tedious and often destroys skeletal elements. Several microphotographs are needed to demonstrate zonation throughout a single skeletal element which presents more

difficulty. Another approach is necessary to study and to correlate zones throughout an interambulacrum.

Despite these problems, scanning electron microscopy supplements our general understanding of growth zonation in echinoids and is the best means of observing microstructural zonation. SEM observations may be particularly critical in documenting growth zones in the skeletal material of fossil echinoids. In theory, the occurence of microstructural zonation within the middle layers of coronal plates should inhibit complete destruction of growth zones by diagenetic processes.

SKELETAL GROWTH

General observations and measurements of test dimensions and features are a traditional approach to investigating the skeletal morphology and growth of regular echinoids (e.g., Vasseur, 1952; Swan, 1966). While this widely used approach is informative, analysis of the accretionary growth of individual coronal plates can also provide a more complete understanding of overall echinoid growth. Both approaches are used in this study of *Strongylocentrotus* to more thoroughly understand how growth and form are interrelated.

Major features of test growth

Preliminary observations of the *Strongylocentrotus droebachiensis* specimens used in this study reveal some general characteristics of coronal morphology. For example, the number of ambulacral plates greatly outnumbers the number of interambulacral plates. A particularly interesting observation is the proportionally larger size of the peristomial opening in smaller (presumably younger) individuals relative to the size of the opening in larger (presumably older) individuals. This is especially important in explaining growth of the peristome and surrounding circumoral plates.

Limited quantitative analysis of test dimensions confirms these initial observations and demonstrates other, less apparent growth-related variability. Only a few parameters are needed to describe the dimensions of the symmetric test form typical of regular echinoids. A schematic diagram, Figure B-1 in the appendix, shows some standard dimensions used

in morphometric analysis of regular echinoids.

Of the four parameters shown in Figure B-1, "horizontal diameter" is most widely recorded in biometric studies of echinoids (e.g., Swan, 1966). It is defined as the width of the test at the ambitus, measured from the midpoint of an interambulacrum to the midpoint of the opposite ambulacrum (Mortensen, 1928, p. 10). "Vertical diameter" denotes height of the test and can be measured from an interambulacrum or an ambulacrum. "Apical diameter" refers to the maximum diameter of the apical system and enclosed periproctal plates. The diameter of the peristomial opening is simply the "peristomial diameter". While all these parameters were often recorded in early studies (e.g., Mortensen, 1943), measurements of the apical and peristomial diameters are generally omitted in more recent work (e.g., Moss and Meehan, 1968). This is unfortunate because such data can be useful in understanding test growth.

Vernier calipers were used to measure all four parameters in specimens of *S. droebachiensis* used in this study. The data are shown in Table B-2 of the appendix (columns B through E). Vertical, apical and peristomial diameters were also each recalculated as a proportion of the horizontal diameter. The resulting percentages are shown paranthetically in columns C, D and E of Table B-2. A brief survey of the data in Table B-2 indicates that the peristomial opening grows anisometrically.

Examining these measurements through graphs is especially helpful. Figure 4 shows a graph of recalculated vertical, apical and peristomial diameters each plotted against the corresponding horizontal diameter, using data from Table B-2. The linear relationship between the apical system and the horizontal diameter (represented by triangles) implies

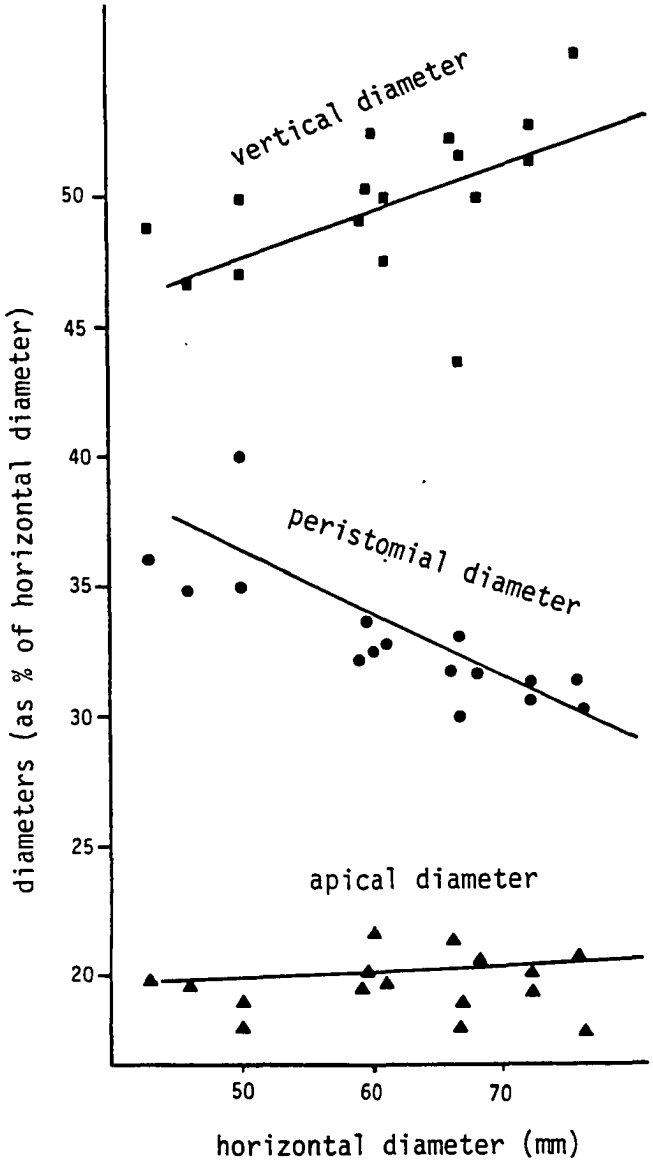

Figure 4. Vertical, apical and peristomial diameters (all expressed as a percentage of horizontal diameter) relative to horizontal diameter of *S. droebachiensis*. Squares designate vertical diameter; triangles indicate apical diameter; circles show peristomial diameter. Data shown in Table B-2 of the appendix.

that the apical system grows isometrically with respectto the test, over the size range examined here. When the peristomial diameter is plotted against horizontal diameter (indicated with circles), it appears that the peristomial opening is proportionally larger in smaller (presumably younger) individuals. This may indicate that the peristome too is larger in smaller individuals compared to their larger counterparts. The anisometric relationship between peristomial opening and horizontal diameter is critical in considering the growth of circumoral plates in older individuals. When vertical diameter is plotted against horizontal diameter (indicated by squares in Figure 4), it seems that test height increases more significantly in larger (presumably older) individuals than in younger individuals. That is, larger individuals have a more spherical test form compared to their smaller counterparts. This observation is even more striking if extremely large (>120 mm in horizontal diameter) individuals of *S. droebachiensis* are compared with small (< 25 mm in horizontal diameter) individuals of the same species. Why this change in form occurs during the course of adult growth is not known, but may be related to a functional importance.

Deviations from isometric growth observed here are similar to those reported by Markel (1981, p. 33) in the cidaroid *Eucidaris*. They may, in fact, be present in all regular echinoids (ibid., p. 33). More importantly, observations of anisometric growth must be considered in any growth model for *Strongylocentrotus*. In particular, the proportional decrease of the peristomial diameter in older individuals implies that resorption of circumoral plates is not necessary during growth. A tendency for more spherical test form may accommodate unlimited addition of plates.

Addition and growth of coronal plates

In regular echinoids, test size increases through the addition of new coronal plates and their subsequent accretionary growth. Little is known about how these two processes interact and whether they influence overall test form. Thorough examination of the addition of plates and accretionary growth of interambulacral plates may furnish some insights regarding ontogenetic variation in test form.

Addition of coronal plates

A dissecting microscope was used to count the number of plates in each ambulacrum and each interambulacrum of the *S. droebachiensis* specimens in this study. Using the microscope alleviated difficulty in distinguishing the small circumoral plates and provided more accurate counting.

Surprisingly, the number of plates per ambulacrum is not constant in all the ambulacra of a single echinoid. The number of plates per ambulacrum can vary by as much as five (plates per ambulacrum) within an individual urchin. It is for the sake of simplicity that only the average numbers, rounded to the nearest whole number, are recorded in columns F and G of Table B-2.

When these averages are plotted against corresponding horizontal and vertical diameters, it seems that plate addition may influence test form (see Figure 5). The number of coronal plates is fairly proportional to horizontal diameter (Figure 5A). In the analogous graph of vertical diameter (Figure 5B), however, the linear relationship between plate number and vertical diameter seems to level off when the diameter reaches 30 to 40 mm.

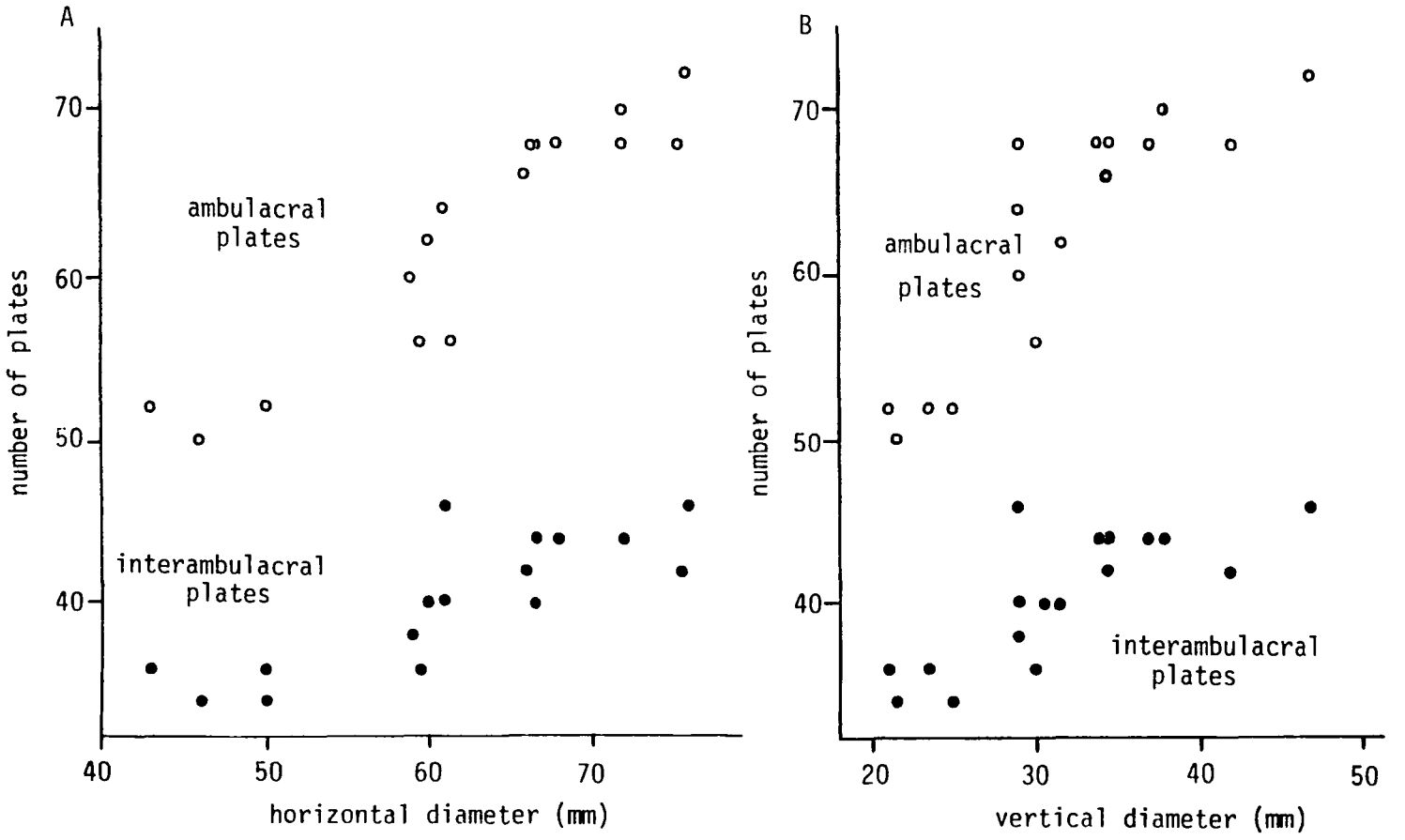

Figure 5. Number of coronal plates relative to (A) horizontal diameter and (B) vertical diameter in *S. droebachiensis*. Open circles indicate ambulacral plates; closed circles indicate interambulacral plates. Data shown in Table B-2 of the appendix.

A similar unexplained pattern was observed by Swan (1966, p. 411) in his studies of *Strongylocentrotus*. Perhaps this pattern indicates that an upper limit to the total number of coronal plates does exist. It may also explain why test form becomes more spherical as the test size increases. There is evidence that the linear portion of the curve varies from species to species and from population to population (Swan, 1958, p. 509; Markel, 1981, p. 33). This probably results from geographic variation in test size that in turn is caused by localized environmental differences such as temperature and food supply (see Moore, 1935, p. 111; Ebert, 1968, p. 1086; Ebert, 1980, p. 473 for a more thorough discussion).

Accretionary growth of coronal plates

Test size and form are also controlled by the accretionary growth of individual coronal plates (Moss and Meehan, 1968, p. 437). How accretionary growth influences the corona can be best investigated by distinguishing growth zones in individual plates and correlating synchronous zones.

Several methods can be used to distinguish growth zones in echinoids (reviewed on p. 7-8, this study). In the case of *Strongylocentrotus*, alternative methods, i.e., cathodoluminescence and scanning electron microscopy, can also be used. These methods are, however, time-consuming and tedious, with the exception of x-radiography. X-radiography is the most efficient and quickest means of recording the growth zones present in echinoids. Sample preparation is minimal and the procedures are familiar to many researchers (Zangerl, 1965, p. 306).

A Faxitron 805 X-ray unit was used to take x-radiographs for this study. Most of the coronal plates in this portion of the study originated

a specimen of *S. franciscanus* . Tubercles generally were removed by abrasion with a 600 mesh paper to reveal growth zones more clearly. Plates were then arranged on Kodak AA film and exposed at 20 kv (exposure time was set automatically).

Growth zones can be easily recognized in radiographs of coronal plates from disarticulated interambulacra (Plate 4A). Dark circular areas present in this radiograph are caused by the dense tubercles. The lighter areas surrounding the dark circles are probably caused by tubercle bases. These features obscure growth zones to some extent and were therefore removed by abrasion in subsequent study.

When tubercles are removed by abrasion, growth zones can be seen with greater clarity (compare Plate 4A with Plate 4B). Both radiographs show the identical pair of interambulacral plates, before and after abrasion. Removal of tubercles may also remove the outermost skeletal layers, thus enhancing the contrast between opaque and translucent zones. In removing tubercles, it is difficult to carry out abrasion evenly over the entire plate. That is, thickness of the skeletal component can become uneven, resulting in "fade-out" of growth zones in some portions of the radiograph (lower right-hand area of the bottom interambulacral in Plate 4B).

Radiographs also reveal some of the morphological distinctions between ambulacral and interambulacral skeletal components (Plate 4C). Large, paired pores readily define ambulacral plates. Radiography also shows that ambulacral plates in *Strongylocentrotus* are compound structures, made up of smaller demi-plates. Suture areas between demi-plates appear quite dark in radiographs and obscure growth zones present in ambulacral plates. Interambulacral plates are, by comparison, simpler forms.

Plate 4. Radiographs of (A) interambulacrals with tubercles; (B) same interambulacrals with tubercles removed; and (C) ambulacrals derived from a test of *S. franciscanus* (scale bar equals 0.5 cm).

Correlation of growth zones in interambulacral plates

Radiographs of homologous plates from different interambulacra of the same individual illustrate how growth zones can be correlated (Plate 5 A; synchronous zones are outlined on acetate overlay). Correlation of zones is based entirely on similarities in the banding patterns common to both interambulacrals. In this respect, correlating growth zones is much like correlating banding patterns in magnetic stratigraphy. While both interambulacrals are more or less homologous, correlation shows that new components are not added synchronously throughout all the columns within an individual. For this reason, homologous plates vary slightly in form.

Like correlated zones in homologous plates, growth zones in adjacent interambulacrals of the same column are also interrelated (Plate 5B; correlations shown with arrows on acetate overlay). Similarities in the banding patters provide one basis for correlation. Another useful criterion is that synchronous zones must compliment one another in form. Just as adjacent plates fit together, synchronous growth zones must also fit together because they represent previous margins of the interambulacral. This greatly facilitates correlation of synchronous zones in adjacent interambulacrals. Only a few correlated zones are indicated on the acetate overlay so that correlations can be observed more clearly.

Note "lines" that radiate from the central nucleus of the interambulacral to the periphery of the component (indicated by wide arrows in Plate 5). These are areas where there is a change in orientation of the skeletal microstructure. They also represent a series of "triple junction points", i.e., points where three interambulacrals meet in the articulated test.

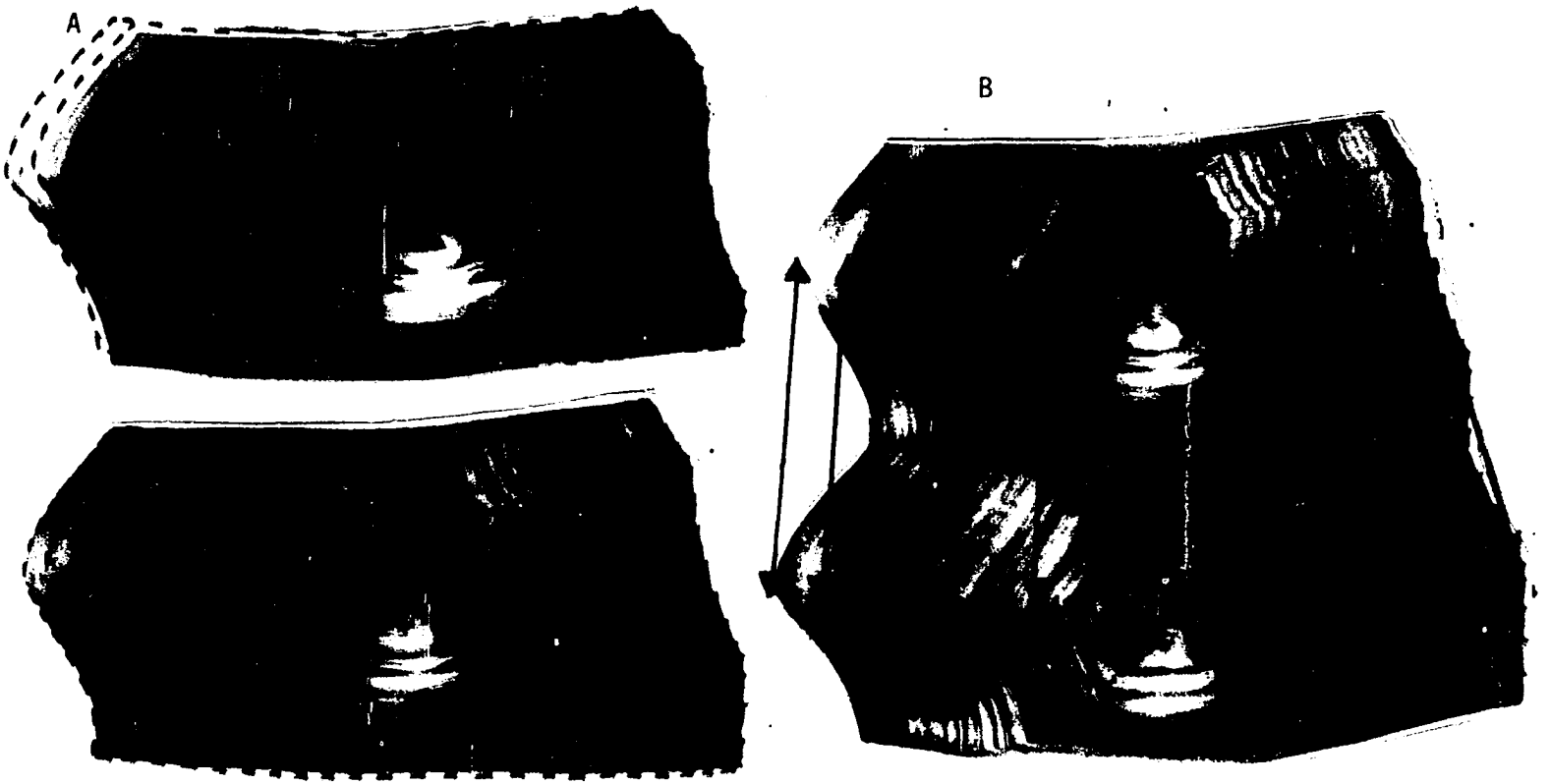

Plate 5. Radiographs of (A) homologous interambulacrals from different columns of the same individual and (B) adjacent interambulacrals of the same column. All interambulacrals originated from a test of *S. franciscanus*. Transparent overlay shows synchronous growth zones (scale bar equals 0.5 cm).

Correlation of zones throughout an interambulacrum

If growth zones can be correlated in pairs of interambulacrals, then synchronous zones can also be correlated throughout an entire interambulacrum. This is best achieved by picking out a few, easily recognized zones to develop an accurate, simplified set of correlations. Radiographs can be illuminated from below with a light table which enhances the contrast between opaque and translucent zones. Synchronous zones can be drawn directly on acetate overlays.

Radiography of an entire interambulacrum, together with correlation of selected synchronous zones (Plate 6), provides some insights regarding accretionary growth.

(1) Growth zones within any one interambulacral reflect the morphology of later, i.e., younger, plates. Deutler first demonstrated this in his study of zonation in echinoids (Pearse and Pearse, 1975, p. 746).

(2) Resorption of skeletal material is not necessary to accommodate growth of the peristomial opening. This is consistent with results of tetracycline-labeling experiments which show that circumoral plates may grow indefinitely (Markel, 1981, p. 48; Dafni and Erez, 1982, p. 72).

(3) Variable growth rates within individual interambulacrals control interambulacral form and maintain morphological integrity of the column. Resorption of skeletal material, if it occurs at all, plays no role in this regard.

(4) The small, triradial "nucleus" of interambulacrals becomes larger aborally. That is, initial size of new components

Plate 6. Radiograph of entire interambulacrum of *S. franciscanus*. Transparent overlay show some synchronous zones throughout the column (scale bar equals 1 cm).

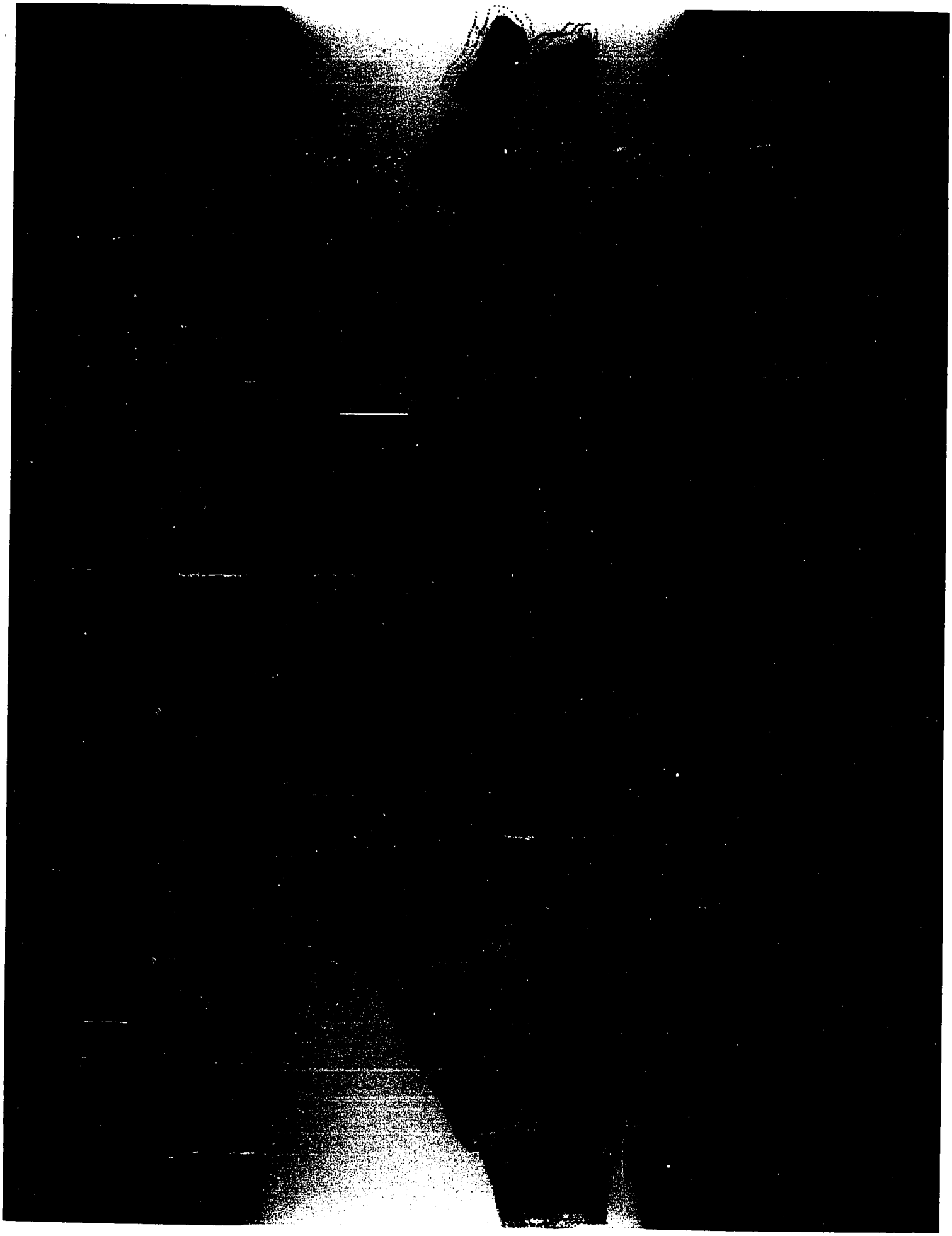

increases as more plates are added.

A growth series of the interambulacrum (Figure 6) can also be reconstructed using the correlations of synchronous zones in Plate 6. Elimination of the outermost, i.e., youngest zones (shown in blue, series "E") produces series "D". Repeated elimination of progressively younger zones produces the entire growth series seen here. Series "A", the oldest interambulacral series that could be recognized, is reproduced with some inaccuracy. This results from problems in distinguishing growth zones of the older interambulacrals, especially the circumoral, primordial plates.

Patterns of skeletal accretion can be seen more clearly with "color-coding". White designates the oldest set of synchronous zones, followed by the addition of yellow zones in series "B", green zones in series "C", orange zones in series "D", and finally blue zones in series "E".

While major changes in form of the column are not apparent, subtle increases in the length of the column with respect to its width seem to occur during growth of the test. This is related to the development of a more spherical test form in large adults and results from both the addition of new components and patterns of accretionary growth.

Careful examination of the reconstructed series reveals that skeletal accretion can be characterized by consistent patterns. Growth of interambulacrals always decreases at the adoral margin first. This is always followed by a decrease in growth along the adapical (aboral) margin. Growth along the interradial-adradial axis, however, does not decrease significantly until the interambulacral plate is positioned near the ambitus. Continued decreases in growth along this axis results in a pattern of converging zones towards the peristome.

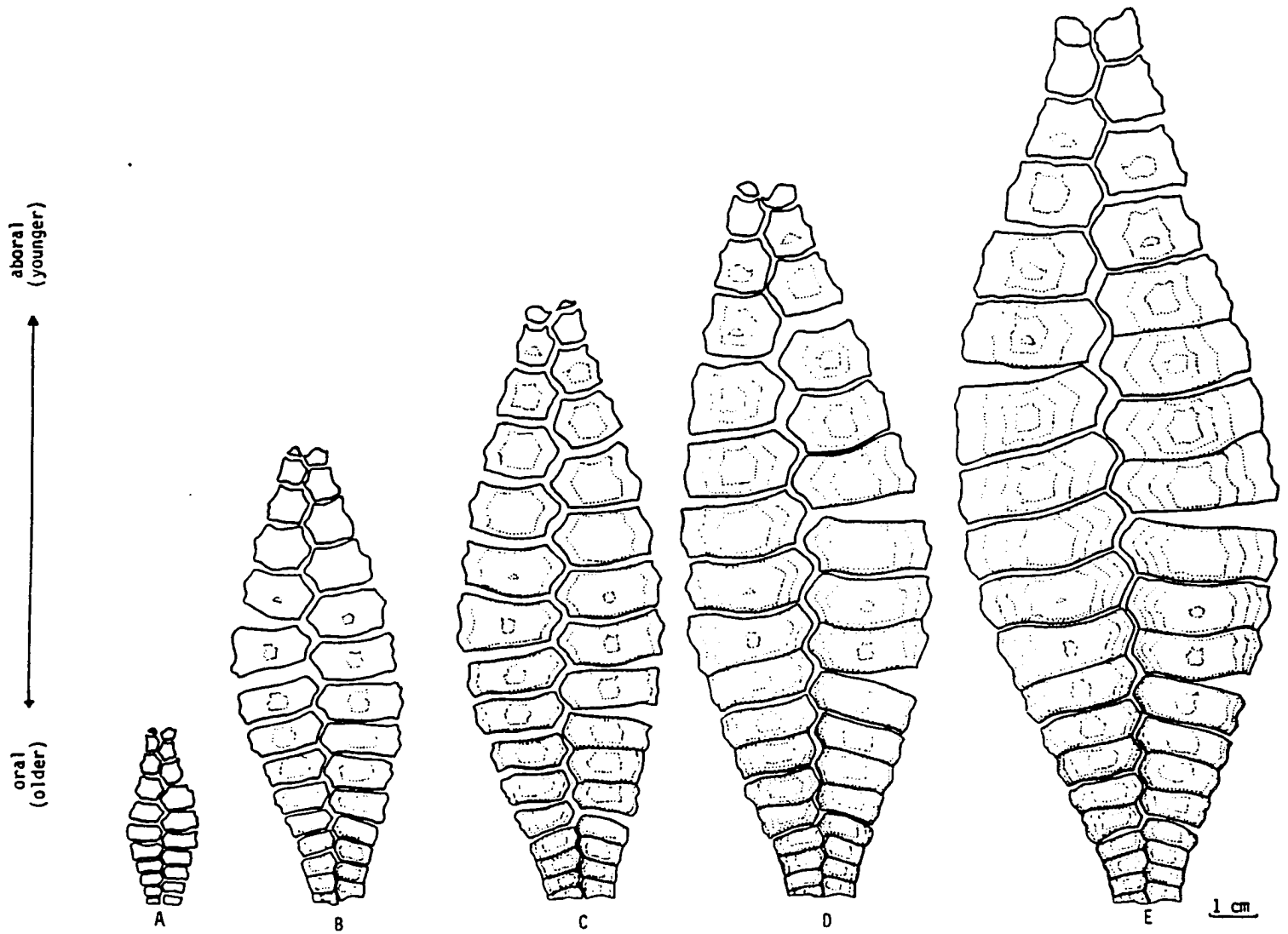

Figure 6. Reconstructed growth series of an interambulacrum: *S. franciscanus*, based on radiograph in Plate 6. "Time-equivalent" growth is shown here by color variation. "A" is shown in white and represents the oldest distinguishable growth; "E", shown in blue, is the youngest or most recent. See text for additional explanation.

This general pattern is similar to that observed in the sea urchin *Tripneustes* by Dafni and Erez (1982, p. 72-73). They suggest that directional components of skeletal accretion in interambulacral plates are closely related to the arrangement of internal tissues, a hypothesis that merits further study.

Morphometric analysis of synchronous zones provides quantitative data that can be used to examine skeletal accretion. Areal measurements taken with a calibrated planimeter are shown in Table B-3 of the appendix. Each column of Table B-3 refers to a set of synchronous zones throughout the interambulacrum, corresponding with the growth series in Figure 6. Measurements in Table B-3 indicate that the size of interambulacral components varies with their relative position in the series. Within each series, the largest interambulacrals always occur at, or slightly above, the ambitus. The smallest interambulacrals in each series are, of course, the circumoral plates.

Figure 7, plotted from data in Table B-3, provides some insight regarding the relationship between accretionary growth and addition of new interambulacrals. Initiation of new interambulacrals produces a "shift" in the position of the ambitus in the aboral direction (approximate position of the ambitus shown by letters "A" through "E" in Figure 7). Growth rates of interambulacrals below the ambitus, i.e., adoral plates, are substantially lower than those of plates above the ambitus in each growth series. It is for this reason that the growth curves appear to be skewed to the right in Figure 7.

Based on these observations, anisometric growth of the test is a

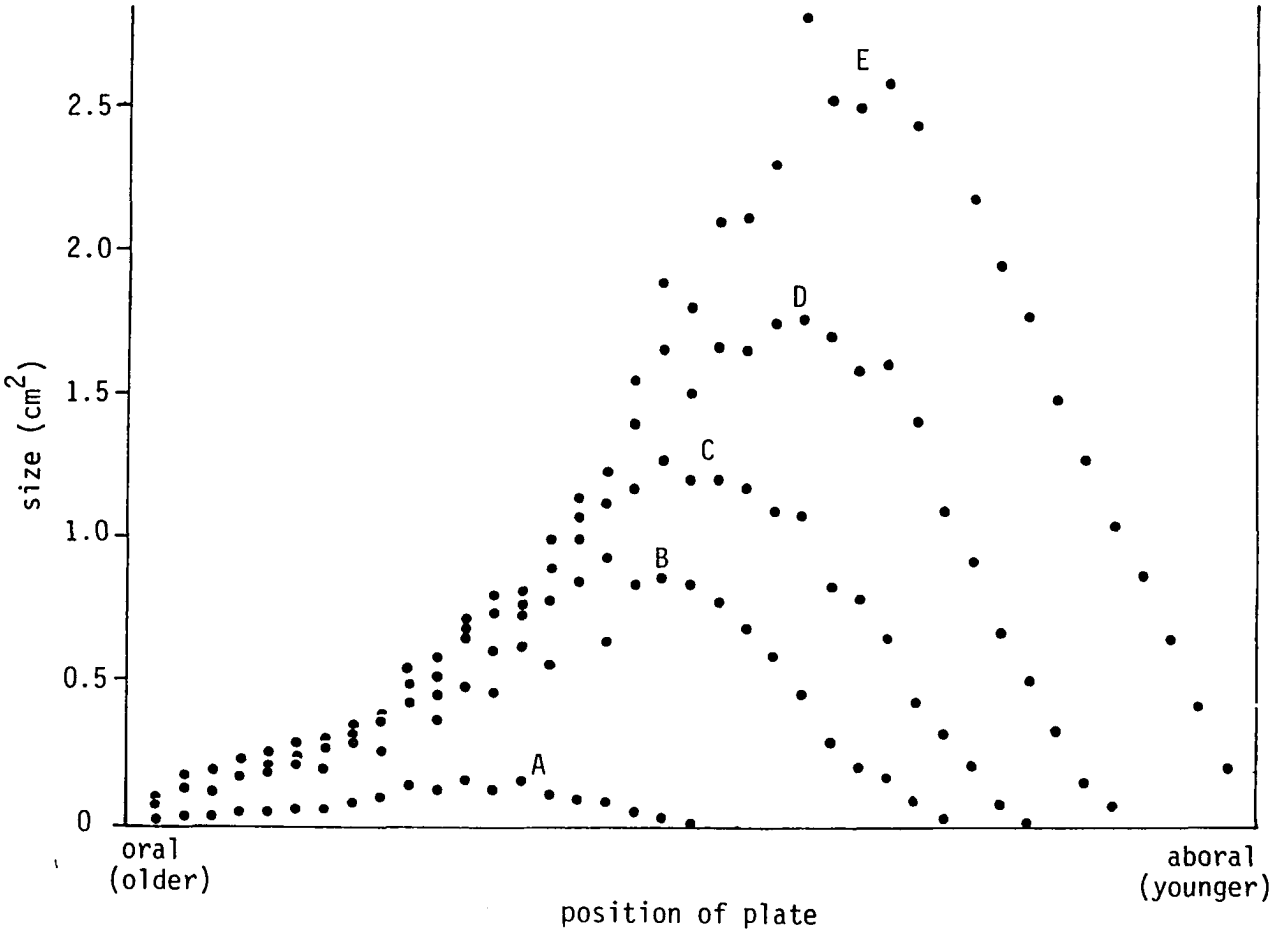

Figure 7. Growth of individual interambulacral plates relative to position of the plate, based on reconstructed growth series in Figure 7. Data shown in Table E-3 of the appendix.

product of both the addition of new coronal plates and their subsequent accretionary growth. In at least one respect, the addition of new plates causes accretionary growth in older plates. When new plates are added, older plates are "readjusted" in form and size to maintain the morphological integrity of the column and test (Markel, 1981, p. 51). This factor should be considered in developing models for growth of the corona and the interambulacrum.

CHEMICAL HETEROGENEITY WITHIN CORONAL PLATES

Previous studies show that the skeletal components of Recent echinoids often are chemically heterogeneous, i.e., elemental composition varies within some skeletal components (see p. 15 of this study). Calcium, for example, is not evenly distributed throughout the regenerating spines of *Arbacia* (Davies et al., 1972, p. 880). Why heterogeneity occurs within monocrystalline skeletal components is not altogether certain but it may be related to accretionary skeletal growth.

This study will describe chemical heterogeneity within the interambulacral plates of *Strongylocentrotus* and document the relationship between chemical heterogeneity and growth zones. Two methods will be used: cathodoluminescence and electron microprobe analysis (also termed "electron beam microanalysis"). Cathodoluminescence is sometimes used to demonstrate chemical heterogeneity in solids, especially minerals such as calcite, dolomite, quartz, feldspar and apatite (Smith and Stenstrom, 1965, p. 628-633). Cathodoluminescence has not been used to distinguish chemical heterogenity within biogenic material of echinodermal origin in earlier studies. Unlike cathodoluminescence, electron microprobe analysis has been applied in previous studies of chemical heterogeneity within echinoid skeletal components. Microprobe work can provide quantitative information regarding elemental composition and its distribution. Together, these two methods should adequately describe most of the chemical heterogeneity present in the skeletal material to be studied here. Cathodoluminescence will also be used to relate chemical heterogeneity to growth zonation.

Methods used in cathodoluminescence

General backround of cathodoluminescence

Ebers and Kopp (1979, p. 908) define cathodoluminescence as the emission of non-thermal radiation from electron beam excitation. Unlike the delayed luminescence observed in phosphorescence, cathodoluminescence occurs immediately upon excitation (Glover, 1977, p. 433). A detailed discussion of the principles and historical development of cathodoluminescence can be found in several sources, including Curie (1963, p. 288-298), Glover (1977, p. 3-51) and Heinrich (1981, p. 494-498).

Divalent manganese acts as a phosphor in carbonates, causing an orange-colored luminescence (Medlin, 1959, p. 452; Sippel and Glover, 1965, p. 1283). Such luminescence may be quenched, or extinguished, in the presence of cobalt, nickel or ferrous iron (Medlin, 1959, p. 456; Sippel and Glover, 1965, p. 1283). Ferrous iron in particular appears to be the major quenching species in calcite.

Luminescence can occur in calcite when manganese concentration is as low as 0.004 wt percent manganese, or 40 ppm manganese (Sommer, 1972, p. 279). Such concentrations are too low to be measured with the electron microprobe. A high concentration of iron (greater than 1.0 wt percent iron, or 10,000 ppm iron) or a low concentration of manganese or a combination of both can quench luminescence (Fairchild, 1983, p. 582). Until there is greater clarification of these thresholds, cathodoluminescence may be of limited use in geochemical studies. Despite this restraint, cathodoluminescence can provide insights regarding chemical heterogeneity in carbonate materials.

Cathodoluminescence in carbonates is often used as a petrographic

tool, to distinguish multiple generations of cements (e.g., Freeman, 1971; Meyers, 1974; Frank et al., 1982; Grover and Read, 1983). The technique may also be applicable in ore exploration (Ebers and Kopp, 1979, p. 918), as well as environmental analysis (Sommer, 1972, p. 278-280).

Smith and Stenstrom (1965, p. 633) suggest that cathodoluminescence might be helpful in paleontological studies. It may distinguish skeletal structures and detect unrecrystallized specimens for isotopic research. Most skeletal materials are not luminescent (Glover, 1977, p. 55). Exceptions include the weakly luminescent skeletal carbonates of oysters, sand dollars and some corals as well as the brightly luminescent exoskeletons of barnacles. In surveying biogenic carbonates, Sommer (1972, p. 281) finds that luminescence is useful in locating regenerative carbonate in mollusc shells. He also indicates that cathodoluminescence could reveal variations in manganese concentration of skeletal material, where present. Such spatial variation may be destroyed during diagenesis, suggesting that uniform luminescence is indicative of diagenetic carbonate (ibid., p. 282). Cathodoluminescence may also be useful in highlighting relict morphological features in ancient organisms such as fossil bryozoans (Ferrigno, 1973, p. II-10). It is surprising, then, that cathodoluminescence is not utilized more extensively in studies of Recent skeletal material.

Sample preparation methods

Skeletal material, particularly that of echinoids, poses some unique difficulties in cathodoluminescence observations. Organic material associated with the mineralogical portion of the skeleton usually obscures

luminescence. The porous nature of the echinoderm skeleton further magnifies this problem because organic material is often trapped within the fenestrate skeleton. Impure sodium hypochlorite, i.e., commercial bleach, which is commonly used to oxidize soft tissues in skeletal preparations presents additional difficulties. Sommer (1972, p. 280) notes that some skeletal material is lost during oxidation. Unknown contaminants that affect luminescence may also be present in the sodium hypochlorite.

Most of the skeletal material examined here originated from the interambulacrum of *Strongylocentrotus*. Generally, disarticulated interambulacral components were hand polished to remove surficial tubercles and ornamentation. Interambulacrals were then bleached (in many cases this was a second oxidation) to eliminate remnants of organic material. These components were rinsed in two ultrasonic baths of distilled water to remove remaining traces of the oxidizing agent. After air-drying, samples were ready for luminoscope observations. Prepared samples were handled with forceps to minimize contamination from manual contact.

A Nuclide Corporation luminoscope, Model 2b , was used for all luminescence observations in this study. The operating parameters used here are recorded in the appendix (Table C-1; recorded in a manner suggested by Marshall, 1978). In order to save time in pumping down the sample chamber, five to six samples were loaded simultaneously. Prolonged exposure of skeletal material to the electron beam can cause deterioration and thus should be avoided.

Microphotographs recorded several observations of cathodoluminescence in *Strongylocentrotus* . An experimental roll of film was also necessary to determine appropriate exposure times for the 400 ASA Ektacolor film used

in this study. Under the luminoscope conditions outlined in Table C-1, for the samples examined here, exposure times of 60 to 90 seconds were most effective. To some extent, correct exposure time is variable and some trial and error is necessary in determining the appropriate time.

Observations with cathodoluminescence

Preliminary observations of unpolished interambulacrals of *S. droebachiensis* show that these skeletal elements are indeed luminescent (see Plate 7A). Luminescence is not uniform and is generally absent at the tips of tubercles. This implies that tubercles are low in manganese and/or high in iron, relative to the adjacent skeletal material. Closer inspection reveals that the bases of some larger tubercles are zoned (shown with arrows, Plate 7A). This banded pattern of concentric zones, where present, suggests that chemical heterogeneity arises during accretionary growth of these tubercle bases.

Cursory examination of the underlying, "unornamented" surface of interambulacrals also revealed faint traces of a banded pattern. This pattern suggested that zonation was not restricted to tubercle bases and that outer skeletal layers obscure an internal zonation.

A microphotograph of a polished interambulacral of *S. droebachiensis* shows that this is indeed the case (Plate 7B). A distinct banded pattern of alternating luminescent and non-luminescent zones occurs below tubercles and surficial skeletal layers. Like zoned tubercle bases, zoning here also indicates a chemical heterogeneity of manganese and/or iron concentrations. Clearly such heterogeneity is caused by elemental variation in the calcifying environment (i.e., the site of calcification in

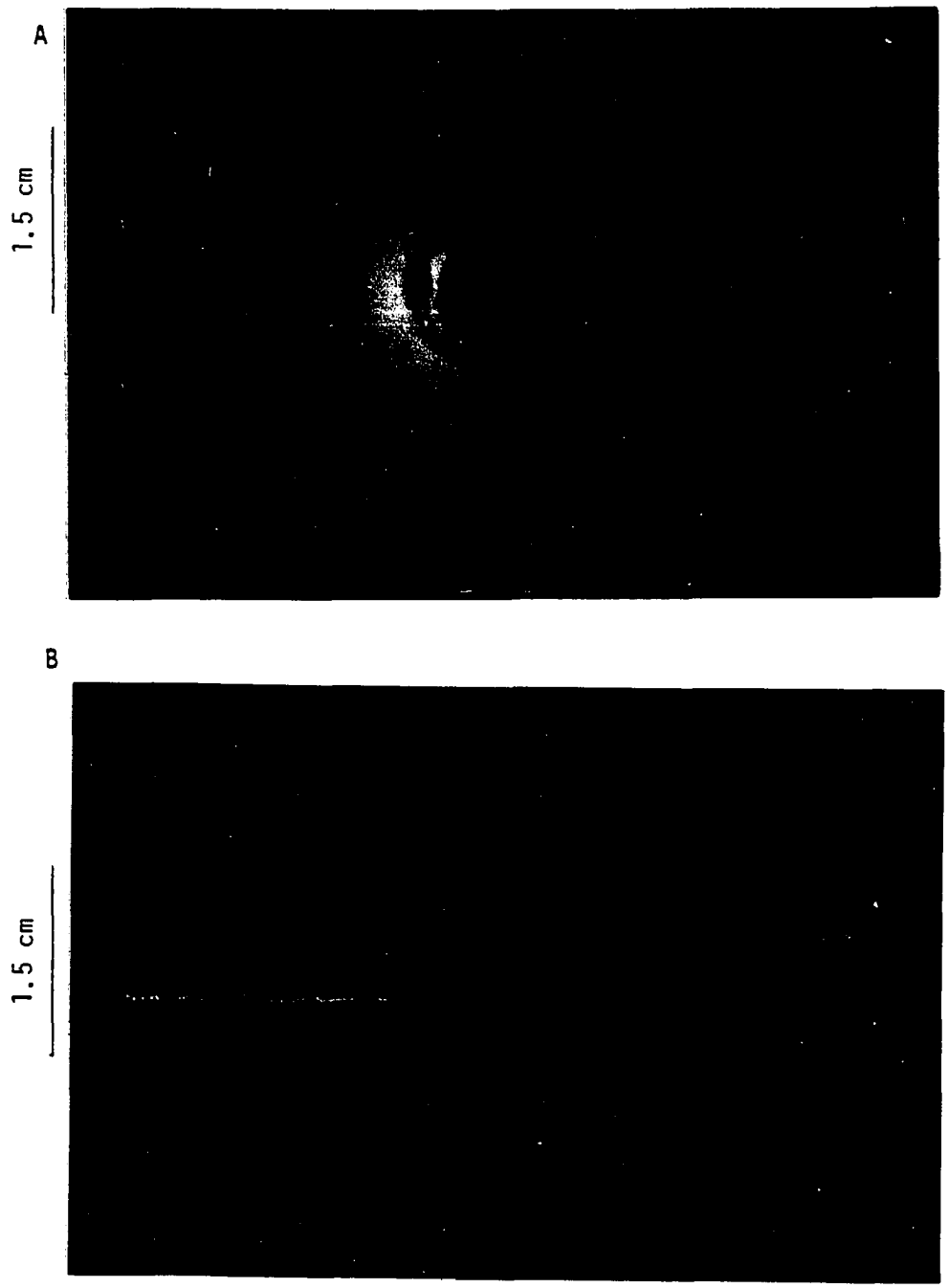

Plate 7. Luminoscope photomicrographs of (A) an unpolished interambulacral of *S. droebachiensis* (scale bar equals 1.5 mm); and (B) polished interambulacral of *S. droebachiensis* (scale bar equals 1.5 mm). Note luminescent bands in middle skeletal layers of interambulacral (Plate 7B).

the organism which can be influenced by intrinsic, physiological factors or extrinsic, ecological factors) during skeletal accretion. There is minor variation in luminescence intensity of different luminescent zones, perhaps reflecting small differences in manganese concentration. Boundaries between luminescent and non-luminescent zones are distinct but not sharp. This may result, in part, from the coarse (600 mesh) paper used in polishing the surface.

Overall zoning observed within interambulacrals bears a striking resemblance to radiographic patterns shown by Pearse and Pearse (1975). A composite photograph combining a radiograph with a luminoscope photomicrograph of an individual interambulacral shows the relationship between growth zones and chemical zonation (Plate 8). Luminescent zones (orange) are generally correlated with x-ray opaque (dark) zones; non-luminescent zones are correlated with x-ray translucent (light) growth zones. Some broad non-luminescent bands correspond to several narrow growth zones. Perhaps chemical zonation is seasonal in periodicity whereas zonation revealed by radiography is more variable in periodicity.

Correlation of non-luminescent zones with x-ray translucent zones formed during the summer/spring season can be supported by another line of reasoning. Because this organism was collected during the summer, the most recently formed chemical zone at the plate periphery should be typical of summer growth. In this interambulacral, the most recently formed zone is non-luminescent. It appears then that non-luminescent zones do form during the spring/summer and luminescent zones develop during the fall/winter. Note the characteristic features associated with seasonal growth zones recorded in Table 2 of this study (p. 10).

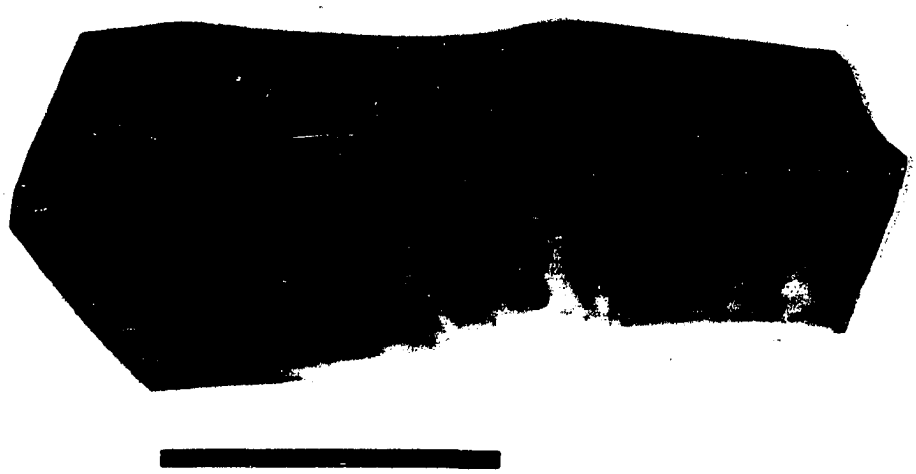

Plate 8. Composite photograph combining a radiograph and luminoscope photomicrograph of a sin le interambulacral of *S. droebachiensis* (scale bar equals 2.5 mm).

A mosaic of luminoscope photomicrographs of skeletal components from the same interambulacrum gives additional insights to chemical zonation (see oversize insert). Most interambulacrals have a non-luminescent core. This implies that new interambulacrals normally originate during spring/summer months and that the addition of new interambulacrals is perhaps related to patterns of reproduction and metamorphosis. Whether this is actually the case should be investigated with living echinoids.

Synchroneity of zones from different interambulacrals can be observed in adjacent components. Synchronous zones become progressively narrow in older (adoral) interambulacrals, often disappearing altogether in oldest plates. The most recent non-luminescent zone separating the youngest (aboral) interambulacrals, for example, cannot be seen in the oldest circumoral plates. This results presumably from the decrease in growth rate as interambulacrals are shifted toward the oral end of the column.

Few zones can be distinguished in the oldest interambulacrals which originate during the larval stage. This, together with decreasing growth rate and resorption, may account for the mottled luminescence present in these interambulacrals.

It is unknown whether chemical zonation occurs in each species of *Strongylocentrotus*. Personal observations (not photographically recorded) indicated that interambulacrals derived from other echinoid genera, e.g., *Lytechinus*, are also chemically zoned. This is not the case in all echinoids, however. Interambulacrals of *Dendraster* (sand dollar), for example, are uniformly luminescent. A more thorough survey of luminescence features in echinoids and other echinoderms would provide considerable insight regarding the origin of luminescence in skeletal materials.

Methods used in electron microprobe analysis

Calcium and magnesium, critical components of echinoid calcites, should be considered in examining chemical heterogeneity of interambulacral plates. In many echinoid genera, calcium and magnesium are distributed in a heterogeneous manner within interambulacrals (Fowler, 1972, p. 81-100). Electron microprobe analysis is used in this study to determine how and if calcium and magnesium vary within interambulacrals of *Strongylocentrotus droebachiensis*.

Electron microprobe analysis developed as a technological outgrowth of both electron microscopy and x-ray spectrochemical analysis (Birks, 1971, p. 1). Microprobe analysis is a particularly effective means of demonstrating spatial variation in elemental composition of solids on a quantitative basis. Despite some limitations (see Heinrich, 1981, p. 444) the application of microprobe analysis has increased in geological and biological studies. Several sources discuss the instrumentation and physics involved in microprobe analysis (e.g., Birks, 1971; Reed, 1975; and Heinrich, 1981).

A few adjacent interambulacral plates from an individual *S. droebachiensis* were selected for electron microprobe analysis. When the organism was alive, these plates were located at the ambitus. Cursory examination of the interambulacrals did not reveal any resorption or dissolution.

Sample interambulacral plates were impregnated in Hilquist thin section epoxy and mounted on a round thin section. The coarse-ground, uncovered thin section was hand polished with a silicon carbide (600-1000

mesh) grit. Raybrite B (.05 μm) was the final polishing powder used in preparing the sample. After polishing was completed, orientation marks were drawn on the sample and the thin section was carbon-coated.

Analyses for calcium and magnesium were carried out at the Department of Geology and Geophysics, University of Chicago, with an ARL electron microprobe unit. The composition of standards used in electron microprobe work is presented in Table C-2 of the appendix. Ten-second count times were used for all data and standards.

Raw counts for each element for each point are shown in Tables C-3 through C-5 of the appendix. The Bence-Albee Routine for Carbonates was used to convert raw data to mole percent values, also shown in Tables C-3 through C-5.

Observations with electron microprobe analysis

Data from electron microprobe analyses of interambulacrals are best understood when presented in graphic form. Figure 8 represents a traverse of 130 points along the long axis of a polished interambulacral, from the interradial (X) to the adradial (X') margin of the plate. Diagramatic inset on Figure 8 shows orientation and direction of the traverse. The traverse covers the middle skeletal layer of the plate. Data points, shown with circles, are converted from counts at 100 μm intervals across the entire plate. See Table C-3 in the appendix for a complete set of data from this traverse.

Overall, $MgCO_3$ concentration falls between 4.9 and 8.2 mole percent within the interambulacral. $CaCO_3$ ranges from 91.8 to 95.1 mole percent.

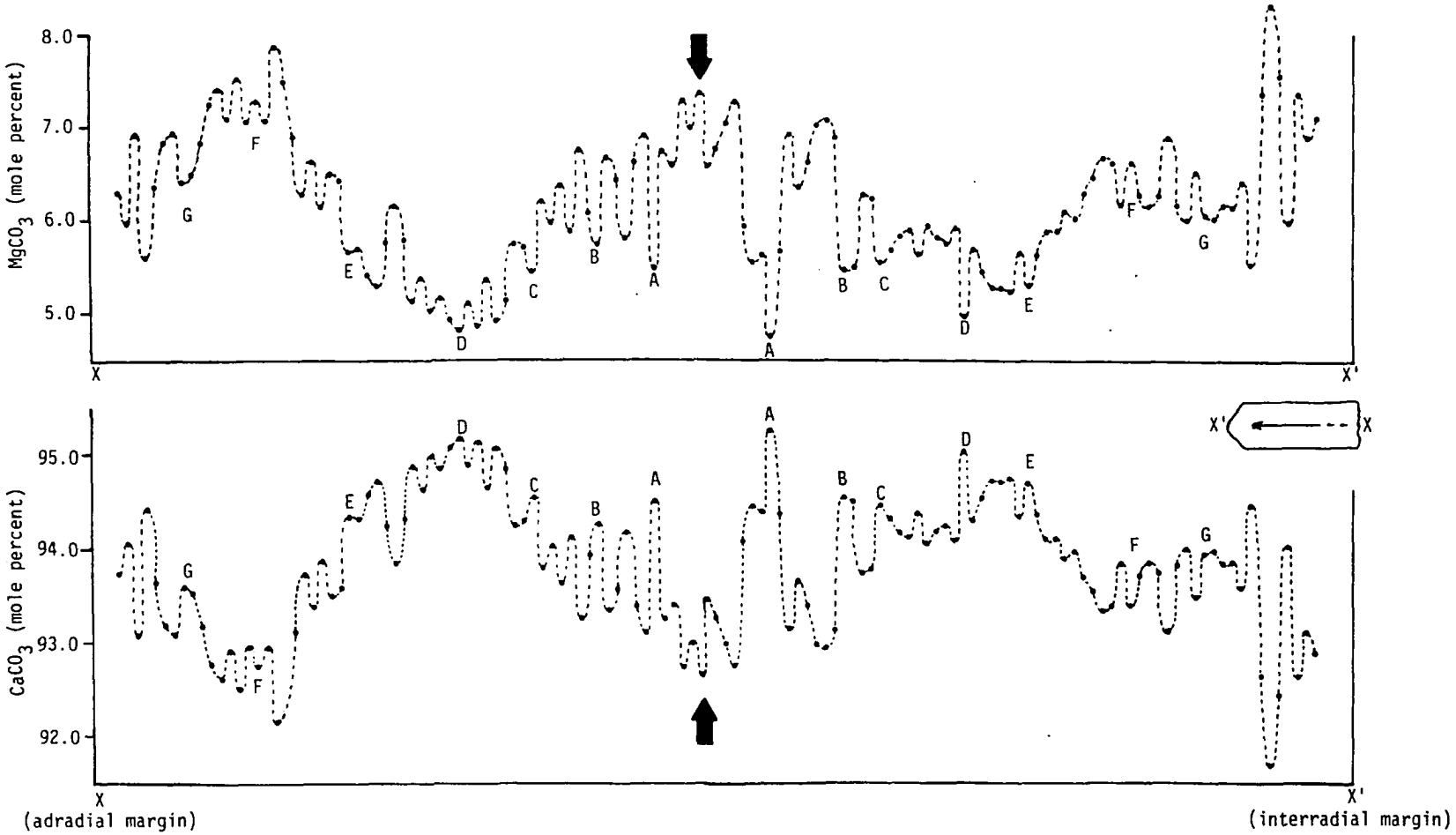

Figure 8. $CaCO_3$ and $MgCO_3$ variation (mole percent) along adradial-interradial axis of an ambital interambulacral of *S. droebachiensis*. Traverse covers middle skeletal layer of interambulacral and passes near center of plate. Dark arrows indicate center of traverse and of plate. Diagram inset shows orientation and direction of traverse. Data shown in Table C-3 of appendix.

Adjacent points may differ considerably in elemental composition, in some cases by as much as two mole percent. $CaCO_3$ and $MgCO_3$ levels oscillate throughout the interambulacral, making it difficult to distinguish trends in elemental composition on a larger scale.

Closer scrutiny reveals a mirror pattern in alternating $CaCO_3$ and $MgCO_3$ concentrations. The pattern is reflected on either side of the central portion of the traverse, underlying the primary tubercle (indicated with arrows in Figure 8). Some corresponding points on each side are labelled with identical letters to show symmetry more clearly. $CaCO_3$ and $MgCO_3$ levels vary cyclically, indicating that deposition of calcium and magnesium in skeletal material fluctuates periodically. Major shifts in $CaCO_3$ and $MgCO_3$, i.e., changes involving 0.5 or more mole percent, segregate high calcium, low magnesium phases from low calcium, high magnesium phases. Note compositional changes at "B" and "E".

An analogous traverse along the inner surface of an adjacent interambulacral shows a similar, but slightly asymmetric compositional variation. See Figure C-6 in the appendix. A traverse across the entire interambulacral was not possible in this case, which may account for the observed asymmetry.

Results of a traverse along the adapical-adoral axis provides some interesting observations (Figure 9). The traverse is perpendicular to the interradial-adradial axis, passing very close to the center of the interambulacral. See diagramatic inset on Figure 9. $CaCO_3$ and $MgCO_3$ levels are comparable to those observed in the longitudinal traverse of the same plate (compare with Figure 9). $CaCO_3$ and $MgCO_3$ vary more in the adoral portion than in the adapical portion of the traverse, perhaps in

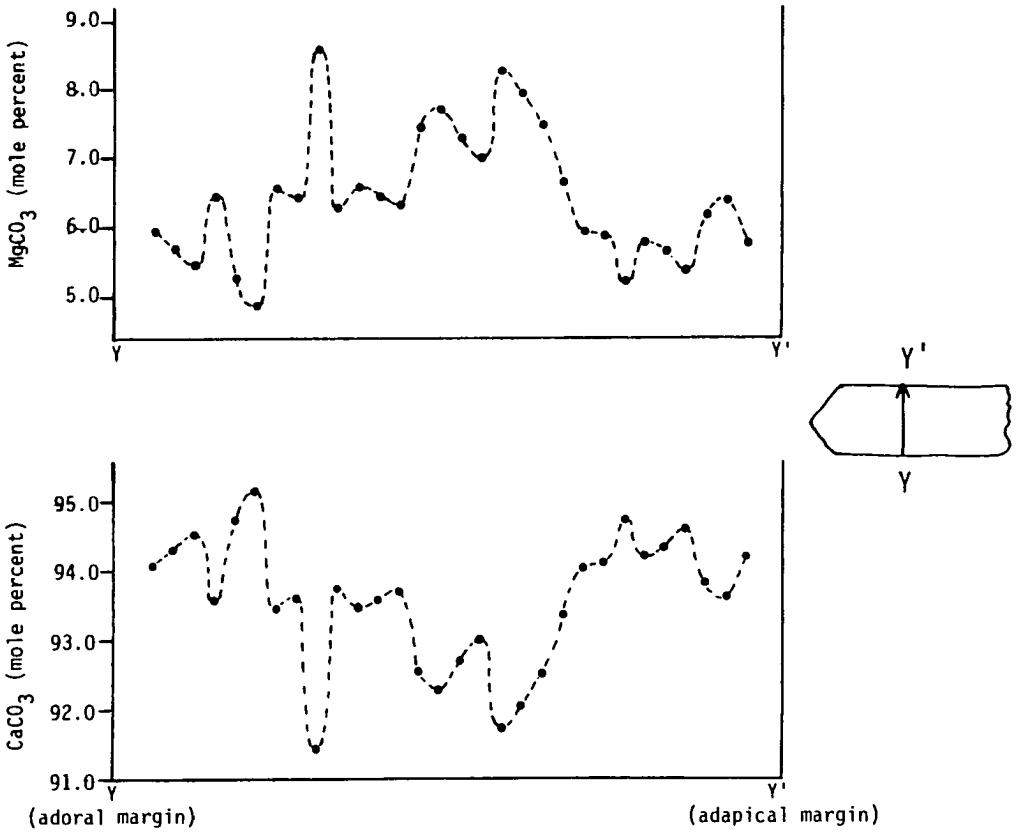

Figure 9. $CaCO_3$ and $MgCO_3$ variation (mole percent) along adoral-adapical axis of an ambital interambulacral of *S. droebachiensis*. Traverse covers middle skeletal layer and passes near center of plate. Diagram inset shows orientation and direction of traverse; dark arrows show approximate center of traverse and plate. Data shown in Table C-4 of appendix.

scent zones. Salinity also influences uptake and incorporation of manganese (Rucker and Valentine, 1961, p. 1099; Pilkey and Harriss, 1966, p. 384; Bryan and Hummerstone, 1973b, p. 871). Seasonal variation in salinity may therefore contribute to zonation of manganese. It is especially interesting to note that the organism's position in the tidal column influences the uptake and incorporation of manganese (Blanchard and Chasteen, 1967, p. 1366; Bryan and Hummerstone, 1973a, p. 710-711). Generally, organisms growing above mean low water level contain more divalent manganese than those growing below this level. This appears to be related to substantial variations of salinity in this portion of the water column (Pilkey and Harriss, 1966, p. 383).

Biological factors, moreover, moderate the effects of environmental factors on the incorporation of manganese and iron in biogenic calcites. In many echinoid genera, including *Strongylocentrotus*, for example, the amount of iron and manganese within the skeleton reflects iron and manganese levels present in their diet (Stevenson and Ufret, 1966, p. 16; Bohn, 1979, p. 325). The inverse relationship between skeletal manganese and salinity is probably regulated by the process of osmoregulation in many organisms (Bryan, 1973, p. 159; Bryan and Hummerstone, 1973b, p. 871). Trace elements composition and zonation is moderated by a number of interacting factors. Additional research is needed to understand the origin of luminescence in echinoids.

Variation of magnesium within interambulacral components is largely attributed to seasonal changes in water temperature (Fowler, 1972, p. 210). This is consistent with the widely accepted observation that the

correspondence with some variation in skeletal accretion.

Both traverses show results similar to those observed in *Echinometra lucunter* (Fowler, 1972, p. 85, 92). Fowler suggested that higher concentrations of $MgCO_3$ within the interambulacral are correlated with x-ray translucent growth zones (ibid., p. 86, 210). Conversely, lower levels of $MgCO_3$ are correlated with x-ray opaque growth zones. It is difficult to document the relationship between growth zones and $MgCO_3$ composition directly, because growth zones are not readily apparent in thin sections of echinoid skeletal material. Some correlationship between growth zones and $MgCO_3$ composition within the interambulacral probably does exist and should be documented in future studies.

Chemical heterogeneity within interambulacral components

Formation of manganese-rich, iron-poor (luminescent) zones during fall/winter skeletal growth of *Strongylocentrotus* indicates that incorporation of manganese is inversely correlated with water temperature. This is consistent with observations that the proportion of manganese in skeletal calcite generally increases as water temperature decreases in echinoids (Harriss and Pilkey, 1966, p. 237) and other marine organisms (Pilkey and Goodell, 1963, p. 147).

Other environmental factors should be considered in understanding the heterogeneity of trace elements within skeletal components. Seasonal increases of manganese present in sea water (Bertine and Goldberg, 1972, p. 881; Hunt, 1983, p. 920-921), for example, may produce lumine-

overall proportion of magnesium within the test is positively correlated with water temperature (e.g., Chave, 1954, p. 272; Dodd, 1967, p. 1322). Experimental studies of calcification in echinoids, however, indicates that the amount of skeletal magnesium is actually related to temperature-induced changes in calcification and growth rates (Davies et al., 1972, p. 881; Weber, 1973, p. 553).

Incorporation of minor and trace elements in interambulacral components results from an interaction of both environmental and biological factors (Weber, 1973, p. 554-555). That is, skeletal chemistry is controlled by so many variables that it is difficult, at best, to distinguish a cause-and-effect relationship (Harriss, 1964, p. 29).

CHEMICAL VARIATION BETWEEN CORONAL PLATES

Studies of growth-related variation in skeletal chemistry are infrequent (Rosenberg, 1980, p. 134). In the case of marine organisms, such studies often relate skeletal chemistry to ecological and environmental factors (e.g., Lerman, 1965; Dodd, 1967). Others concern the relationship between skeletal chemistry and taxonomic differences (e.g., Harriss and Almy, 1964; Riley and Segar, 1970). A few studies investigate how skeletal composition is influenced by both taxonomic and environmental factors (e.g., Chave, 1954). In the case of echinoderms, most studies of skeletal chemistry examine the relationship between skeletal magnesium and environmental factors such as temperature (see Pilkey and Hower, 1960; Davies et al., 1972).

Analysis of the skeletal chemistry of *Strongylocentrotus* can therefore largely increase general understanding of the echinoid skeleton. Analyses of individual plates from entire interambulacra are particularly useful in investigating the importance of ontogeny in skeletal chemistry. Coupled with some knowledge of chemical heterogeneity within interambulacrals, it may be possible to learn how skeletal chemistry and growth are interrelated. By analyzing skeletal material from cogeneric species, it is also possible to determine if chemical variation occurs at lower taxonomic levels.

Several methods can provide quantitative chemical analyses: atomic emission spectrography, x-ray diffraction and x-ray fluorescence. In this study, however, atomic absorption spectroscopy is used for analytical work because it is an efficient means of determining a variety of elements in a large number of samples. Its widespread use in investigating skeletal

chemistry demonstrates that atomic absorption is an accurate method for such studies (see Harriss, 1965). An important distinction between atomic absorption spectroscopy and methods such as electron microprobe analysis is that atomic absorption is a wet chemistry procedure. Samples and standards must be converted to liquid form for analysis. Several references review atomic absorption in detail and provide a comprehensive discussion of the underlying principles and instrumentation (e.g., Angino and Billings, 1967; Slavin, 1968; Reeves and Brooks, 1978).

Sample preparation and methods used for atomic absorption

Disarticulated ambulacral and interambulacral plates were cleaned in commercial sodium hypochlorite and thoroughly rinsed in an ultrasonic bath of deionized, distilled water. After oven-drying at 100°C for approximately 24 hours, coronal plates were weighed. Plates were weighed promptly upon removal from the oven because skeletal material would begin to adsorb atmospheric moisture as it cooled. This phenomenom was probably related to the porous nature of the echinoderm skeleton and was more pronounced in more porous material, i.e., ambulacral components. Ideally, skeletal components should be kept warm during weighing to minimize moisture adsorbance which produces inaccurate weight measurements. Skeletal components were reweighed after a second rinsing and drying and the average of both readings was recorded for subsequent calculations.

Each component was dissolved in a minimal volume (a few drops) of concentrated (37.6% acid/volume), reagent-grade hydrochloric acid. After dissolution in a 25 ml volumetric flask, the sample solution was brought to volume with deionized, distilled water (except where otherwise noted).

A small amount of acid-insoluble organic material (collagen fibers?) often remained in the solution. Dilution of these "original sample" solutions was necessary for calcium and magnesium analyses (as well as strontium in some cases). Sample preparation methods discussed here were similar to those suggested by other workers (e.g., Dodd, 1965, p. 385; Bischoff et al., 1983, p. 1184).

Dilution of concentrated stock solutions (usually 1000 µg element/ml solution) provided standards for atomic absorption readings. Stock solutions were prepared by dissolving pure metals or their carbonate salts in a minimal volume of concentrated (37.6% acid/volume), reagent-grade hydrochloric acid. The amount of material dissolved was sufficient to produce one liter of stock solution at the concentration noted above. When dissolution was complete, solutions were brought to a one liter volume with deionized, distilled water and stored in polyethylene jugs. Deionized, distilled water spiked with hydrochloric acid served as a blank solution for analysis.

A Perkin-Elmer Model 403 atomic absorption spectrophotometer was used to measure absorbance. Analyses for calcium, magnesium, strontium, iron, and manganese all required a mixed air-acetylene flame. Maximum sensitivity was achieved by following the general procedures recommended in the Perkin-Elmer manual. All raw data (readings for blanks, standards, and samples) were recorded initially in atomic absorbance units. Each sample was analyzed in replicate.

Each replicate reading was converted to concentrations (µg element/ml solution) by extrapolation from calibration curves (some of the curves used in this study are shown in Figures D-1 through D-5 in the appendix).

Calibration curves were drawn by plotting the absorbance reading (atomic absorbance units) for each standard dilution with the known concentration (μg element/ml) of the dilution. The slopes of calibration curves also gave some indication of the sensitivity of the spectrophotometer for a set of analyses. Sensitivity for calcium (Figure D-1), for example, was about 25 atomic absorbance units per μg Ca/ml solution over most of the range examined. Sensitivity for magnesium (Figure D-2), on the other hand, was approximately 35 atomic absorbance units for one-tenth (0.1) μg Mg/ml solution. Most, but not all, of the calibration curves used in this study are shown in appendix figures.

Concentrations read off the calibration curves were easily converted to more useful weight percents with a calculator. The equation below, modified from the Perkin-Elmer manual, was used for all conversions:

$$\text{element (wt \%)} = \frac{(\mu g/ml)(\text{dilution factor})(0.0025\ dkl)}{\text{gm sample}}$$

, where

μg/ml is concentration read from a calibration curve;

dilution factor is a correction component incorporating dilution from an original sample solution primarily in analyses for Ca and Mg;

0.0025 dkl is volume of the original sample solution and varies if the original sample solution was not 25 ml;

gm sample is sample weight.

Duplicate weight percent were calculated from the replicate analyses and were recorded in data tables. Mole fractions and mole percents were computed from an average of the duplicate weight percents and were also recorded in the data tables.

Results of chemical analyses

All data from atomic absorption analyses are recorded in Tables D-6 through D-10 of the appendix. The tables include a complete set of raw readings, concentrations and weight percent from replicate analyses for each element analyzed. Mean weight percents, mole fractions and mole percents for each element are also shown. All figures for a single coronal plate are organized in a single row, with replicate data segregated into couplets within the row. Residuals (not shown in order to conserve space) can be determined by calculating the absolute difference of weight percents.

Compositional differences between ambulacrals and interambulacrals

Examination of the data for a series of ambital plates, both ambulacrals and interambulacrals, provides insights regarding chemical variation and accuracy of analytical methods. A specimen of *Strongylocentrotus droebachiensis* is used in this portion of the study because of its availability. Data from this set of analyses (Table D-6 of the appendix) reveals two major observations. Analyses of ambulacral plates are less accurate than similar analyses of their interambulacral counterparts. Equally important, ambulacral and interambulacral components can be distinguished on the basis of compositional variation.

These observations are more apparent in graphic form. Graphs of replicate weight percents (Figure 9A), for example, show greater disparity in the weight percent values of ambulacrals than in the values for interambulacrals. Residual analyses also indicate greater error in analysis of ambulacral components compared to analysis of interambulacral components (Figure 9B). This may be related to the very high porosity present

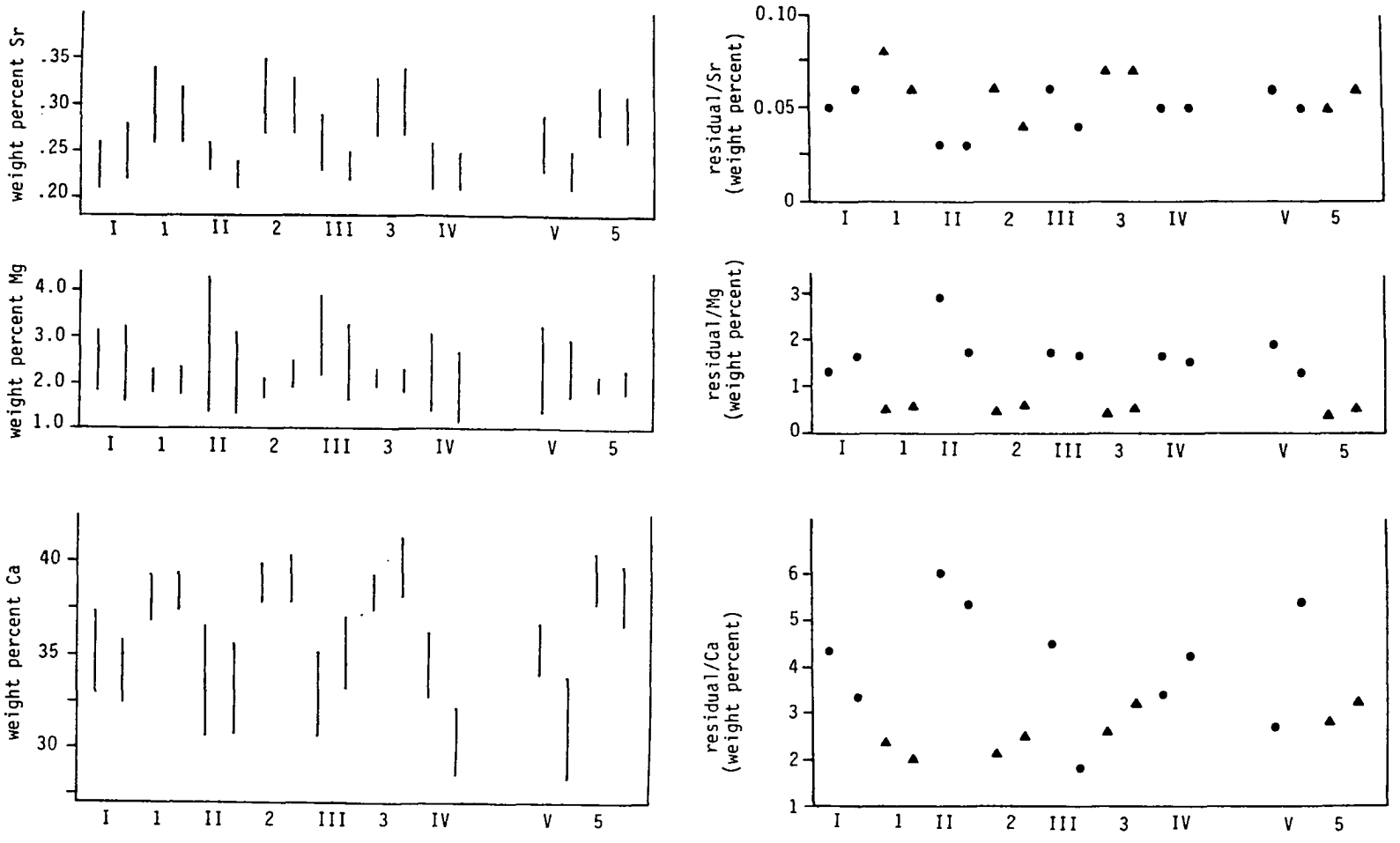

Figure 9. $CaCO_3$, $MgCO_3$ and $SrCO_3$ (weight percent) variation and corresponding residual analysis for ambital plates of *S. drocbachiensis*. Ambulacral plates: circles and Roman numerals; interambulacral plates: triangles and Arabic numerals. Data shown in Table D-6 of the appendix.

in ambulacral plates and a corresponding increase in contamination by the oxidizing agent.

Comparison of weight percent values reveals some major compositional differences between ambulacral and interambulacral components. Interambulacral plates typically have more calcium (an average 91.7 mole% Ca) and less magnesium (an average 8.0 mole% Mg) than ambulacral plates (with an average 89.1 mole% Ca, 10.6 mole% Mg). It is not altogether clear if the concentration of strontium is significantly higher in interambulacrals than ambulacrals. These distinctions can be visualized more readily if the data are presented graphically (Figure 10). Points are plotted according to the position of the corresponding skeletal component around the ambitus. The graphs therefore reflect the morphological arrangement of ambital plates. Higher calcium values are associated with lower magnesium values (conversely, lower calcium values are associated with higher magnesium values). This is not surprising because these two elements are the major cations that occur in the calcite of echinoderms. Strontium levels seem to vary with calcium in a subtle manner.

Another approach to determining if compositional distinctions occur is to compare compositional ranges of ambulacral and interambulacral components. Calcium, for example, ranges from 86.49 to 90.31 mole% in ambulacral plates, but ranges from 91.18 to 92.30 mole% in interambulacral plates. Magnesium extends from 9.37 to 13.21 mole% in ambulacrals and from 7.37 to 8.51 mole% in interambulacrals. There is no overlap in Ca and Mg levels of the two different plate types. When ranges of strontium are compared (0.27 to 0.32 mole% in ambulacrals; 0.31 to 0.36 mole% in interambulacrals), there is a slight degree of overlap.

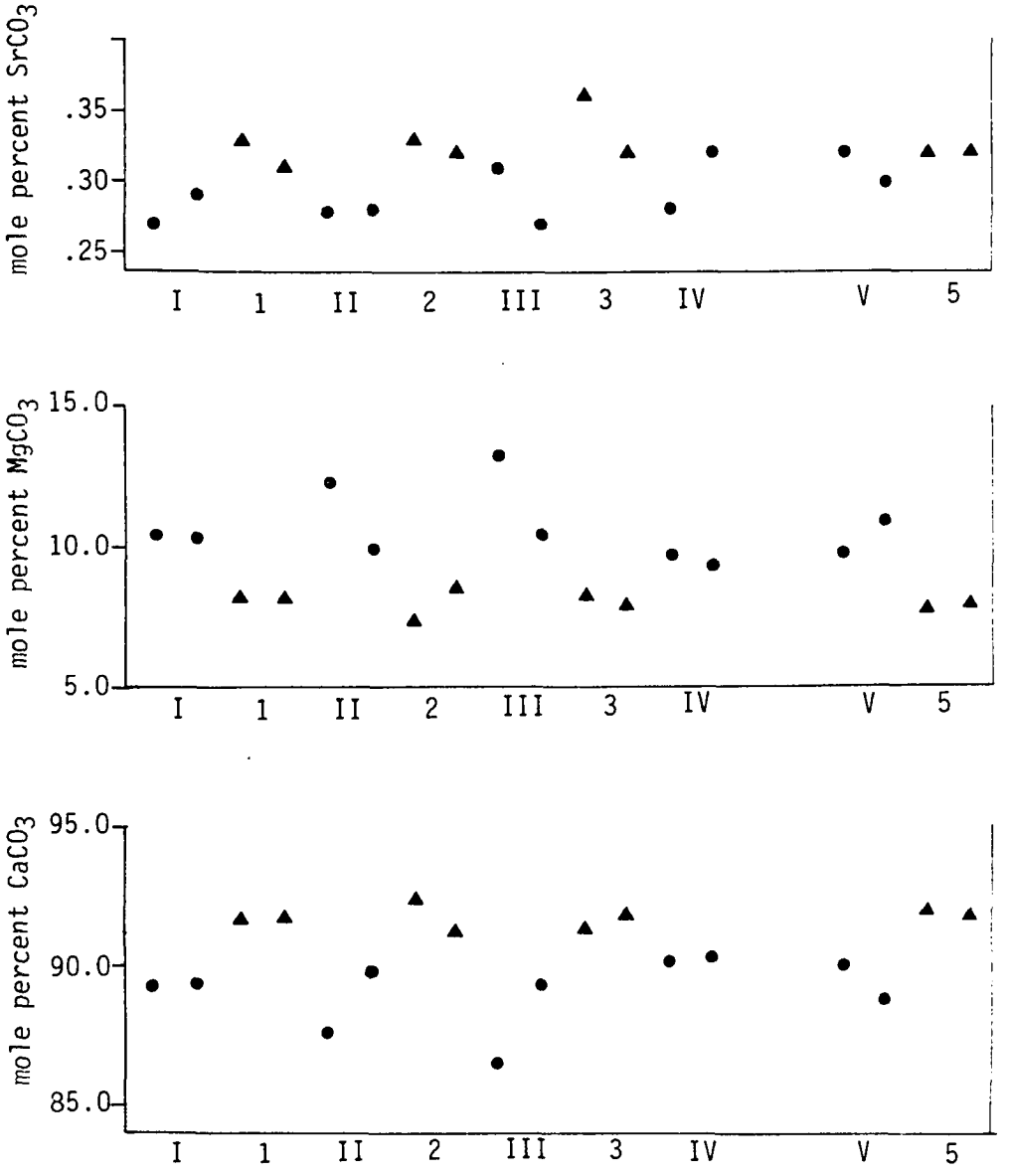

Figure 10. $CaCO_3$, $MgCO_3$ and $SrCO_3$ variation (mole percent) of ambital plates of *S. droebachiensis*. Ambulacral plates: circles and Roman numerals; interambulacral plates: triangles and Arabic numerals. Data shown in Table D-6 of the appendix.

Compositional variation within interambulacral series

Analyses of individual interambulacral plates of *S. franciscanus* (Table D-7 of the appendix) indicates some variation in skeletal composition may be growth-related. Replicate weight percents calculated for each interambulacral are plotted against the position of the plate for calcium, magnesium, strontium, iron and manganese. These are shown, together with corresponding residual analyses, in Figures D-11 through D-15 of the appendix. Residual analyses for calcium, magnesium and strontium indicate that analytical error occurs randomly. In the case of iron and manganese, error seemingly increases in the analysis of adoral (older) interambulacrals, but may not be significant. Note that residuals for calcium, magnesium and strontium here are lower than residuals from the analysis of ambital plates. Decreased solution decay and greater proficiency in analytical methods might explain this.

Graphs of replicate weight percents for magnesium and iron suggest that magnesium and iron increase in adoral (i.e., older) interambulacrals. No general trends are obvious in the analogous graphs for calcium, strontium and manganese. If, in fact, magnesium and iron increase adorally, there should be a corresponding decrease in at least one of the other components such as calcium.

Plotting the mole percent values for each element against the position (and hence, the relative age) of the corresponding interambulacral may clarify whether a change in chemical composition occurs throughout the interambulacral series. Data graphed in this manner more clearly reveal ontogenetic trends in chemical composition (see Figure 11). Calcium, for example, decreases slightly from 91.0 mole percent to 90.5 mole

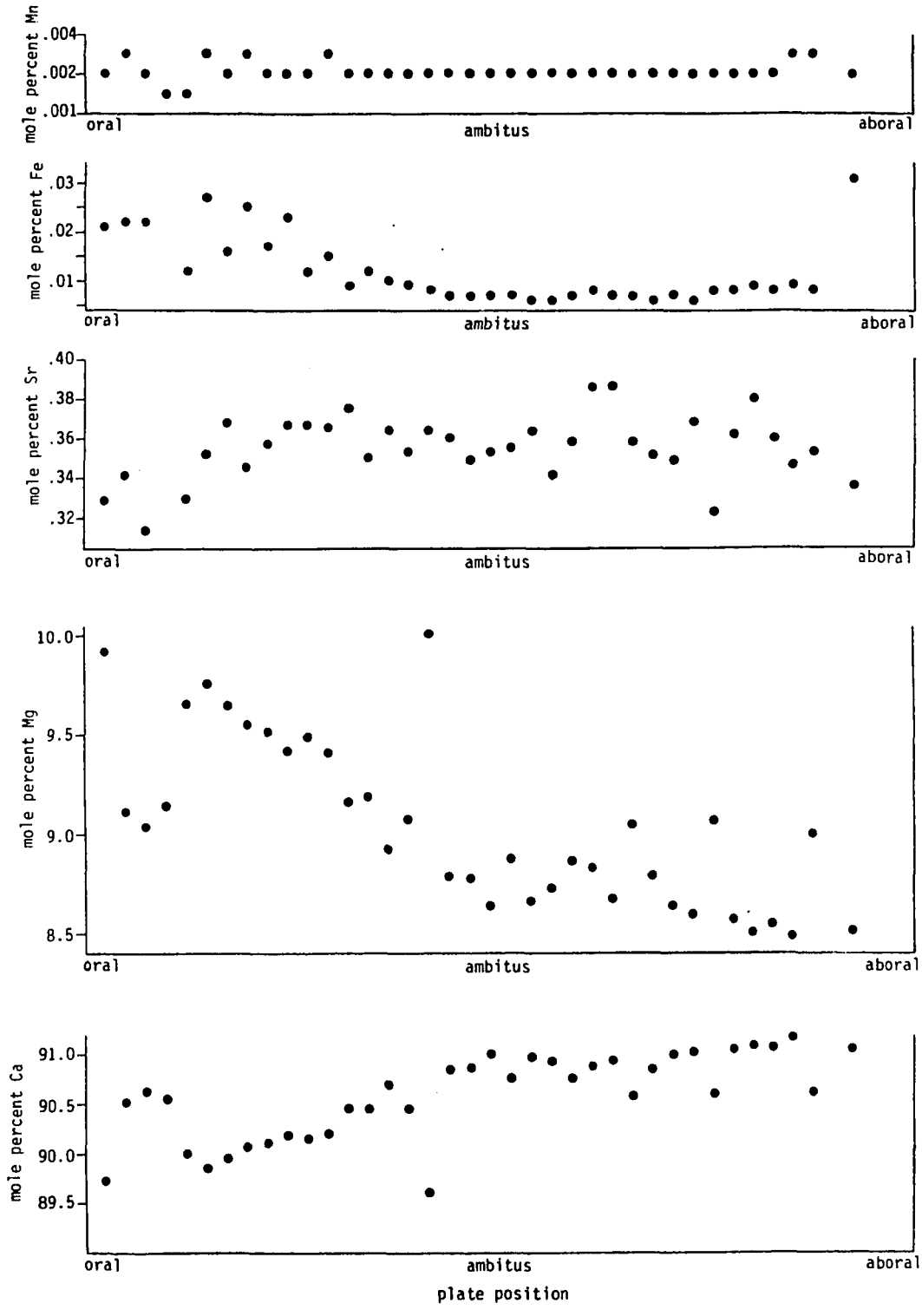

Figure 11. $CaCO_3$, $MgCO_3$, $SrCO_3$, $FeCO_3$ and $MnCO_3$ variation (mole percent) of an interambulacral series: *S. franciscanus*. Data shown in Table F-7 of the appendix.

percent in progressively older interambulacrals. Magnesium shows a corresponding increase in older plates, approximately from 8.5 to 9.0 mole percent. No consistent variation in strontium concentration (about 0.35 mole percent) is apparent. Like magnesium, iron also increases in successfully older interambulacrals, up to 0.02 mole percent. A somewhat aberrant (0.031 mole percent) amount of iron occurs in the youngest plate and cannot be explained. Trace levels of manganese (0.002 mole percent) are fairly constant throughout the interambulacrum. Trace amounts of barium can also be noted in the skeletal material but are not recorded here because of extreme difficulty in obtaining absorbance measurements for this element.

Similar analyses of the interambulacra of *S. droebachiensis* and *S. purpuratus* are also recorded (Tables D-8 through D-10; Figs. 12 and 13. This information provides additional documentation regarding variation in skeletal chemistry throughout the interambulacrum. It is also a means of detecting the presence of genetic variability in skeletal chemistry at lower taxonomic levels. Neither iron nor manganese could be determined, however, because small plate mass prohibited detection of trace elements. For the sake of simplicity, only mole percent values are included in subsequent discussion.

Overall, the average chemical composition of *S. droebachiensis* interambulacrals (90.68 mole percent calcium, 8.99 mole percent magnesium, 0.36 mole percent strontium) does not vary significantly from that of *S. franciscanus*. Trends revealed by plotting the mole percent value of each element against the position of the corresponding interambulacral are similar to those observed in *S. franciscanus* (compare Figures 11 and 12).

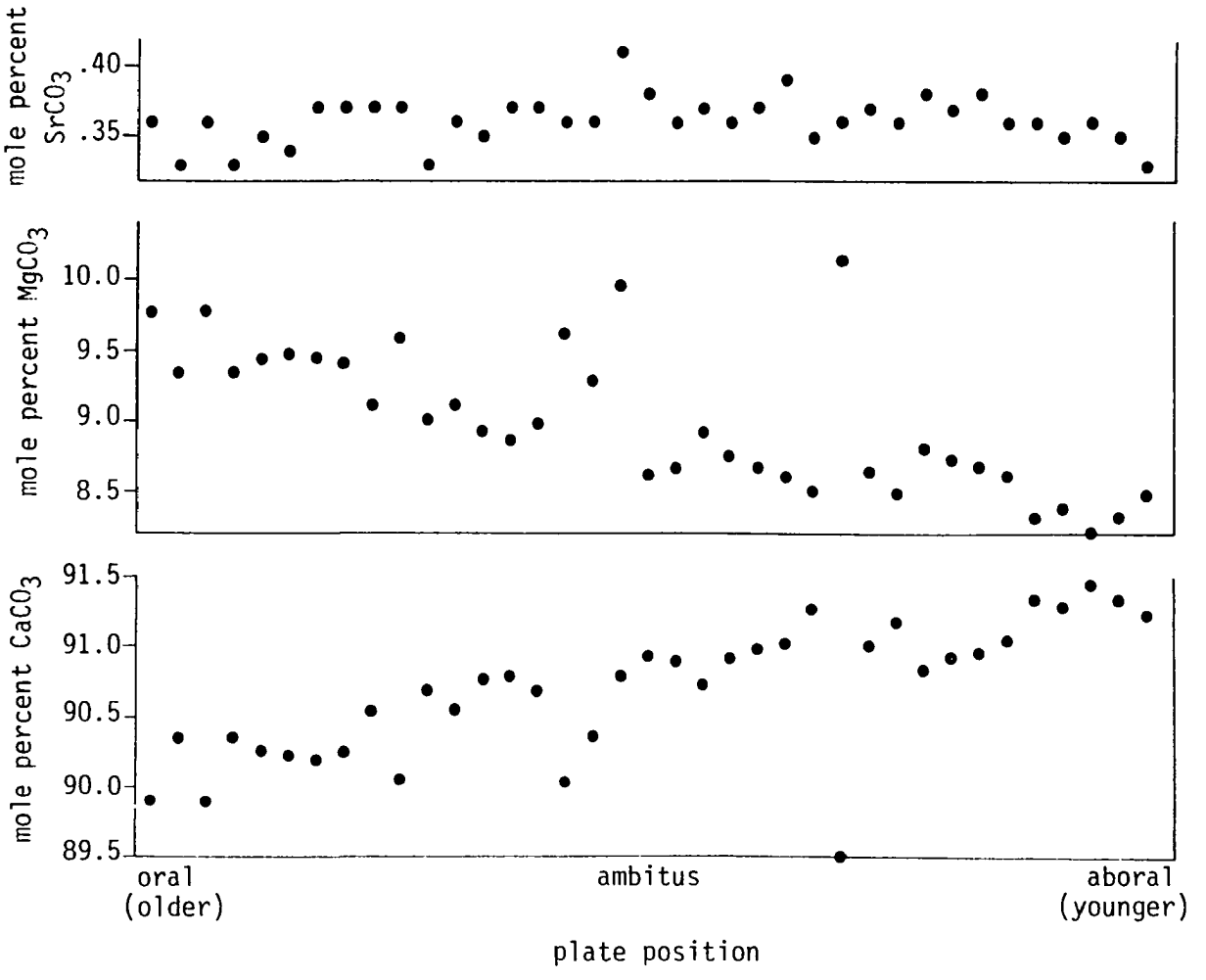

Figure 12. $CaCO_3$, $MgCO_3$ and $SrCO_3$ variation (mole percent) of an interambulacral series: *S. droebachiensis*. Data shown in Table D-8 of the appendix.

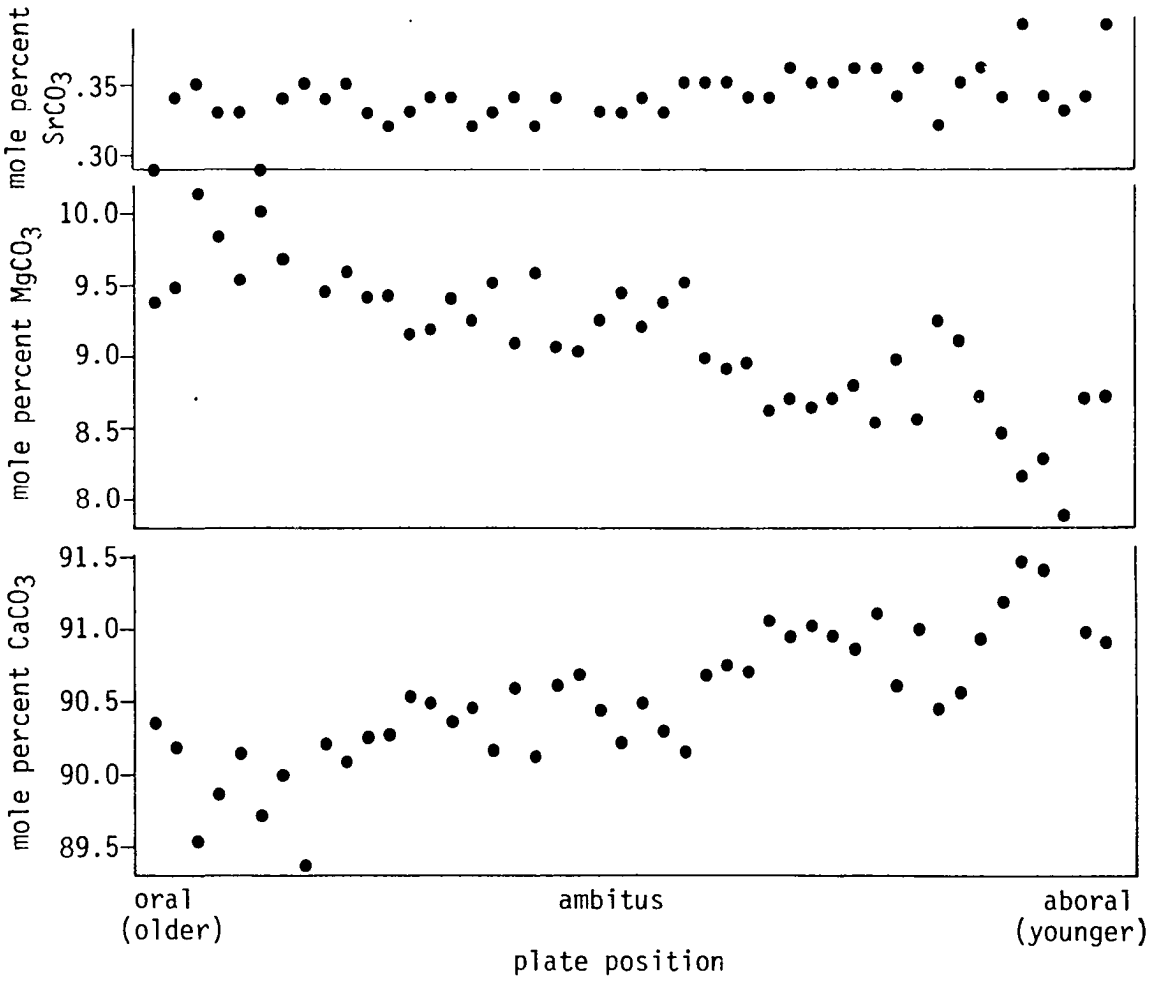

Figure 13. $CaCO_3$, $MgCO_3$ and $SrCO_3$ variation (mole percent) of an interambulacral series: *S. purpuratus*. Data shown in Table D-10 of the appendix.

Calcium decreases adorally (from around 91.3 to 90.0 mole percent) as magnesium increases (from about 8.3 to 9.8 mole percent). Strontium is relatively constant from plate to plate.

Analysis of *S. purpuratus* reveals that interambulacrals have a composition averaging 90.54 mole percent calcium, 9.12 mole percent magnesium, 0.34 mole percent strontium. This does not differ significantly from the composition of *S. franciscanus* and *S. droebachiensis*. More importantly, the same ontogenetic trends seen in other species of *Strongylocentrotus* are observed in *S. purpuratus* (Figure 13). Calcium ranges from approximately 91.4 mole percent in the youngest plates to 89.8 mole percent in oldest plates. Magnesium ranges from around 8.3 mole percent in aboral interambulacrals to 9.9 mole percent in adoral interambulacrals. Again, strontium shows no major variation.

Another approach to understanding the chemical composition is to examine the magnesium to calcium ratios and magnesium to strontium ratios of these interambulacrals. Magnesium to calcium ratios shown in Table D-16 of the appendix are computed in the following manner:

$$\frac{\text{mole \% Mg}}{\text{mole \% Ca}} \times 100 = \text{Mg:Ca ratio.}$$

Ratios are plotted against the position of the corresponding interambulacral (see Figure 14). As expected, this graph indicates that Mg:Ca ration increases adorally. Generally, the ratios of *S. purpuratus* (designated with circles) and those of *S. franciscanus* (shown with squares) are similar in magnitude. Mg:Ca ratios are lowest in *S. droebachiensis* (designated with triangles).

Magnesium to strontium ratios are computed in the following way:

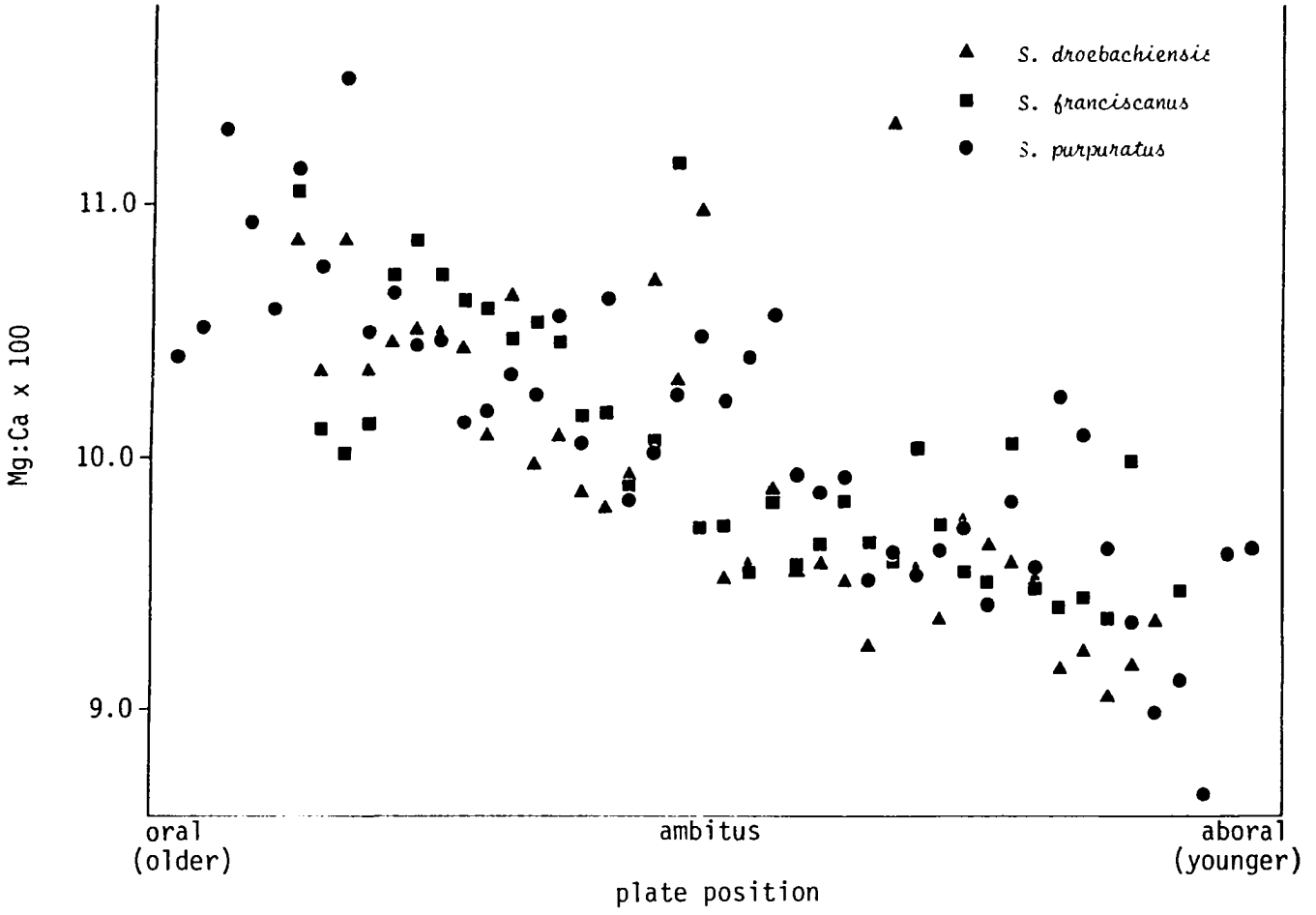

Figure 14. Mg:Ca ratios relative to position of the interambulacral in *Strongylocentrotus* species. Data shown in Table D-16 of the appendix.

$$\frac{\text{mole \% Mg}}{\text{mole \% Sr}} \times 0.1 = \text{Mg:Sr ratio.}$$

Resulting ratios are shown in Table D-17 of the appendix. A graph of Mg:Sr ratios plotted against the position of corresponding interambulacrals (Figure 15) shows that the ratios increase adorally. In most cases, Mg:Sr ratios are larger in *S. purpuratus* (shown with circles) than in *S. franciscanus* (indicated by squares). Mg:Sr ratios of *S. franciscanus*, in turn, are higher than those of *S. droebachiensis* (represented by triangles).

Variation in Mg:Ca and Mg:Sr ratios between different species appears to be minor and of little consequence. Graphic analysis of these ratios underscores the initial observation that magnesium levels increase in adoral (older) interambulacrals.

Variation of skeletal chemistry within the individual

Considerable variation in skeletal chemistry can occur within individuals of *Strongylocentrotus*. One source of variability lies in morphological differences, i.e., differences between ambulacral and interambulacral plates. Analysis of the ambital series in this study shows that magnesium is higher and strontium is lower in ambulacrals than in interambulacrals. This is consistent with similar observations by Fowler (1973) on the echinoids *Echinometra* (p. 119), *Tripneustes* (p. 120), *Lytechinus* (p. 121), *Arbacia* (p. 123) and *Eucidaris* (p. 126). Earlier studies of *S. franciscanus* (Terentieva, 1932, p. 50; Weber, 1969a, p. 544), however, show that magnesium is higher in interambulacrals than in ambulacrals. Additional investigation may resolve this

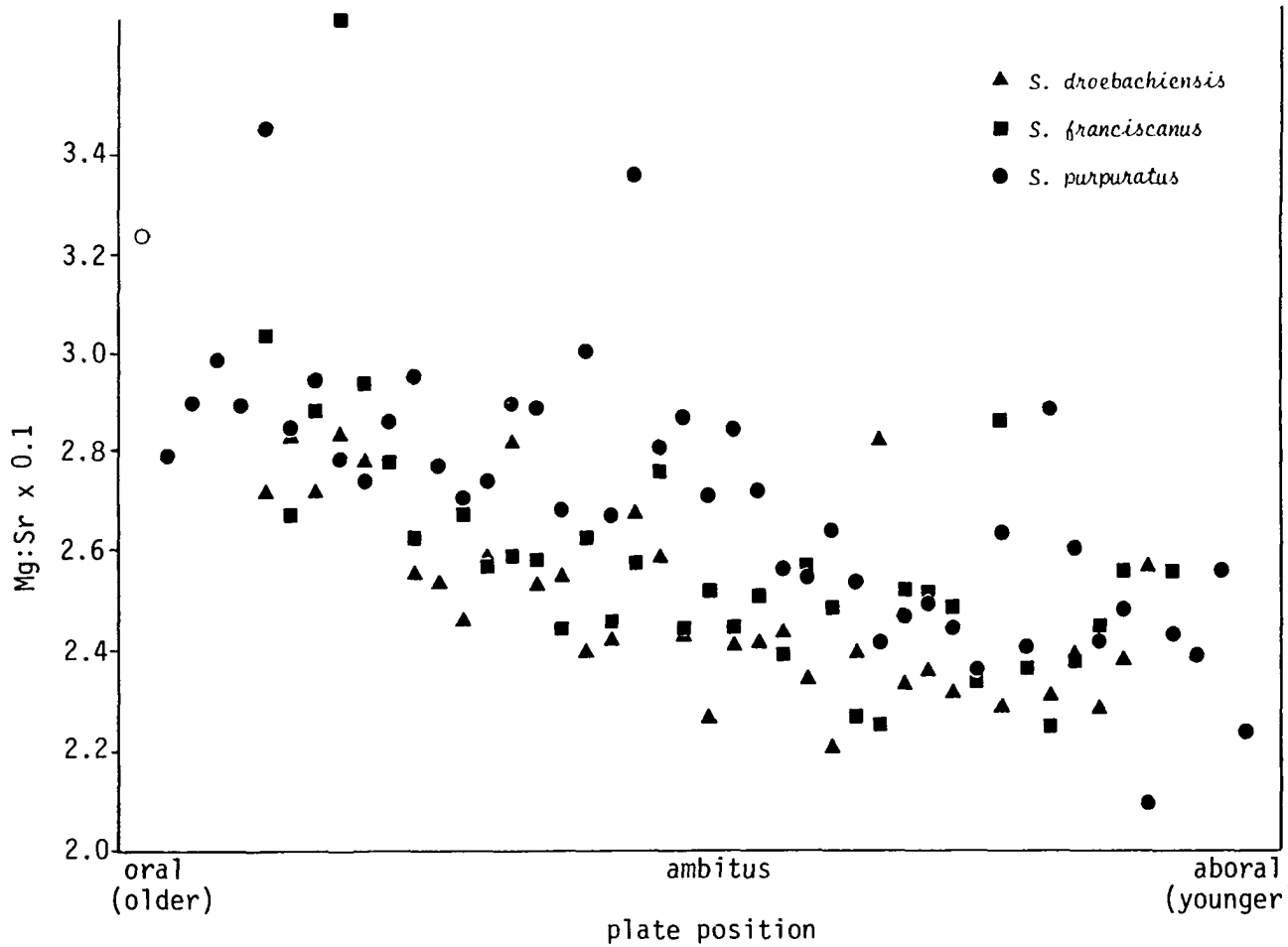

Figure 15. Mg:Sr ratios relative to position of the interambulacral in *Strongylocentrotus* species. Data shown in Table D-17 of the appendix.

conflict. Compositional differences that do exist may be related to variations in porosity, tubercularity and/or mode of growth.

Another major source of compositional differences within an individual is growth-related variation, i.e., differences between the older adoral interambulacrals and the younger aboral interambulacrals. In all three species examined here, magnesium increases as calcium decreases in progressively older plates. This is consistent with limited observations by Fowler and Dodd (1969, p. 24), Weber (1969a, p. 544), and Riley and Segar (1970, p. 727). These observations may be attributed to a constant change in growth rate (see Pilkey and Goodell, 1963, p. 141-146; Weber, 1973, p. 553) or variation in "structural maturity" (Davies et al., 1972, p. 881). Bioaccumulation may also account for increased levels of trace elements in older interambulacrals (see Bohn, 1979; Buchanan et al., 1980 for a discussion of iron accumulation in the skeleton of echinoids).

Chemical heterogeneity within coronal plates (see appropriate chapter of this study) is, of course, another source of compositional variation within an individual test. It is not clear how compositional variation within interambulacrals is related to variation between a interambulacrals.

Graphs of Mg:Ca and Mg:Sr ratios included in this study suggest that little or no compositional differences occur at subgeneric levels. This may result from similarities in environment and geographic range and therefore should not be considered conclusive.

Summary/Conclusions

Compositional and microstructural variation occurs within the middle skeletal layers of interambulacrals derived from *Strongylocentrotus*. These variations are correlated with other growth zone characteristics so that:

(1) large pores and thin trabeculae characteristic of spring/summer skeletal accretion are associated with high magnesium, low calcium, low manganese phases;

(2) small pores and thick trabeculae characteristic of fall/winter skeletal accretion are associated with low magnesium, high calcium, high manganese phases;

(3) compositional and microstructural variation within interambulacral components is closely related to changes in growth rate;

(4) changes in growth rate, in turn, are a function of seasonal variation in temperature and nutrient availability.

Growth zones also record the changes in form and size of individual interambulacral plates and the entire interambulacral column. Analysis of growth zones shows that the form of each interambulacral depends primarily on its position. The size of each interambulacral depends on its position and the total number of coronal plates. Changes in form of the growing interambulacral are produced by directional components in skeletal accretion and differential growth rates. Anisometric growth of the test results from the addition of new coronal plates, together with their subsequent accretionary growth.

Analysis of coronal plates by atomic absorption spectrophotometry reveals that the "bulk chemistry" of coronal plates varies considerably within an individual test. Ambulacral plates contain more magnesium and less calcium and strontium than their interambulacral counterparts. In all three species examined here, older interambulacrals contain more magnesium and less calcium than younger interambulacrals (strontium is more or less constant throughout the interambulacrum). Why magnesium levels increase in progressively older interambulacrals has not been demonstrated and should be determined in future studies.

BIBLIOGRAPHY

ANGINO, E.E. and G.K. BILLINGS. 1967. Atomic Absorption Spectrometry in Geology. 144 pp. Elsevier; New York, N.Y.

BERTINE, K.K. and E.D. GOLDBERG. 1972. Trace elements in clams, mussels and shrimp. Limnol. Oceanogr. 17: 877-884.

BEVELANDER, G. and H. NAKAHARA. 1960. Development of the sand dollar (*Echinarachnius parma*). Am. Assoc. Adv. Sci. Publ. 64: 41-56.

BIRKS, L.S. 1971. Electron Probe Microanalysis. 2nd ed. 190 pp. Wiley-Interscience; New York, N.Y.

BISCHOFF, W.D., F.C. BISHOP and F.T. MACKENZIE. 1983. Biogenically produced magnesian calcite: inhomogeneities in chemical and physical properties; comparison with synthetic phases. Am. Mineral. 68: 1183-1188.

BLANCHARD, S.C. and N.D. CHASTEEN. 1976 Electron paramagnetic resonance spectrum of a seashell. J. Phys. Chem. 80: 1362-1367.

BOERSMA, A. 1978. Foraminifera. Pp. 19-77. In: Haq, B.U. and A. Boersma, eds. Introduction to Marine Micropaleontology. Elsevier; New York, N.Y.

BOHN, A. 1979. Trace metals in fucoid algae and purple sea urchins near a high Arctic lead/zinc ore deposit. Mar. Pollut. Bull. 10: 325-327.

BOURGET, E. 1980. Barnacle shell growth and its relationship to environmental factors. Pp. 469-491. In: Rhoads, D.C. and R.A. Lutz, eds. Skeletal Growth of Aquatic Organisms. Plenum Press; New York, N.Y.

BRAND, U. 1983. Mineralogy and chemistry of the Lower Pennsylvanian Kendrick fauna, Eastern Kentucky, U.S.A. Chem. Geol. 40: 167-181.

BROMLEY, R.G. and U. ASGAARD. 1975. Sediment structures produced by a spatangoid echinoid: a problem of preservation. Bull. Geol. Soc. Den. 24: 261-281.

BRYAN, G.W. 1973. The occurence and seasonal variation of trace metals in the scallops *Pecten maximus* (L.) and *Chlamys opercularis* (L.). J. Mar. Biol. Assoc. U.K. 53: 145-166.

BRYAN, G.W. and L.G. HUMMERSTONE. 1973a. Brown seaweed as an indicator of heavy metals in estuaries in South-West England. J. Mar. Biol. Assoc. U.K. 53: 705-720.

BRYAN, G.W. and L.G. HUMMERSTONE. 1973b. Adaptation of the polychaete *Nereis diversicolor* to manganese in estuarine sediments. J. Mar. Biol. Assoc. U.K. 53: 859-872.

BUCHANAN, J.B., B.E. BROWN, T.L. COOMBS, B.J.S. PIRIE and J.A. ALLEN. 1980. The accumulation of ferric iron in the guts of some spatangoid echinoderms. J. Mar. Biol. Assoc. U.K. 60: 631-640.

CHAVE, K.E. 1954. Aspects of the biogeochemistry of magnesium. 1. Calcareous marine organisms. J. Geol. 62: 266-283.

CLARKE, F.W. and W.C. WHEELER. 1915. The inorganic constituents of echinoderms. U.S. Geol. S. Professional Paper 90-L: 191-196.

CURIE, D. 1963. Luminescence in Crystals. G.F.J. Garlick, trans. 332 332 pp. Wiley; New York, N.Y.

CURREY, J.D. and D. NICHOLS. 1969. The question of the organic matrix of echinoderm skeletons. Proc. Malacol. Soc. Lond. 38: 546-547.

DAFNI, J. and J. EREZ. 1982. Differential growth in *Tripneustes gratilla* (Echinoidea). Pp. 71-75. In: Lawrence, J.M., ed. Echinoderms: Proceedings of the International Conference, Tampa Bay. A.A. Balkema; Rotterdam, Netherlands.

DAVIES, T.T., M.A. CRENSHAW and B.M. HEATFIELD. 1972. The effect of temperature on the chemistry and structure of echinoid spine regeneration. J. Paleont. 46: 874-883.

DEUTLER, F. 1926. Uber das Wachstum der Seeigelskeletts. Zool. Jahrb., Abt. Anat. Ont. Tiere 48: 119-200.

DILLAMAN, R.M. and H.V. HART. 1981. X-ray evaluation of a SEM technique for determining the crystallography of echinoid skeletons. Scanning Electron Microscopy 1981. III: 313-320.

DODD, J.R. 1965. Preparing fossils and shells for chemical analysis. Pp. 384-388. In: Kummel, B. and D. Raup, eds. Handbook of Paleontological Techniques. W.H. Freeman and Co.; San Francisco, California.

DODD, J.R. 1967. Magnesium and strontium in calcareous skeletons: a review. J. Paleont. 41: 1313-1329.

DODD, J.R. and R.J. STANTON, JR. 1981. Paleoecology, Concepts and Applications. 559 pp. Wiley and Sons; New York, N.Y.

DONNAY, G. and D.L. PAWSON. 1969. X-ray diffraction studies of echinoderm plates. Science 166: 1147-1150.

DUGGINS, D.O. 1981. Sea urchins and kelp: the effects of short term changes in urchin diet. Limnol. Oceanogr. 26: 391-394.

DURHAM, J.W. 1955. Classification of clypeasteroid echinoids. Univ. Calif. Publ. Geol. Sci. 31: 73-198.

DURHAM, J.W. 1966. Evolution among the Echinoidea. Biol. Rs. 41: 368-391.

EANES, E.D. and A.S. POSNER. 1970. Structure and chemistry of bone material. Pp. 1-26. In: Schraer, H., ed. Biological Calcification. Cellular and Molecular Aspects. Appleton-Century-Crofts; New York, N.Y.

EBERS, M.L. and O.C. KOPP. 1979. Cathodoluminescent microstratigraphy in gangue dolomite, the Mascot-Jefferson City District, Tennessee. Econ. Geol. 74: 908-918.

EBERT, T.A. 1967. Growth and repair of spines in the sea urchin *Strongylocentrotus purpuratus* (Stimpson). Biol. Bull. 133: 141-149.

EBERT, T.A. 1968. Growth rate of the sea urchin *Strongylocentrotus purpuratus* related to food availability and spine abrasion. Ecology 49: 1075-1091.

EBERT, T.A. 1980. Relative growth of sea urchin jaws: an example of plastic resource allocation. Bull. Mar. Sci. 30: 467-474.

EISLER, R. 1981. Trace Metal Concentrations in Marine Organisms. 685 pp. Pergamon Press; New York, N.Y.

EISMA, D., W.G. MOOK and H.A. DAS. 1976. Shell characteristics, isotopic composition and trace element contents of some euryhaline molluscs as indicators of salinity. Palaeogeogr. Palaeoclimatol. Palaeoecol. 19: 39-62.

FAIRCHILD, I.J. 1983. Chemical controls of cathodoluminescence of natural dolomites and calcites: new data and review. Sedimentology 30: 579-584.

FERRIGNO, K.F. 1973. The use of cathodoluminescence in the study of limestones and fossils in thin sections. Pp. 8-10. In: Kopp, O.C., ed. Geological Applications of Cathodoluminescence - A Short Course. Univ. of Tennessee; Knoxville, Tennessee.

FOWLER, M.L. 1972. Distribution of magnesium and strontium in the skeletons of modern regular echinoids from the U.S. Atlantic Coast and Caribbean Sea. 291 pp. Ph.D. dissertation, Geology Dept., Indiana Univ.; Bloomington, Indiana.

FOWLER, M.L. and J.R. DODD. 1969. Magnesium and strontium variation within echinoid skeletons. (abst.). Geol. Soc. Am., S.E. Section: Program, Ann. Meeting: 24-25.

FRANK, J.R., A.B. CARPENTER and T.W. OGLESBY. 1982. Cathodoluminescence and compaction of calcite cement in the Taum Sauk Limestone (Upper Cambrian), Southeast Missouri. J. Sed. Petrol. 52: 631-638.

FREEMAN, T. 1971. Morphology and composition of an Ordovician vadose cement. Nature Phys. Sci. 233: 133-134.

GLOVER, E.D. 1977. Cathodoluminescence, iron and manganese content, and the early diagenesis of carbonates. 444 pp. Ph.D. dissertation, Geology Dept., Univ. Wisconsin; Madison, Wisconsin.

GORDON, C.M., R.A. CARR and R.G. LARSON. 1970. The influence of environmental factors on the sodium and manganese content of barnacle shells. Limnol. Oceanogr. 15: 461-466.

GORDON, I. 1926. The development of the calcareous test of *Echinus miliaris*. Philos. Trans. R. Soc. Lond. B Biol. Sci. 214: 259-312.

GORDON, I. 1929. Skeletal development in *Arbacia*, *Echinarachnius* and *Leptasterias*. Proc. R. Soc. Lond. B Biol. Sci. 215: 255-313.

GROSS, M.G. 1964. Variations in the O^{18}/O^{16} and C^{13}/C^{12} ratios of diagenetically altered limestones in the Bermuda Islands. J. Geol. 72: 170-194.

GROVER, G. JR. and J.F. READ. 1983. Paleoaquifer and deep burial related cements defined by regional cathodoluminescent patterns, Middle Ordovician carbonates, Virginia. Am. Assoc. Pet. Geol. Bull. 67: 1275-1303.

GROVER, J. and F. KUBANEK. 1983. The formation of ordered dolomite from high-magnesian calcite at 250 to 350 C and 1500 bars: epitactic growth with optimal phase orientation, and implications for carbonate diagenesis. Am. J. Sci. 283-A: 514-539.

HARRISS, R.C. 1964. The transfer of strontium, iron, and magnesium from sea water to skeletal carbonate material. 43 pp. M.S. thesis, Geology Department, Rice Univ.; Houston, Texas.

HARRISS, R.C. 1965. Trace element distribution in molluscan skeletal material. I. Magnesium, iron, manganese, and strontium. Bull. Mar. Sci. 15: 265-273.

HARRISS, R.C. and C.C. ALMY, JR. 1964. A preliminary investigation into the incorporation and distribution of minor elements in the skeletal material of scleractinian corals. Bull. Mar. Sci. 14: 418-423.

HARRISS, R.C. and O.H. PILKEY. 1966. Temperature and salinity control of the concentration of skeletal Na, Mn, and Fe in *Dendraster excentricus* Pac. Sci. 20: 235-238.

HEINRICH, K.F.J. 1981. Electron Beam X-Ray Microanalysis. 578 pp. Van Nostrand Reinhold Co.; New York, N.Y.

HOOPER, K. 1965. Analytical techniques applied to fossils and shells. Pp. 360-383. In: Kummel, B. and D. Raup, eds. Handbook of Paleontological Techniques. W.H. Freeman and Co.: San Francisco, California.

HUNT, C.D. 1983. Variability in the benthic Mn flux in coastal marine ecosystems resulting from temperature and primary production. Limnol. Oceanogr. 28: 913-923.

HYMAN, L.H. 1955. The Invertebrates. Echinodermata. The Coelomate Bilateria. Vol. IV. 763 pp. McGraw-Hill Book Co.; New York, N.Y.

JENSEN, M. 1969. Age determination of echinoids. Sarsia 37: 41-44.

JENSEN, M. 1972. The ultrastructure of the echinoid skeleton. Sarsia 48: 39-48.

JENSEN, M. 1974. The Strongylocentrotidae (Echinoidea), a morphologic and systematic study. Sarsia 57: 113-148.

JENSEN, M. 1982. Pedicellariae in classification of echinoids. Pp. 111-115. In: Lawrence, J.M., ed. Echinoderms: Proceedings of the International Conference, Tampa Bay. A.A. Balkema; Rotterdam, Netherlands.

JOHNSON, C.R. and K.H. MANN. 1982. Adaptations of *Strongylocentrotus droebachiensis* for survival on barren grounds in Nova Scotia. Pp. 277-283. In: Lawrence, J.M., ed. Echinoderms: Proceedings of the International Conference, Tampa Bay. A.A. Balkema; Rotterdam, Netherlands.

KIER, P.M. 1965. Evolutionary trends in Paleozoic echinoids. J. Paleont. 39: 436-465.

KIER, P.M. 1974. Evolutionary trends and their functional significance in the post-Paleozoic echinoids. 95 pp. J. Paleont. 48, Mem. 5.

KLING, S.A. 1978. Radiolaria. Pp. 203-244. In: Haq, B.U. and A. Boersma, eds. Introduction to Marine Micropaleontology. Elsevier; New York.

KOZLOFF, E.N. 1973. Seashore Life of Puget Sound, the Strait of Georgia, and the San Juan Archipelago. 282 pp. Univ. Washington Press; Seattle, Washington.

LERMAN, A. 1965. Paleoecological problems of magnesium and strontium in biogenic calcites in light of recent thermodynamic data. Geochim. Cosmochim. Acta 29: 977-1002.

LOEPER, B. and J.S. PEARSE. 1982. Scanning electron microscope observations of sea urchin coronal plates. P. 83. In: Lawrence, J.M., ed. Echinoderms: Proceedings of the International Conference, Tampa Bay. A.A. Balkema; Rotterdam, Netherlands.

LUTZ, R.A. and D.C. RHOADS. 1980. Growth patterns within the molluscan shell: an overview. Pp. 203-254. In: Rhoads, D.C. and Lutz, eds. Skeletal Growth of Aquatic Organisms. Plenum Press; New York, N.Y.

MACQUEEN, R.W. and E.D. GHENT. 1970. Electron microprobe study of magnesium distribution in some Mississippian echinoderm limestones from western Canada. Can. J. Earth Sci. 7: 1308-1316.

MACQUEEN, R.W., E.D. GHENT and G.R. DAVIES. 1974. Magnesium distirbution in living and fossil specimens of the echinoid *Peronella lesueuri* Agassiz, Shark Bay, Western Australia. J. Sed. Petrol. 44: 60-69.

MACURDA, D.B., JR. 1966. The ontogeny of the Mississippian blastoid genus *Orophocrinus*. J. Paleontol. 40: 92-124.

MARKEL, K. 1981. Experimental morphology of coronor growth in regular echinoids. Zoomorphology 97: 31-52.

MARSHALL, D.J. 1978. Suggesting standards for the reporting of cathodoluminescence results. J. Sed. Petrol. 48: 651-653.

MATTHEWS, J.L. et al. 1982. Structure, properties, and function of mineralized tissue components. Pp. 327-348. In: Nancollas, G.H., ed. Biological Mineralization and Demineralization - Dahlem Konferezen 1982. Springer-Verlag; New York, N.Y.

MCALESTER, A.L. 1968. The History of Life. 151 pp. Prentice-Hall; Englewood Cliffs, N.J.

MCLEAN, R.F. 1967. Erosion of burrows in beachrock by the tropical sea urchin, *Echinometra lucunter*. Can. J. Zool. 45: 586-588.

MEDLIN, W.L. 1959. Thermoluminescent properties of calcite. J. Chem. Phys. 30: 451-458.

MELVILLE, R.V. and DURHAM, J.W. 1966. Skeletal morphology. Pp. U220-U257. In: Moore, R.C., ed. Treatise on Invertebrate Paleontology. Part U. Echinodermata 3. Volume 1.

MEYER, D.L. 1965. Plate growth in some platycrinid crinoids. J. Paleont. 39: 1207-1209.

MEYERS, W.J. 1974. Carbonate cement stratigraphy of the Lake Valley Formation (Mississippian) Sacramento Mountains, New Mexico. J. Sed. Petrol. 44: 837-861.

MOORE, H.B. 1935. Comparison of the biology of *Echinus esculentus* in different habitats. Part II. J. Mar. Biol. Assoc. U.K. 20: 109-128.

MOORE, H.B. 1966. Ecology of echinoids. Pp. 73-85. In: Boolootian, R.A., ed. Physiology of Echinodermata. Interscience Publ., New York, N.Y.

MORTENSEN, T. 1928. A Monograph of the Echinoidea. V. 1. Cidaroidea. No. 1. 551 pp. University Press; London, England.

MORTENSEN, T. 1943. A Monograph of the Echinoidea. V. 3. Camarodonta II. No. 3. 446 pp. University Press; London, England.

MOSS, M.L. and M.M. MEEHAN. 1968. Growth of the echinoid test. Acta Anat. 69: 409-444.

NODDACK, I. and W. NODDACK. 1939. Die Haufigkeiten der Schwermetalle in Meerestieren. Arh. Zool. 32A (I), no. 4: 1-35.

OKAZAKI, K. 1975. 7. Normal development to metamorphosis. Pp. 177-232. In: Czihak, G., ed. The Sea Urchin Embryo. Biochemistry and Morphogenesis. Springer-Verlag; New York, N.Y.

OKAZAKI, K., R.M. DILLAMAN and K.M. WILBUR. 1981. Crystalline axes of the spine and test of the sea urchin *Strongylocentrotus purpuratus* determination by crystal etching and decoration. Biol. Bull. 161: 402-402-415.

OKAZAKI, K., K. MCDONALD and S. INOUE. 1980. Sea urchin larval spicule observed with the scanning electron microscope. Pp. 159-168. In: Omori, M. and N. Watabe, eds. The Mechanisms of Biomineralization in Animals and Plants. Proceedings of the Third International Biomineralization Symposium. Tokai Univ. Press; Tokyo, Japan.

OLDFIELD, S.C. 1976. Surface ornamentation of the echinoid test and its ecologic significance. Paleobiology 2: 122-130.

O'NEILL, P.L. 1981. Polycrystalline echinoderm calcite and its fracture-mechanics. Science 213: 646-648.

PEARSE, J.S. and V.B. PEARSE. 1975. Growth zones in the echinoid skeleton. Amer. Zool. 15: 731-753.

PILKEY, O.H. and H.G. GOODELL. 1963. Trace elements in recent mollusc shells. Limnol. Oceanogr. 8: 137-148.

PILKEY, O.H. and R.C. HARRISS. 1966. The effect of intertidal environment on the composition of calcareous skeletal material. Limnol. Oceanogr. 11: 381-385.

PILKEY, O.H. and J. HOWER. 1960. The effect of environment on the concentration of skeletal magnesium and strontium in *Dendraster*. J. Geol. 68: 203-216.

PRENANT, M. 1926. Notes histologiques sur la structure et la croissance des dents d'oursin. Arch. Zool. exp. gen. Note et Rev. 65: 25-38.

RAUP, D.M. 1958. The relation between water temperature and morphology in *Dendraster*. J. Geol. 66: 668-677.

RAUP, D.M. 1959. Crystallography of echinoid calcite. J. Geol. 67: 661-674.

RAUP, D.M. 1960. Ontogenetic variation in the crystallography of echinoid calcite. J. Paleont. 34: 1041-1050.

RAUP, D.M. 1962. The phylogeny of calcite crystallography in echinoids. J. Paleont. 36: 793-810.

RAUP, D.M. 1965. Crystal orientations in the echinoid apical system. J. Paleont. 39: 934-951.

RAUP, D.M. and S.M. STANLEY. 1978. Principles of Paleontology. 2nd ed. 481 pp. Freeman; San Francisco, California.

REED, S.J.B. 1975. Electron Microprobe Analysis. 400 pp. Cambridge Press; London, England.

REEVES, R.D. and R.R. BROOKS. 1978. Trace Element Analysis of Geological Materials. 421 pp. Wiley and Sons; New York, New York.

REGIS, M.B. 1977. Orgaisation microstructurale du stereome de l'echinoide *Paracentrotus lividus* (Lmk) et ses eventuelles incidences physiologiques. C.R. Hebd. Seanc. Acad. Sci., Paris 285: 189-192.

RILEY, J.P. and SEGAR, D.A. 1970. The distribution of the major and some minor elements in marine animals. 1. Echinoderms and coelenterates. J. Mar. Biol. Assoc. U.K. 50: 721-730.

ROSENBERG, G.D. 1980. An ontogenetic approach to the environmental significance of bivalve shell chemistry. Pp. 133-168. In: Rhoads, D.C. and R.A. Lutz, eds. Skeletal Growth of Aquatic Organisms. Plenum Press; New York, N.Y.

ROUX, M. 1975. Microstructural analysis of the crinoid stem. 7 pp. Univ. Kans. Paleontol. Contrib. Pap. 75.

RUCKER, J.B. and J.W. VALENTINE. 1961. Salinity response of trace element concentration in *Crassostrea virginica*. Nature (London) 190: 1099-1100.

SCHROEDER, J.H. 1969. Experimental dissolution of calcium, magnesium, and strontium from Recent biogenic carbonates: a model of diagenesis. J. Sed. Petrol. 39: 1057-1073.

SCHROEDER, J.H., E.J. DWORNIK and J.J. PAPIKE. 1969. Primary protodolomite in echinoid skeletons. Geol. Soc. Amer. Bull. 80: 1613-1616.

SEILACHER, A. 1979. Constructional morphology of sand dollars. Paleobiology 5: 191-221.

SHIMIZU, M. and J. YAMADA. 1980. Sclerocytes and crystal growth in the regeneration of sea urchin test and spines. Pp. 169-178. In: Omori, M. and N. Watabe, eds. The Mechanisms of Biomineralization in Animals and Plants. Proceedings of the Third International Biomineralization Symposium. Tokai Univ. Press; Tokyo, Japan.

SIPPEL, R.F. and E.D. GLOVER. 1965. Structures in carbonate rocks made visible by luminescene petrography. Science 180: 1283-1287.

SLAVIN, W. 1968. Atomic Absorption Spectroscopy. 307 pp. Interscience Pub.; New York, N.Y.

SMITH, A.B. 1978. A functional classification of the coronal pores of regular echinoids. Palaeontology 21: 759-789.

SMITH, A.B. 1980. Stereom microstructure of the echinoid test. 81 pp. Spec. Papers in Palaeontology 25. Palaeont. Assoc. London.

SMITH, J.F. and R.C. STENSTROM. 1965. Electron-excited luminescence as a petrologic tool. J. Geol. 73: 627-635.

SOMMER, S.E. 1972. Cathodoluminescence of carbonates, 2. Geological applications. Chem. Geol. 9: 275-284.

STEPHENS, R.E. 1972. Studies on the development of the sea urchin *Strongylocentrotus droebachiensis*. I. Ecology and normal development. Biol. Bull. 142: 132-144.

STEVENSON, R.A. and S.L. UFRET. 1966. Iron, manganese, and nickel in skeletons of the sea urchins *Tripneustes esculentus* and *Echinometra lucunter*. Limnol. Oceanogr. 11: 11-17.

SWAN, E.F. 1956. The meaning of strontium-calcium ratios. Deep Sea Research 4: 71.

SWAN, E.F. 1958. Growth and variation in sea urchins of York, Maine. J. Mar. Res. 17: 505-522.

SWAN, E.F. 1966. Growth, autonomy, and regeneration. Pp. 397-434. In: Boolootian, R.A., ed. Physiology of Echinodermata. Wiley and Sons; New York, N.Y.

TEGNER, M.J. and L.A. LEVIN. 1982. Do sea urchins and abalones compete in California kelp forest communities? P. 265. In: Lawrence, J.M., ed. Echinoderms: Proceedings of the International Conference, Tampa Bay. A.A. Balkema; Rotterdam, Netherlands.

TERENTIEVA, K.F. 1932. Mineralinyia sostov skeletov nekotorykh sovremennykh iglokozhikh. Akaademiia nauk SSSR, Leningrad. Biogeokhimicheskaia laboratoriia. Trudy 2: 45-62.

TOWE, K.M. 1967. Echinoderm calcite: single crystal or polycrystalline aggregate. Science 157: 1048-1050.

TRAVIS, D.F. 1970. The comparative ultrastructure and organization of five calcified tissues. Pp. 203-311. In: Schraer, H., ed. Biological Calcification: Cellular and Molecular Aspects. Appleton-Century-Crofts; New York, N.Y.

ULBRICHT, R.J. and A.W. PRITCHARD. 1972. Effect of temperature on the metabolic rate of sea urchins. Biol. Bull. 142: 178-185.

URAKAMI, H., I. UEMURA and K. OKAZAKI. 1980. A study of the ultrathin section of sea urchin larval spicule. Pp. 170-185. In: Omori, M. and N. Watabe, eds. The Mechanisms of Biomineralization in Animals and Plants. Proceedings of the Third International Biomineralization Symposium. Tokai Univ. Press; Tokyo, Japan.

VASSEUR, E. 1952. Geographic variation in the Norwegian sea-urchins *Strongylocentrotus droebachiensis* and *S. pallidus*. Evolution 6: 87-100.

VINOGRADOV, A.P. 1953. The Elementary Chemical Composition of Marine Organisms. (trans. from Russian) 647 pp. Sears Found. Mar. Res.; New Haven, Conn.

WEBER, J.N. 1969a. The incorporation of magnesium into the skeletal calcites of echinoderms. Am. J. Sci. 267: 537-566.

WEBER, J.N. 1969b. Origin of concentric banding in the spines of the tropical echinoid *Heterocentrotus*. Pac. Sci. 23: 452-466.

WEBER, J.N. 1973. Temperature dependence of magnesium in echinoid and asteroid skeletal calcite: a reinterpretation of its significance. J. Geol. 81: 543-556.

WEBER, J.N. and D.M. RAUP. 1966a. Fractionation of the stabel isotopes of carbon and oxygen in marine calcareous organisms - the Echinoidea. Part I. Variation of C^{13} and O^{18} content within individuals. Geochim. Cosmochim. Acta 30: 681-703.

WEBER, J.N. and D.M. RAUP. 1966b. Fractionation of the stable isotopes of carbon and oxygen in marine calcareous organisms - the Echinoidea. Part II. Environmental and genetic factors. Geochim. Cosmochim. Acta 30: 705-736.

WEBER, J.N. and D.M. RAUP. 1968. Comparison of C^{13}/C^{12} and O^{18}/O^{16} in the skeletal calcite of recent and fossil echinoids. J. Paleont. 42: 37-50.

WEBER, J.N. and E.W. WHITE. 1973. Carbonate minerals as precursors of new ceramic, metal, and polymer materials for biomedical applications. Miner. Sci. Eng. 5: 151-165.

WEST, C.D. 1937. Note on the crystallography of the echinoderm skeleton. J. Paleont. 11: 458-459.

WHITE, R.A., J.N. WEBER, and E.W. WHITE. 1972. Replaminiform: a new process for preparing porous ceramic, metal, and polymer prosthetic materials. Science 176: 922-924.

WILBUR, K.M. 1980. Cells, crystals and skeletons. Pp. 3-11. In: Omori, M. and N. Watabe, eds. The Mechanisms of Biomineralization in Animals and Plants. Proceedings of the Third International Biomineralization Symposium. Tokai Univ. Press; Tokyo, Japan.

WOLLAST, R. and D. REINHARD-DERIE. 1972. Equilibrium and mechanism of dissolution of magnesian calcites. Pp. 479-492. In: Andersen, N.R. and A. Malahoff, eds. The Fate of Fossil Fuel CO_2 in the Oceans. Plenum Press; New York, N.Y.

ZANGERL, R. 1965. Radiographic techniques. Pp. 305-320. In: Kummel, B. and D. Raup, eds. Handbook of Paleontological Techniques. W.H. Freeman and Co.; San Francisco, California.

Appendix Figures and Tables

Table A-1 : Test dimensions of some *S. droebachiensis* specimens.

	h. d.	v. d.	Apical system	Peristome	Number of plates A.	Number of plates I. A.
1	78 mm	42 mm	17.5 mm (22.5 % h. d.)	22 mm (28.2 % h. d.)	34—35	24—25
2	70 —	37 —	15 — (21.4 - —)	22 — (31.4 - —)	35—36	23—24
3	65 —	35 —	14 — (23.1 - —)	21 — (32.3 - —)	29—30	19—20
4	58 —	34 —	15 — (25.9 - —)	20 — (34.5 - —)	30—31	19—20
5	56 —	29 —	13 — (23.2 - —)	19 — (33.9 - —)	25—26	19—20
6	52 —	24 —	10.5 — (20.2 - —)	19 — (36.5 - —)	20—21	13—14
7	47 —	22 —	10.5 — (22.4 - —)	17 — (36.2 - —)	18—19	14—15
8	46 —	25 —	11 — (23.9 - —)	17 — (37.0 - —)	29—30	21—22
9	46 —	35 —	11 — (23.9 - —)	17 — (37.0 - —)	23—24	15—16
10	30 —	14 —	7.5 — (25.0 - —)	12 — (40.0 - —)	15—16	12—13
11	25 —	12.5 —	7 — (28.0 - —)	11 — (44.0 - —)	13—14	11—12
12	20 —	10 —	5.5 — (27.5 - —)	8.5 — (42.5 - —)	13—14	10—11
13	67 —	31 —	15 — (22.4 - —)	21 — (30.8 - —)	34—35	24—25
14	66 —	35 —	14 — (21.2 - —)	20 — (30.3 - —)	33—34	21—22
15	64 —	32 —	13.5 — (21.2 - —)	19.5 — (30.5 - —)	30—31	20—21
16	59 —	32 —	12 — (20.4 - —)	19 — (32.2 - —)	30—31	20—21
17	50 —	25 —	10 — (20.0 - —)	17 — (34.0 - —)	27—28	18—19
18	45 —	24 —	10 — (22.2 - —)	14.5 — (32.3 - —)	25—26	16—17
19	76 —	41 —	17 — (22.4 - —)	24 — (31.6 - —)	28—29	20—21
20	70 —	32 —	16 — (22.8 - —)	21.5 — (30.7 - —)	23—24	16—17
21	68 —	37 —	16.5 — (24.3 - —)	21 — (30.9 - —)	29—30	23—24
22	60 —	27 —	15 — (25.0 - —)	20.5 — (34.2 - —)	21—22	15—16
23	55 —	22 —	13.5 — (24.6 - —)	19.5 — (35.5 - —)	18—19	15—16
24	52 —	26 —	14 — (26.9 - —)	18.5 — (35.6 - —)	19—20	15—16
25	63 —	33 —	13 — (20.7 - —)	21 — (33.3 - —)	29—30	19—20
26	59 —	37 —	12.5 — (21.2 - —)	19 — (32.3 - —)	31—32	19—20
27	56 —	33 —	13 — (23.2 - —)	18 — (32.2 - —)	28—29	18—19
28	53 —	29 —	11.5 — (21.9 - —)	18 — (34.0 - —)	26—27	18—19
29	48 —	28 —	11.5 — (24.0 - —)	18 — (37.5 - —)	22—23	15—16
30	43 —	23 —	11 — (25.6 - —)	16.5 — (38.4 - —)	23—24	15—16
31	36 —	20 —	8 — (22.2 - —)	14 — (38.9 - —)	22—23	15—16
32	32 —	18 —	8 — (25.0 - —)	11 — (34.4 - —)	23—24	17—18
33	23 —	14 —	5 — (21.7 - —)	10 — (43.5 - —)	20—21	14—15
34	41 —	21 —	9 — (22.0 - —)	15 — (36.6 - —)	26—27	16—17
35	28 —	13 —	7 — (25.0 - —)	12 — (41.9 - —)	17—18	14—15
36	27 —	13 —	6.5 — (24.1 - —)	10.5 — (39.0 - —)	17—18	14—15
37	26 —	14 —	6.5 — (25.0 - —)	10 — (38.5 - —)	17—18	14—15
38	26 —	13 —	6 — (23.1 - —)	10.5 — (40.5 - —)	20—21	15—16

Table copied from Mortensen (1943, p. 206)

Figure B-1: Stylized sketch of regular echinoid test showing measurable test dimensions: B: "horizontal diameter"; C: vertical diameter; D: apical diameter; E: peristomial diameter.

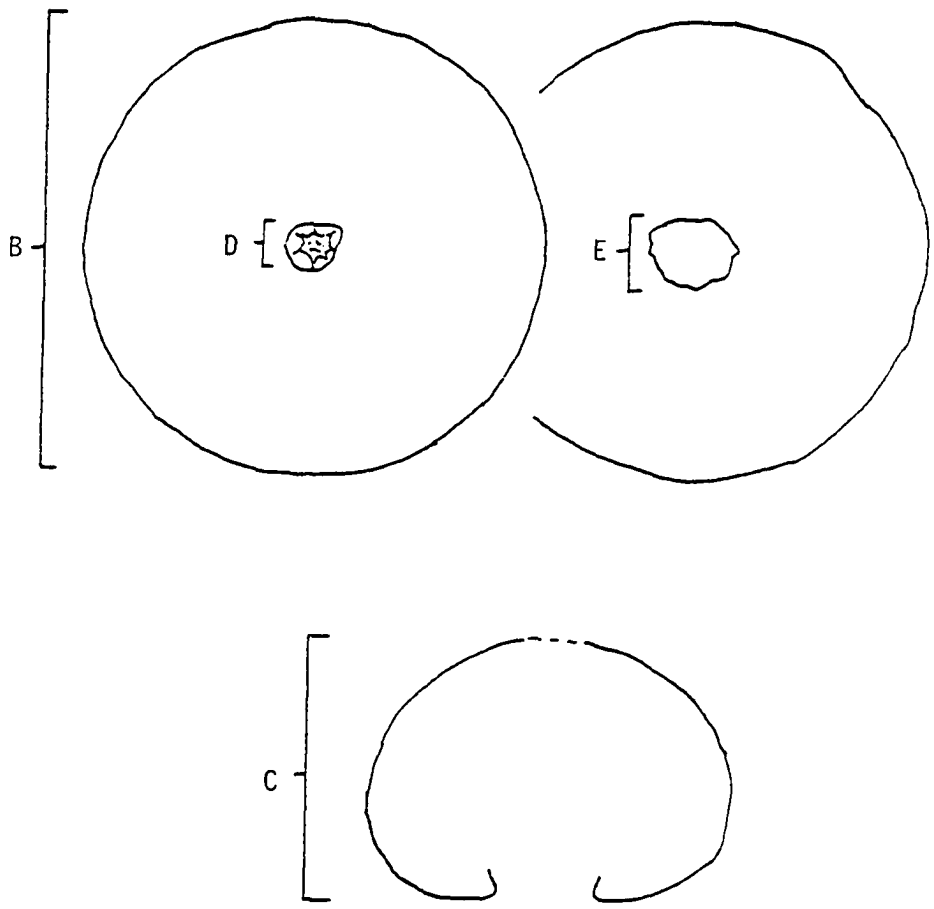

Table B-2: Test dimensions of *S. droebachiensis* specimens used in this study.

A	B	C	D	E	F	G
1	67	34.5(51.7%)	12.7(19.0%)	20.0(30.0%)	68	44
2	76	42.0(55.6%)	15.7(20.8%)	23.7(31.4%)	68	42
3	60	31.5(52.5%)	13.0(21.7%)	19.5(32.5%)	62	40
4	66	34.5(52.3%)	14.4(21.8%)	21.0(31.8%)	66	42
5	72	37.0(51.4%)	14.5(20.1%)	22.0(30.6%)	68	44
6	68	34.0(50.0%)	14.0(20.6%)	21.5(31.6%)	68	44
7	72	38.0(52.8%)	14.0(19.4%)	22.5(31.3%)	70	44
8	60	30.0(50.4%)	12.0(20.2%)	20.0(33.6%)	56	36
9	61	30.5(50.0%)	12.0(19.7%)	20.0(32.8%)	56	40
10	50	25.0(50.0%)	9.5(19.0%)	17.5(35.0%)	52	34
11	46	21.5(46.7%)	9.0(19.6%)	16.0(34.8%)	50	34
12	43	21.0(48.8%)	8.5(19.8%)	15.5(36.0%)	52	36
13	59	29.0(49.2%)	11.5(19.5%)	19.0(32.2%)	60	38
14	76	47.0(61.8%)	13.5(17.8%)	23.0(30.3%)	72	46
15	50	23.5(47.0%)	9.0(18.0%)	20.0(40.0%)	52	36
16	61	29.0(47.5%)	12.0(19.7%)	20.0(32.8%)	64	46
17	67	29.0(43.6%)	12.0(18.0%)	22.0(33.1%)	68	40

Explanation

A: specimen number
B: horizontal diameter (mm)
C: vertical diameter (mm); proportion of vertical diameter to horizontal diameter multiplied by 100%, in parentheses
D: apical diameter (mm); proportion of apical diameter to horizontal diameter multiplied by 100%, in parentheses
E: peristomial diameter (mm); proportion of peristomial diameter to horizontal diameter multiplied by 100%, in parentheses
F: average number of ambulacral plates present
G: average number of interambulacral plates present

Table B-3: Plate sizes throughout the reconstructed growth series

	A	B	C	D	E
1	.015/.005/.033	.034/.012/.075	.046/.016/.101	-	-
2	.020/.007/.044	.060/.020/.132	.081/.028/.178	-	-
3	.017/.006/.037	.054/.018/.119	.088/.030/.193	-	-
4	.025/.009/.055	.076/.026/.167	.108/.037/.237	-	-
5	.025/.009/.055	.082/.028/.180	.092/.031/.202	.118/.040/.259	-
6	.029/.010/.064	.100/.034/.220	.108/.037/.237	.136/.046/.299	-
7	.030/.010/.066	.090/.031/.198	.125/.043/.274	.138/.047/.303	-
8	.040/.014/.088	.128/.044/.281	.150/.051/.329	.163/.056/.358	-
9	.050/.017/.110	.123/.042/.270	.168/.057/.369	.175/.060/.384	-
10	.064/.022/.141	.198/.067/.435	.225/.077/.494	.248/.084/.544	-
11	.060/.020/.132	.168/.057/.369	.208/.071/.457	.238/.081/.522	.265/.090/.582
12	.072/.025/.158	.218/.074/.479	.298/.101/.654	.318/.108/.698	.325/.111/.713
13	.058/.020/.127	.210/.072/.461	.280/.095/.615	.340/.116/.746	.365/.124/.801
14	.070/.024/.154	.285/.097/.626	.333/.113/.731	.353/.120/.775	.378/.129/.830
15	.054/.018/.119	.253/.086/.555	.363/.124/.797	.410/.140/.900	.458/.156/1.005
16	.045/.015/.099	.385/.131/.845	.460/.157/1.010	.495/.168/1.087	.523/.178/1.148
17	.037/.013/.081	.293/.100/.643	.430/.146/.944	.518/.176/1.137	.565/.192/1.240
18	.023/.008/.050	.385/.131/.845	.540/.184/1.185	.640/.218/1.405	.710/.242/1.559
19	.016/.005/.035	.390/.133/.856	.585/.199/1.284	.765/.260/1.679	.863/.294/1.895
20	.010/.003/.022	.380/.129/.834	.548/.187/1.203	.690/.235/1.515	.823/.280/1.807
21	.003/.001/.007	.353/.120/.775	.553/.188/1.214	.765/.260/1.679	.960/.327/2.108
22	*	.316/.108/.694	.538/.183/1.181	.760/.259/1.668	.970/.330/2.129
23	*	.265/.090/.582	.505/.172/1.109	.800/.272/1.756	1.048/.357/2.301
24	*	.205/.070/.450	.500/.170/1.098	.808/.275/1.774	1.286/.438/2.823
25	*	.135/.046/.296	.380/.129/.834	.780/.265/1.712	1.150/.391/2.525
26	*	.098/.033/.215	.360/.123/.790	.725/.247/1.592	1.140/.388/2.503
27	*	.075/.026/.165	.300/.102/.659	.735/.250/1.614	1.178/.401/2.586
28	*	.040/.014/.088	.200/.068/.439	.648/.221/1.423	1.113/.379/2.443
29	*	.012/.004/.026	.150/.051/.329	.505/.172/1.109	.700/.238/1.537
30	*	*	.100/.034/.220	.420/.143/.922	.996/.339/2.187
31	*	*	.040/.014/.088	.305/.104/.670	.890/.303/1.954
32	*	*	.012/.004/.026	.230/.078/.505	.813/.277/1.785
33	*	*	*	.152/.052/.334	.676/.230/1.484
34	*	*	*	.070/.024/.154	.585/.199/1.284
35	*	*	*	.032/.011/.070	.480/.163/1.054
36	*	*	*	*	.400/.136/.878
37	*	*	*	*	.300/.102/.659
38	*	*	*	*	.195/.066/.428
39	*	*	*	*	.100/.034/.220

Explanation

Rows "1" through "39" represent individual interambulacral (1 is oldest).
Columns "A" through "E" correspond to reconstructed series in Figure 7 (A is oldest, E most recent).
Triplicate readings: 1st entry, raw reading (in^2); 2nd entry, plate size, corrected for enlargement (in^2); 3rd entry, plate size converted to metric equivalent (cm^2); "-", no measureable growth; "*", plate unformed.

Table C-1

Operating parameters for luminoscope observations

Microscope:	Leitz, 1.25x ocular, 4.3x objective
Instrument:	Nuclide Corp. Luminoscope, Model ELM 2b
Chamber window:	clear to pale yellow
Sample preparation:	coarse-ground (400 grit) whole interambulacral components, with organic components removed

Instrument parameters		Photographic parameters	
Beam energy:	8-10 kV	Camera:	Pentax K-1000
Beam current:	40-60 microamperes	Film type:	Kodak Ektacolor
Spot diameter:	5-10 mm	Film size/speed:	35 mm, 400 ASA
Gun type:	cold cathode	Development:	normal
Ambient gas:	air @ 100 millitorrs	Exposure:	60-90 seconds

Standards reported according to criteria sugessted by Marshall, 1978.

Table C-2: Standards used for electron microprobe analysis.

(1) Dolomite H.U. #10971

CaO	30.71
MgO	22.20
CO_2	47.45

(2) Dolomite #105064

CaO	30.43
MgO	21.78
MnO	.02
FeO	.08
CO_2	47.37

(3) Kutnahorite #85670

CaO	27.44
MgO	2.21
MnO	28.31
FeO	.50
CO_2	41.80

(4) Aragonite (Herongrund, Hungary)

CaO	56.00

All standards from University of Chicago, Dept. of Geology and Geophysics

Table C-3: Electron microprobe analysis along adradial-interradial axis of an ambital interambulacral: *S. droebachiensis* (data graphed in Figure 3).

A	B	C	D	E	F	G
1	623	631990	17275	204014	93.72	6.28
2	548	585701	15382	202616	94.06	5.94
3	566	582428	17729	204295	93.09	6.91
4	618	612355	14988	200988	94.41	5.59
5	538	566463	15961	203886	93.65	6.35
6	580	553375	16656	203241	93.19	6.81
7	572	560609	17115	203947	93.09	6.91
8	500	574483	16352	203842	93.60	6.40
9	552	583337	16657	203837	93.53	6.47
10	545	573944	17299	203591	93.18	6.82
11	564	578810	18461	203453	92.77	7.23
12	550	573938	18748	203814	92.61	7.39
13	545	577682	18090	203797	92.91	7.09
14	570	591987	19526	203882	92.50	7.50
15	525	601732	18693	203571	92.96	7.04
16	553	584268	18681	203614	92.75	7.25
17	587	575291	17864	202871	92.95	7.05
18	598	556968	19284	203871	92.16	7.84
19	541	553383	18341	204045	92.53	7.47
20	538	583261	17722	203540	93.12	6.88
21	577	597336	16454	202292	93.73	6.27
22	565	627005	18130	204496	93.39	6.61
23	554	593318	16041	204843	93.87	6.13
24	626	580053	16493	201142	93.51	6.49
25	575	582107	16447	201133	93.59	6.41
26	532	566532	14293	201289	94.34	5.66
27	584	597486	14978	202072	94.31	5.69
28	546	620713	14831	201979	94.58	5.42
29	569	633391	14718	201091	94.71	5.29
30	581	625589	15794	203145	94.24	5.76
31	883	497449	13214	201168	93.84	6.16
32	561	557218	14355	201162	94.21	5.79
33	593	640463	14405	201315	94.87	5.13
34	540	599756	14295	201372	94.62	5.38
35	548	564166	12679	201428	94.98	5.02
36	576	609085	13869	201154	94.84	5.16
37	567	620946	13532	201361	95.07	4.93
38	530	635838	13576	201287	95.18	4.82
39	613	586337	13204	201197	94.90	5.10
40	626	638195	13582	201783	95.14	4.86
41	625	634555	14840	201371	94.64	5.36
42	629	646512	13923	201309	95.07	4.93
43	586	638886	14412	201134	94.86	5.14
44	566	610890	15435	203761	94.26	5.74
45	570	611590	15342	201484	94.30	5.70
46	543	579335	14039	201437	94.55	5.45
47	560	577096	15811	203981	93.80	6.20
48	570	552370	14656	203985	94.03	5.97
49	556	555406	15687	203328	93.63	6.37
50	619	564799	14630	201246	94.12	5.88

A	B	C	D	E	F	G
51	538	547310	16394	203340	93.27	6.73
52	609	583868	15581	203287	93.93	6.07
53	526	561335	14363	201442	94.27	5.73
54	487	546617	16290	204739	93.34	6.66
55	607	581109	16398	203924	93.58	6.42
56	665	578528	14706	201256	94.19	5.81
57	567	567259	16581	204043	93.39	6.61
58	568	560107	17062	203041	93.11	6.89
59	519	517880	12860	201195	94.51	5.49
60	550	541189	16191	204080	93.27	6.73
61	543	542383	15905	204122	93.41	6.59
62	502	513057	16741	201126	92.73	7.27
63	574	588979	18103	201143	93.01	6.99
64	556	584112	18959	201192	92.64	7.36
65	563	590149	17040	201516	93.44	6.56
66	577	569725	16968	201139	93.25	6.75
67	573	575371	17842	201643	92.97	7.03
68	590	562732	18027	203889	92.74	7.26
69	591	567642	14871	201049	94.07	5.93
70	661	574333	13970	201153	94.45	5.55
71	567	580767	14418	203867	94.39	5.61
72	632	588621	12344	201069	95.25	4.75
73	593	596020	14855	201939	94.34	5.66
74	584	610645	14566	201702	94.58	5.42
75	554	592778	14813	202908	94.35	5.65
76	630	594047	17838	201472	93.13	6.87
77	572	584437	16353	202549	93.65	6.35
78	516	537595	15886	203800	93.39	6.61
79	543	504828	15871	202736	92.98	7.02
80	596	540734	16896	201359	92.94	7.06
81	573	554572	16847	203048	93.13	6.87
82	535	614107	14808	200866	94.54	5.46
83	574	639365	15395	203265	94.50	5.50
84	566	637905	17493	202147	93.73	6.27
85	570	610971	16680	202320	93.78	6.22
86	552	642135	15608	201798	94.46	5.54
87	544	645979	16089	202563	94.32	5.68
88	550	635613	16268	203079	94.17	5.83
89	603	601140	15512	200754	94.12	5.88
90	525	568402	14272	200886	94.37	5.63
91	583	619286	16130	202615	94.06	5.94
92	596	614137	15645	203110	94.19	5.81
93	604	616533	15478	202540	94.26	5.74
94	592	606703	15724	202392	94.09	5.91
95	533	634115	13932	203305	95.03	4.97
96	562	602407	15120	203504	94.31	5.69
97	708	542483	12969	200481	94.55	5.45
98	754	557995	12820	200529	94.72	5.28
99	717	592786	13613	200586	94.72	5.28
100	705	625296	14185	200580	94.76	5.24

A	B	C	D	E	F	G
101	599	591051	14670	200651	94.36	5.64
102	624	570229	13332	200731	94.70	5.30
103	582	602843	14915	203470	94.38	5.62
104	550	590845	15392	200751	94.11	5.89
105	550	576750	15046	203263	94.11	5.89
106	569	579257	15598	204435	93.90	6.10
107	573	576991	15368	202906	93.97	6.03
108	582	583310	16161	202201	93.71	6.29
109	566	576125	16431	202581	93.54	6.46
110	514	544253	16167	200819	93.34	6.66
111	530	558518	16388	202940	93.40	6.60
112	590	648873	17399	201526	93.84	6.16
113	569	616173	17836	202034	93.40	6.60
114	584	639497	17506	202341	93.73	6.27
115	533	586592	15956	200553	93.86	6.14
116	574	623193	17096	200726	93.74	6.26
117	493	554449	17027	201449	93.12	6.88
118	546	622215	16843	203886	93.84	6.16
119	550	608044	16064	202006	94.00	6.00
120	568	618344	17630	202362	93.49	6.51
121	560	579436	15530	202462	93.94	6.06
122	587	605876	15973	202342	93.99	6.01
123	517	582756	15924	203473	93.84	6.16
124	539	542796	14868	202733	93.86	6.14
125	518	552783	15779	202805	93.60	6.40
126	543	537750	13310	201531	94.48	5.52
127	523	540037	17721	203672	92.64	7.36
128	549	533358	19726	201344	91.70	8.30
129	563	590889	19603	200887	92.46	7.54
130	667	504828	13385	200757	94.02	5.98
131	558	583431	18871	200726	92.66	7.34
132	567	563826	17182	201351	93.11	6.89
133	564	577752	18086	201818	92.90	7.10

Explanation

A: data for a single point, from "1" (adradial margin) to "133" (interradial margin)
B: iron count (used only to balance computer input; iron levels too low to be measured in samples)
C: calcium count
D: magnesium count
E: backround count
F: mole percent calcium
G: mole percent magnesium

Table C-4: Electron microprobe analysis along adoral-adapical axis of an ambital interambulacral: *S. droebachiensis* (data graphed in Figure 4).

A	B	C	D	E	F	G
1	528	584627	15363	200870	94.08	5.92
2	562	624122	15531	200847	94.34	5.66
3	631	620321	14703	200671	94.57	5.43
4	433	404753	12157	200706	93.59	6.41
5	565	597454	13838	200837	94.77	5.23
6	611	585847	12530	200717	95.17	4.83
7	600	593329	17031	200663	93.46	6.54
8	521	594289	16806	200494	93.60	6.40
9	676	519746	19683	200729	91.43	8.57
10	488	568104	15811	200552	93.76	6.24
11	451	509138	15137	200525	93.44	6.56
12	516	539597	15517	200338	93.57	6.43
13	535	528163	14838	200786	93.72	6.28
14	512	542957	17956	201790	92.58	7.42
15	534	555720	18989	200482	92.30	7.70
16	536	568965	18353	200400	92.72	7.28
17	568	576301	17734	200174	93.02	6.98
18	535	581915	21272	200227	91.74	8.26
19	577	596559	20826	200250	92.06	7.94
20	574	583415	19160	200051	92.54	7.46
21	500	525711	15623	200133	93.38	6.62
22	502	553499	14709	200013	94.06	5.94
23	610	631052	16132	200131	92.14	5.86
24	534	586640	13641	200109	94.78	5.22
25	586	603300	15299	200393	94.23	5.77
26	682	592938	14568	200397	94.36	5.64
27	546	651544	15370	200285	94.63	5.37
28	548	637115	17220	200407	93.83	6.17
29	573	638648	17804	200305	93.62	6.38
30	568	622949	15763	200221	94.24	5.76

Explanation

A: data for a single point, from "1" (adoral margin) to "30" (adapical margin)
B: iron count (used only to balance compute input; iron levels too low to be measured in samples
C: calcium count
D: magnesium count
E: backround count
F: mole percent calcium
G: mole percent magnesium

Table C-5: Electron microprobe analysis along adradial-interradial axis of an ambital interambulacral, from interior surface: (data graphed in Figure C-6).

A	B	C	D	E	F	G
1	479	534207	20967	203919	91.25	8.75
2	489	450790	16782	202088	91.82	8.18
3	499	550739	20560	203440	91.63	8.37
4	540	570650	21829	203149	91.38	8.62
5	562	550187	20015	201405	91.80	8.20
6	507	582791	21854	204898	91.55	8.45
7	575	582474	21495	201171	91.64	8.36
8	581	566668	19469	203986	92.22	7.78
9	564	562989	20972	204113	91.59	8.41
10	547	548239	20136	202362	91.73	8.27
11	558	567816	19544	202911	92.22	7.78
12	508	570075	19444	203589	92.32	7.68
13	518	569702	17127	203260	93.23	6.77
14	567	602999	17229	201181	93.50	6.50
15	563	527381	16216	202973	93.09	6.91
16	508	536738	16388	202496	93.17	6.83
17	565	535508	18402	202309	92.26	7.74
18	615	564325	16980	202508	93.16	6.84
19	614	521290	14682	201389	93.65	6.35
20	592	572632	16640	202651	93.40	6.60
21	583	611186	17101	207771	93.61	6.39
22	545	534669	16142	200853	93.22	6.78
23	555	574338	14562	202185	94.28	5.72
24	567	568158	15493	202198	93.84	6.16
25	548	575711	15010	203205	94.12	5.88
26	540	523303	15495	200877	93.37	6.63
27	532	552993	16386	202916	93.34	6.66
28	560	581398	14256	201524	94.47	5.53
29	593	572909	14200	200796	94.36	5.64
30	901	556083	14534	200650	93.87	6.13
31	581	587180	18093	202152	92.99	7.01
32	577	554882	14391	200983	94.16	5.84
33	561	578113	12479	201572	95.17	4.83
34	570	592134	15895	201871	93.91	6.09
35	552	587702	15438	203167	94.06	5.94
36	565	581587	15765	203420	93.86	6.14
37	581	576703	15950	203601	93.73	6.27
38	535	630214	16192	203392	94.16	5.84
39	530	611610	17252	203805	93.60	6.40
40	531	630903	19589	201220	92.92	7.08
41	502	624770	19503	201669	92.91	7.09
42	518	610915	21005	203143	92.20	7.80
43	535	604671	19902	201853	92.53	7.47
44	526	550878	19561	203243	92.02	7.98

Explanation:

A: data for a single point, from "1" near adradial margin, to "44" near interradial margin
B: iron count (used only to balance computer input; iron levels too low to be measured in samples)
C: calcium count
D: magnesium count
E: backround count
F: mole percent calcium
G: mole percent magnesium

Figure C-6

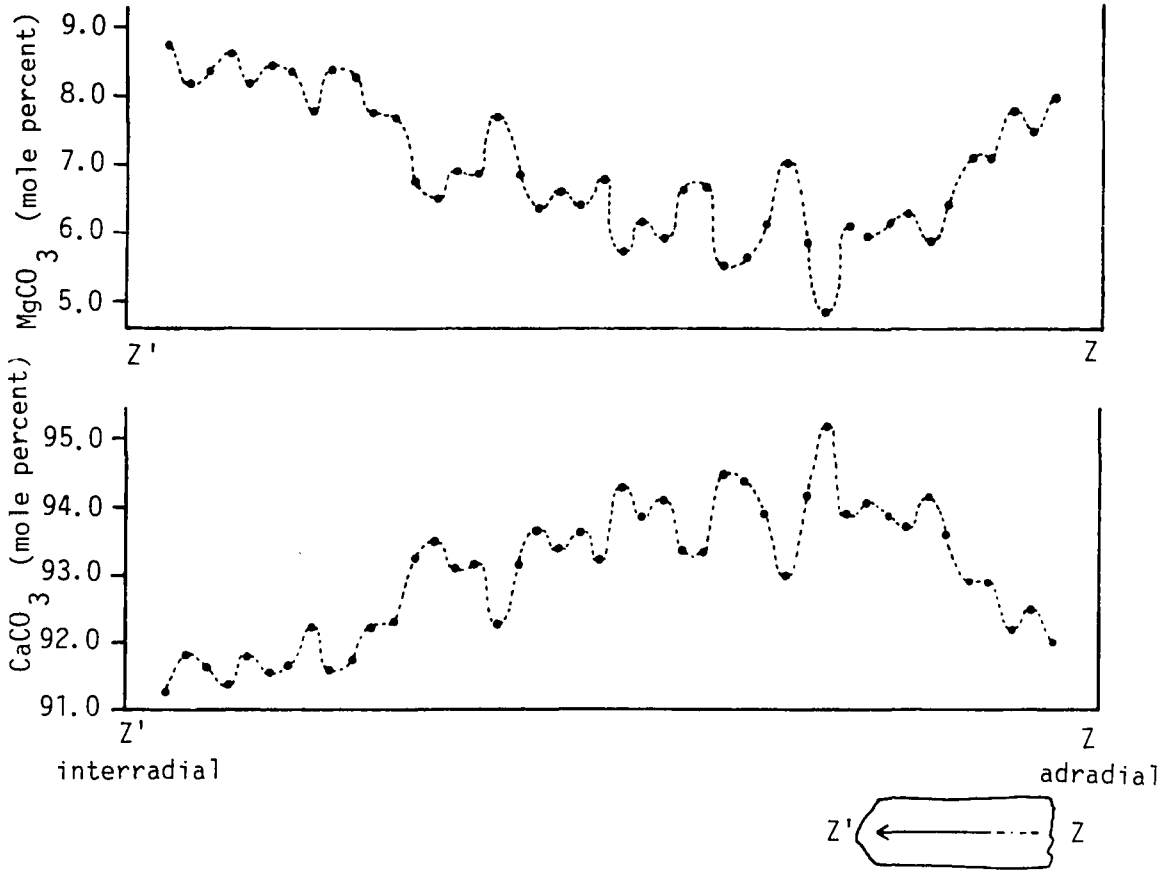

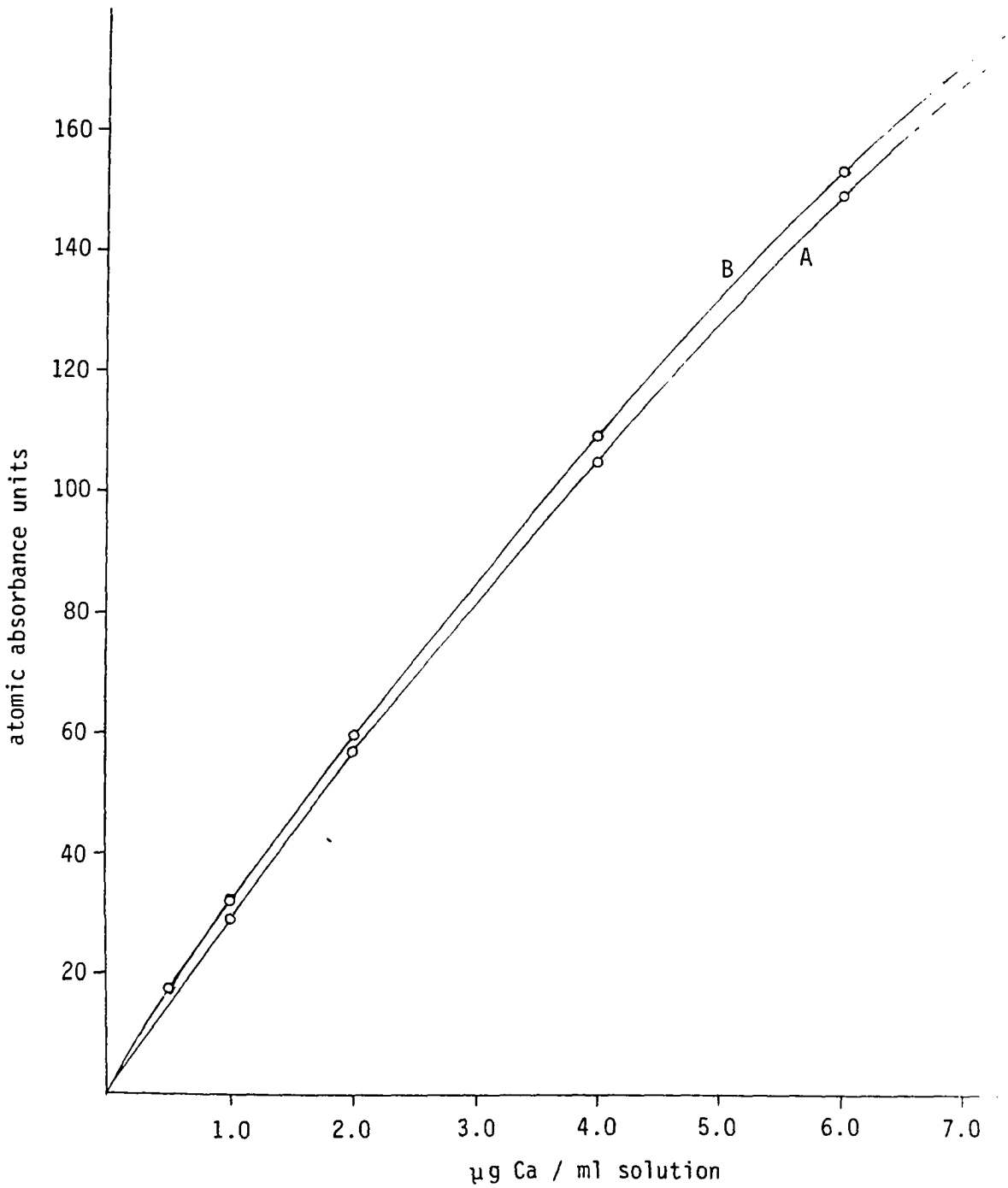

Figure D-1. Calibration curves for determination of Ca by atomic absorption analysis.

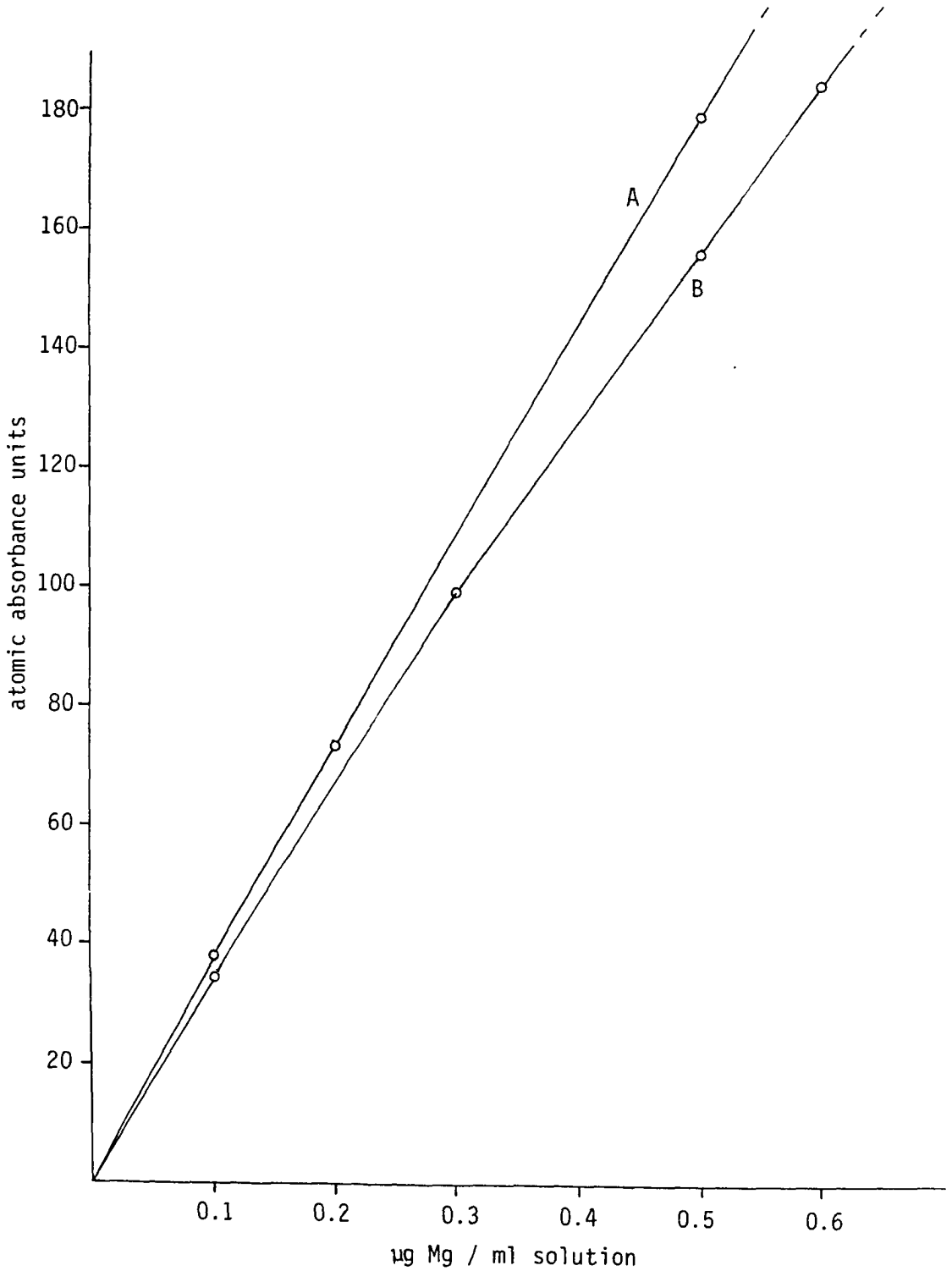

Figure D-2. Calibration curves for determination of Mg by atomic absorption analysis.

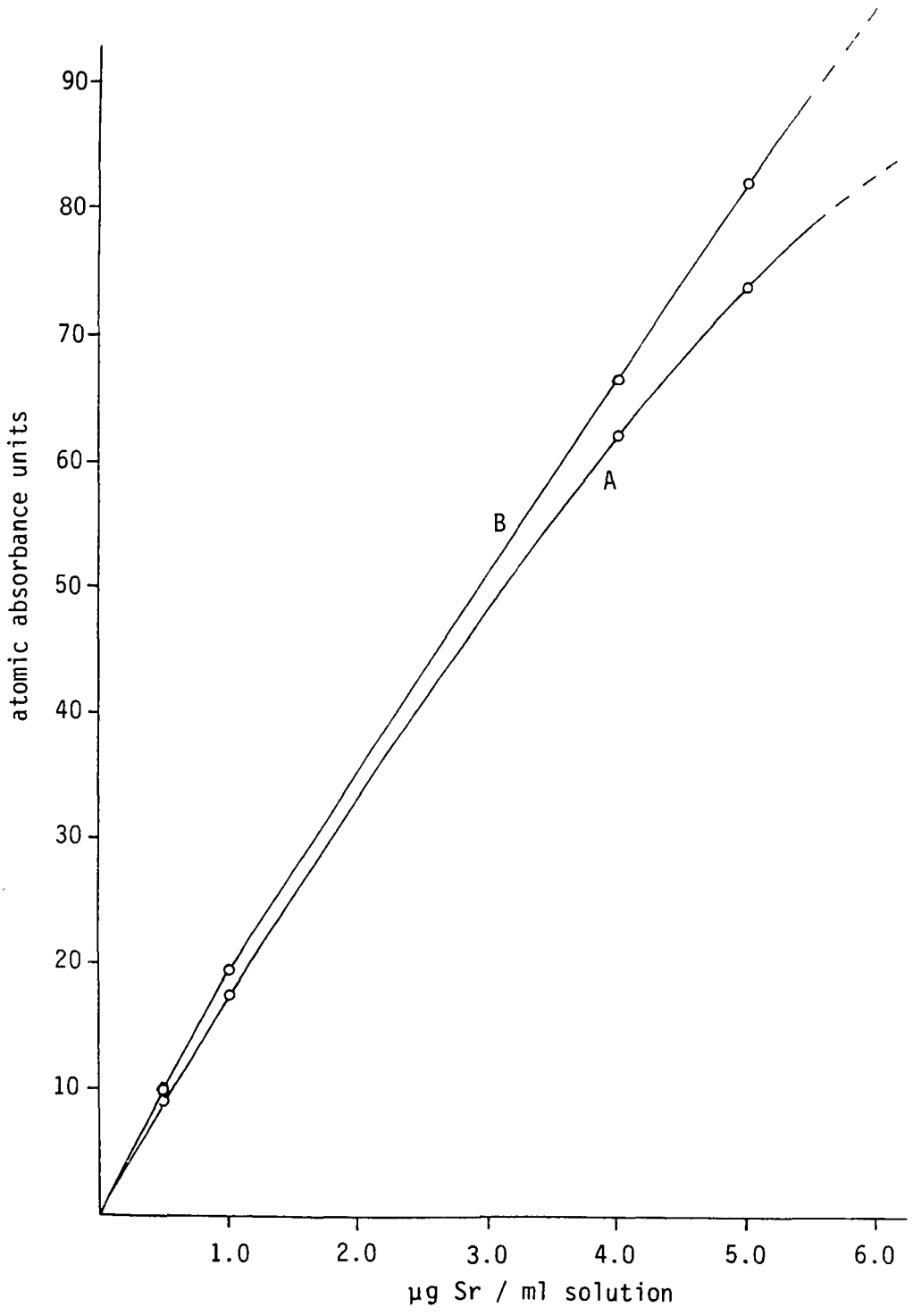

Figure D-3. Calibration curves for determination of Sr by atomic absorption analysis.

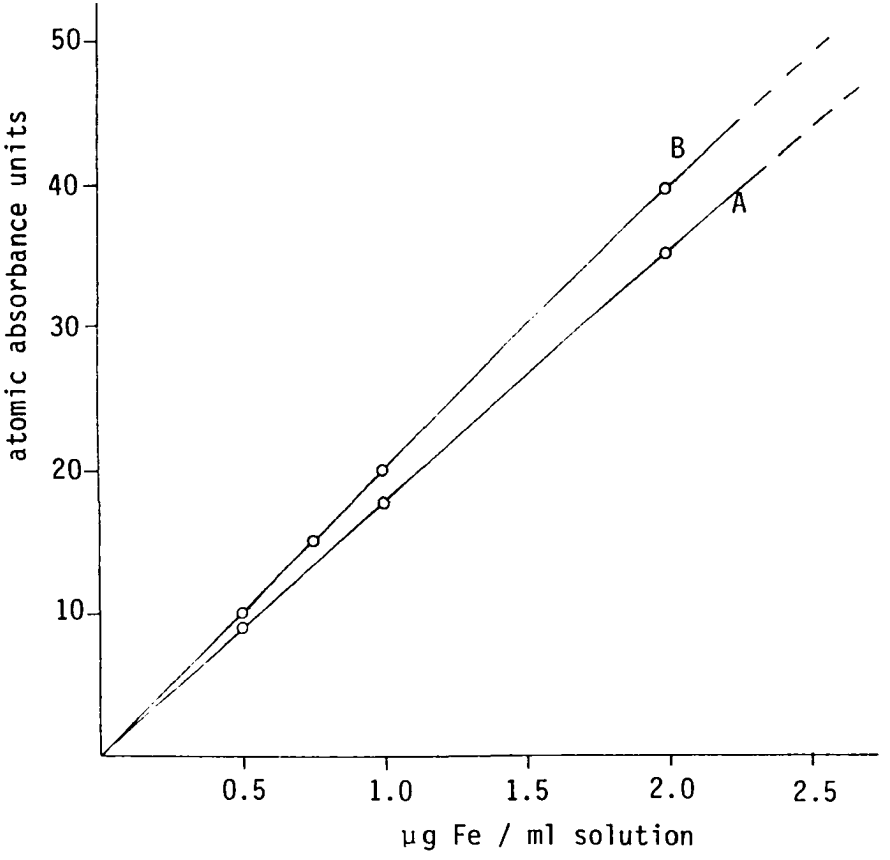

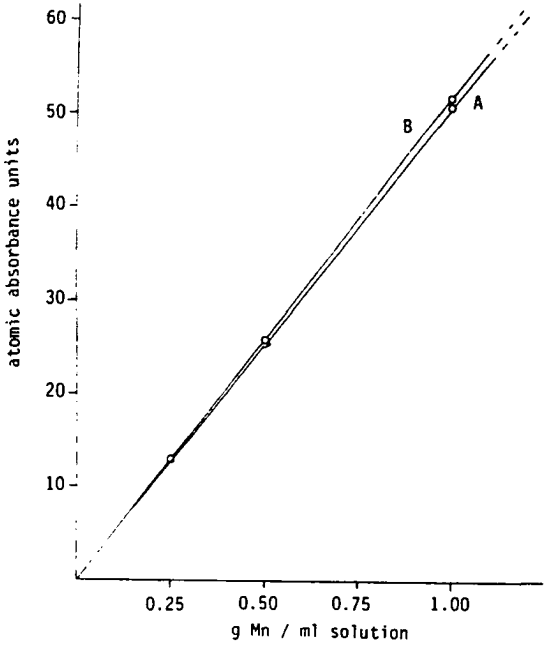

Figure D-4. Calibration curves for determination of Fe by atomic absorption analysis.
Figure D-5. Calibration curves for determination of Mn by atomic absorption analysis.

Explanation for Table D-6

A plate number

B weight of plate (grams)
B' volume of original 25 ml solution added to 20 ml aliquot for calcium and magnesium determinations (ml)

C raw absorbance measurements of calcium in replicate (atomic absorbance units)
C' concentrations of Ca present in solution, converted from replicate readings (µg/ml)
C" weight percent Ca calculated for each replicate [note that volume of original solution added to 20 ml aliquots of distilled water for Ca analysis varied; hence dilution factor used in this calculation varied for each plate; see column B']

D raw absorbance measurements of magnesium in replicate (atomic absorbance units)
D' concentrations of Mg present in solution, converted from replicate readings (µg/ml)
D" weight percent Mg calculated for each replicate [measurements for Mg from solution used for Ca; see note regarding dilution factor for C"]

E raw absorbance measurements of strontium in replicate (atomic absorbance units)
E' concentrations of Sr present in solution, converted from replicate readings (µg/ml)
E" weight percent Sr calculated for each replicate (no dilution factor; original 25 ml solution used]

F mean weight percent Ca and corresponding mole fraction Ca x 100% for each plate
F' mean weight percent Mg and corresponding mole fraction Mg x 100% for each plate
F" mean weight percent Sr and corresponding mole fraction Sr x 100% for each plate

G total of mole fractions of all cations analyzed for each plate

H mole percent Ca for each plate
H' mole percent Mg for each plate
H" mole percent Sr for each plate

Table D-6: Chemical analyses of *S. droebachiensis*: ambital series. (data graphed in Figures 9 and 10)

A	B	C	C'	C"	D	D'	D"	E	E'	E"	F	F'	F"	G	H	H'	H"
I-31	.01585	018	1.13	32.97	017	.063	1.84	20.5	1.36	.21	35.16	2.496	.235	98.26	89.27	10.45	.27
		023	1.28	37.35	038	.108	3.15	023	1.67	.26	87.72	10.27	.27				
I-32	.01510	017	1.06	32.47	014	.052	1.59	020	1.32	.22	34.155	2.405	.25	95.40	89.33	10.38	.29
		021	1.17	35.84	037	.105	3.22	023	1.67	.28	85.22	9.90	.28				
II-27	.01541	16.5	1.02	30.61	10.5	.038	1.38	20.5	1.36	.23	33.615	2.835	.245	95.80	87.55	12.17	.28
		022	1.22	36.62	49.5	.143	4.29	022	1.58	.26	83.87	11.66	.27				
II-28	.01298	014	0.85	30.29	12.5	.046	1.35	16.5	1.07	.21	32.96	2.22	.245	91.63	89.75	9.96	.28
		018	1.00	35.63	31.5	.087	3.09	018	1.27	.24	82.24	9.13	.25				
III-31	.01540	16.5	1.02	30.63	013	.047	2.19	021	1.38	.23	32.885	3.045	.26	94.87	86.49	13.21	.31
		021	1.17	35.14	045	.130	3.90	024	1.74	.29	82.05	12.53	.29				
III-32	.01322	15.5	0.95	33.24	19.5	.073	1.64	017	1.12	.22	35.16	2.46	.235	98.10	89.42	10.32	.27
		019	1.06	37.08	33.5	.094	3.28	18.5	1.32	.25	87.72	10.12	.26				
IV-31	.01495	017	1.06	32.79	12.5	.046	1.42	19.5	1.27	.21	34.495	2.24	.235	95.56	90.07	9.65	.28
		021	1.17	36.20	035	.099	3.06	022	1.58	.26	86.07	9.22	.27				
IV-32	.01477	015	0.91	28.50	010	.037	1.16	019	1.25	.21	30.375	1.91	.23	83.92	90.31	9.37	.32
		18.5	1.03	32.25	031	.085	2.66	021	1.51	.25	75.79	7.86	.27				
V-32	.01537	018	1.13	34.00	12.5	.046	1.38	20.5	1.36	.23	35.355	2.315	.26	98.02	89.99	9.71	.30
		022	1.22	36.71	038	.108	3.25	024	1.74	.29	88.21	9.52	.29				
V-33	.01287	013	0.79	28.39	013	.047	1.69	16.5	1.07	.21	31.086	2.32	.23	87.37	88.77	10.93	.30
		017	0.94	33.78	030	.082	2.95	18.5	1.32	.25	77.56	9.55	.26				
1-19	.03698	048	2.95	36.89	036	.144	1.80	055	3.85	.26	38.08	2.04	.30	103.74	91.58	8.09	.33
		057	3.14	39.27	061	.182	2.28	065	4.96	.34	95.01	8.39	.34				
1-20	.03516	46.5	2.85	37.49	034	.135	1.78	052	3.62	.26	38.475	2.06	.29	104.81	91.59	8.09	.31
		54.5	3.00	39.46	060	.178	2.34	059	4.49	.32	96.00	8.48	.33				
2-19	.03696	049	3.02	37.79	33.5	.133	1.66	057	4.02	.27	38.855	1.88	.31	105.03	92.30	7.37	.33
		058	3.19	39.92	057	.168	2.10	67.5	5.16	.35	96.94	7.74	.35				
2-20	.03332	045	2.73	37.89	035	.139	1.93	051	3.54	.27	39.14	2.215	.30	107.10	91.18	8.51	.32
		053	2.91	40.39	60.5	.180	2.50	058	4.40	.33	97.65	9.11	.34				
3-19	.03567	047	2.88	37.34	037	.148	1.92	055	3.85	.27	38.64	2.115	.30	105.46	91.42	8.25	.36
		056	3.08	39.94	060	.178	2.31	063	4.80	.33	96.41	8.70	.35				
3-20	.03313	045	2.73	38.11	033	.131	1.83	051	3.54	.27	39.715	2.075	.305	107.97	91.78	7.90	.32
		054	2.96	41.32	56.5	.166	2.32	059	4.49	.34	99.09	8.53	.35				
5-19	.03622	048	2.95	37.67	35.5	.142	1.81	055	3.85	.27	39.075	1.995	.295	106.03	91.95	7.74	.32
		57.5	3.17	40.48	058	.171	2.18	61.5	4.67	.32	97.49	8.21	.34				
5-20	.03555	046	2.81	36.56	034	.135	1.76	053	3.69	.26	38.185	2.01	.285	103.87	91.72	7.96	.32
		55.5	3.06	39.81	059	.174	2.26	59.5	4.53	.31	95.27	8.27	.33				

EXPLANATION FOR TABLE D-7

A plate number
"1" designates oldest plate in series, "38" denotes youngest plate in series;
"14A" and "14B" are randomly broken portions of the same plate

B weight of plate (grams)
B' dilution factor required in calculations for strontium, calcium and magnesium, except where "o.s." denotes original solution (25 ml)

C raw absorbance measurements of calcium in replicate (atomic absorbance units)
C' concentrations of Ca present in solution, converted from replicate readings (µg/ml)
C" weight percent Ca calculated for each replicate [note that 0.2 ml of diluted original solution was added to 20 ml aliquots of distilled water for Ca analysis; hence, two dilution factors must be used in this calculation, with the exception of plates where "o.s." indicated]

D raw absorbance measurements of magnesium in replicate (atomic absorbance units)
D' concentrations of Mg present in solution, converted from replicate readings (µg/ml)
D" weight percent Mg calculated for each replicate [measurements for Mg from solution used for Ca and same dilution factor(s) must be used in this calculation]

E raw absorbance measurements of strontium in replicate (atomic absorbance units)
E' concentrations of Sr present in solution, converted from replicate readings (µg/ml)
E" weight percent Sr calculated for each replicate [dilution factor noted in column B' must be used in calculations for Sr]

F raw absorbance measurements of iron in replicate (atomic absorbance units)
F' concentrations of Fe present in solution, converted from replicate readings (µg/ml)
F" weight percent Fe calculated for each replicate [no dilution factor; original solution used]

G raw absorbance measurements of manganese in replicate (atomic absorbance units)
G' concentrations of Mn present in solution, converted from replicate readings (µg/ml)
G" weight percent Mn calculated for each replicate [no dilution factor; original solution used]

H mean weight percent Ca and corresponding mole fraction Ca x 100% for each plate
H' mean weight percent Mg and corresponding mole fraction Mg x 100% for each plate
H" mean weight percent Sr and corresponding mole fraction Sr x 100% for each plate
H"' mean weight percent Fe and corresponding mole fraction Fe x 100% for each plate
H"" mean weight percent Mn and corresponding mole fraction Mn x 100% for each plate

J total of mole fractions of all cations analyzed for each plate

K mole percent Ca for each plate
K' mole percent Mg for each plate
K" mole percent Sr for each plate
K"' mole percent Fe for each plate
K"" mole percent Mn for each plate

Table D-7: Chemical analyses of *S. franciscanus*: interambulacral series.
(data graphed in Figures 11 and D-11 through D-15)

A	B	B'	C	C'	C"	D	D'	D"	E	E'	E"	F	F'	F"	G	G'	G"	H	H'	H"	H"'	H""	J	K	K'	K"	K"'	K""
1	.02723	o.s.	101	3.82	38.97	089	.243	2.48	054	3.38	.31	002	.12	.0110	0.5	.010	.0009	38.11	2.56	.305	.0124	.00135	105.96	89.728	9.921	.328	.021	.002
			101	3.65	37.24	086	.258	2.63	056	3.29	.30	003	.15	.0138	001	.020	.0018	95.07	10.51	.35	.022	.002						
2	.02700	o.s.	097	3.66	37.62	079	.216	2.22	053	3.32	.31	002	.12	.0111	0.5	.010	.0009	36.90	2.255	.305	.0125	.0014	101.72	90.512	9.121	.342	.022	.003
			098	3.52	36.18	075	.223	2.29	055	3.23	.30	003	.15	.0139	001	.020	.0019	92.07	9.28	.35	.022	.003						
3*	.02059	o.s.	080	2.94	39.76	063	.169	2.29	041	2.49	.30	002	.12	.0146	0.5	.010	.0012	38.95	2.365	.295	.0134	.0012	107.23	90.626	9.035	.314	.022	.002
			080	2.82	38.14	061	.179	2.42	042	2.41	.29	002	.10	.0134	0.5	.010	.0012	97.18	9.69	.34	.024	.002						
5	.06783	2.429	102	3.86	38.37	088	.240	2.39	054	3.38	.30	004	.22	.0081	001	.020	.0007	37.525	2.44	.30	.0075	-	104.02	90.007	9.651	.329	.012	.001
			102	3.69	36.68	084	.251	2.49	057	3.36	.30	004	.19	.0070	-	-	-	93.63	10.04	.34	.013	.001						
6	.06705	2.429	095	3.57	35.86	082	.223	2.21	053	3.32	.30	008	.44	.0164	002	.040	.0015	35.005	2.305	.30	.0146	.0015	97.19	89.860	9.758	.352	.027	.003
			095	3.40	34.15	079	.236	2.37	056	3.29	.30	007	.34	.0127	002	.040	.0015	87.34	9.48	.34	.026	.003						
7	.08275	2.66	105	3.99	35.66	090	.246	2.20	060	3.83	.31	006	.33	.0099	002	.040	.0012	34.675	2.225	.31	.0086	.0012	96.16	89.966	9.648	.368	.016	.002
			104	3.77	33.69	086	.258	2.31	065	3.88	.31	005	.24	.0072	002	.040	.0012	86.51	9.28	.35	.015	.002						
8	.09313	2.66	123	4.77	37.91	106	.291	2.31	067	4.39	.31	010	.56	.0150	003	.060	.0016	37.00	2.38	.31	.0148	.0019	102.49	90.072	9.554	.345	.025	.003
			122	4.54	36.09	102	.308	2.45	072	4.34	.31	011	.54	.0145	004	.080	.0021	92.32	9.79	.35	.026	.003						
9	.10861	3	119	4.60	35.26	102	.279	2.14	067	4.39	.30	007	.39	.0090	02.5	.045	.0010	34.57	2.215	.30	.0090	.0012	95.73	90.104	9.520	.357	.017	.002
			119	4.42	33.88	09[illegible]	.[illegible]	2.29	073	4.41	.30	008	.39	.0090	003	.060	.0014	86.25	9.11	.34	.016	.002						
10	.11300	3	119	4.60	33.89	102	.279	2.06	068	4.48	.30	010	.56	.0124	02.5	.045	.0010	33.225	2.105	.295	.0118	.0012	91.92	90.186	9.423	.367	.023	.002
			119	4.42	32.56	097	.292	2.15	073	4.41	.29	010	.50	.0111	003	.060	.0013	82.90	8.66	.34	.021	.002						
11	.14706	4.143	124	4.82	37.67	108	.297	2.32	070	4.64	.33	007	.39	.0066	003	.060	.0010	37.085	2.365	.33	.0066	.0012	102.65	90.139	9.480	.367	.012	.002
			125	4.67	36.50	102	.308	2.41	076	4.62	.33	008	.39	.0066	004	.080	.0014	92.53	9.73	.38	.012	.002						
12	.15167	4.143	134	5.28	40.01	117	.322	2.44	077	5.32	.36	010	.56	.0092	004	.080	.0013	39.405	2.495	.35	.0091	.0015	109.00	90.199	9.418	.366	.015	.003
			135	5.12	38.80	110	.337	2.55	082	5.02	.34	011	.54	.0089	005	.095	.0016	98.32	10.27	.40	.016	.003						
13	.22630	6.5	109	4.17	33.24	089	.243	1.94	064	4.14	.30	007	.39	.0043	005	.095	.0010	32.56	2.00	.295	.0045	.0012	89.81	90.452	9.161	.375	.009	.002
			109	4.00	31.88	086	.258	2.06	067	4.02	.29	009	.44	.0049	006	.115	.0013	81.24	8.23	.34	.008	.002						
14 A	.06216	2.429	087	3.23	35.00	072	.194	2.10	046	2.82	.28	003	.17	.0068	001	.020	.0008	33.915	2.175	.28	.0064	.0012	93.90	90.115	9.530	.341	.012	.002
			086	3.03	32.83	070	.208	2.25	049	2.84	.28	003	.15	.0060	002	.040	.0016	84.62	8.95	.32	.011	.002						
14 B	.16690	4.66	119	4.60	35.69	097	.265	2.06	066	4.31	.30	007	.39	.0058	004	.080	.0012	34.645	2.10	.295	.0058	.0013	95.43	90.580	9.054	.353	.010	.002
			117	4.33	33.60	092	.276	2.14	070	4.22	.29	008	.39	.0058	005	.095	.0014	86.44	8.64	.34	.010	.002						

see next page

15	.28692	8.33	110	4.21	33.93	088	.240	1.93	062	3.99	.29	010	.56	.0049	007	.135	.0012	33.086	1.975	.29	.0048	.0013	91.02	90.696	8.928	.364	.010	.002
			109	4.00	32.24	084	.251	2.02	066	3.94	.29	011	.54	.0047	008	.155	.0014	82.55	8.13	.33	.009	.002						
16	.35786	8.33	136	5.37	34.70	113	.311	2.01	074	5.01	.29	011	.62	.0045	008	.160	.0011	34.05	2.07	.29	.0045	.0012	93.81	90.558	9.079	.353	.009	.002
			136	5.17	33.40	108	.330	2.13	081	4.93	.29	013	.64	.0045	009	.175	.0012	84.96	8.52	.33	.008	.002						
17	.37315	8.33	145	5.79	35.88	138	.381	2.36	082	5.92	.33	012	.67	.0045	010	.195	.0013	36.005	2.44	.32	.0044	.0013	100.25	89.612	10.014	.364	.008	.002
			148	5.83	36.13	130	.406	2.52	090	5.57	.31	013	.64	.0043	010	.190	.0013	89.83	10.04	.37	.008	.002						
18	.40634	12	111	4.25	34.83	088	.240	1.97	062	3.99	.29	012	.67	.0041	008	.160	.0010	34.095	2.00	.296	.0040	.0011	93.64	90.844	8.787	.360	.007	.002
			111	4.07	33.36	083	.248	2.03	067	4.02	.30	013	.64	.0039	009	.175	.0011	85.07	8.23	.34	.007	.002						
19	.48064	12	135	5.32	36.86	110	.302	2.09	074	5.01	.31	012	.67	.0035	010	.195	.0010	36.34	2.13	.305	.0037	.0011	99.7	90.860	8.783	.349	.007	.002
			136	5.17	35.82	103	.313	2.17	080	4.87	.30	015	.75	.0039	011	.210	.0011	90.67	8.76	.35	.007	.002						
20	.54443	12	148	5.93	36.27	120	.330	2.02	081	5.78	.32	014	.78	.0036	011	.215	.0010	35.966	2.07	.305	.0038	.0011	98.61	91.001	8.637	.353	.007	.002
			148	5.83	35.66	113	.347	2.12	086	5.28	.29	017	.85	.0039	013	.250	.0011	89.73	8.52	.35	.007	.002						
21	.58414	12	154	6.25	35.63	126	.357	2.04	090	7.04	.36	016	.90	.0039	013	.300	.0013	35.06	2.08	.30	.0039	.0013	96.38	90.757	8.879	.355	.007	.002
			154	6.05	34.49	120	.372	2.12	094	5.86	.36	018	.90	.0039	015	.290	.0012	87.48	8.56	.34	.007	.002						
22	.52737	12	144	5.74	36.24	115	.316	2.00	085	6.34	.35	013	.73	.0035	011	.215	.0010	35.58	2.056	.33	.0037	.0011	97.59	90.965	8.664	.363	.006	.002
			144	5.53	34.92	109	.334	2.11	088	5.43	.31	016	.80	.0038	012	.230	.0011	88.77	8.46	.35	.006	.002						
23*	.54486	12	146	5.83	36.63	119	.327	2.05	083	6.06	.34	013	.73	.0034	011	.215	.0010	36.00	2.095	.33	.0035	.0011	98.79	90.925	8.726	.341	.006	.002
			146	5.63	35.37	111	.341	2.14	088	5.43	.32	015	.75	.0035	012	.230	.0011	89.82	8.62	.34	.006	.002						
24	.52543	12	148	5.93	37.58	120	.330	2.09	081	5.78	.33	013	.73	.0035	012	.235	.0011	37.105	2.20	.32	.0038	.0012	102.00	90.759	8.874	.358	.007	.002
			149	5.78	36.63	118	.364	2.31	087	5.36	.31	017	.85	.0040	013	.250	.0012	92.58	9.05	.37	.007	.002						
25	.57143	12	146	5.83	33.98	120	.330	1.92	084	6.20	.33	015	.84	.0037	012	.235	.0010	33.98	1.98	.315	.0037	.0010	93.30	90.873	8.731	.386	.008	.002
			148	5.83	33.98	114	.351	2.05	092	5.71	.30	017	.85	.0037	011	.210	.0009	84.78	8.15	.36	.007	.002						
26	.52487	12	136	5.37	34.07	110	.302	1.92	078	5.42	.31	012	.67	.0032	011	.215	.0010	33.436	1.936	.31	.0034	.0010	91.74	90.928	8.678	.386	.007	.002
			136	5.17	32.80	102	.308	1.95	085	5.35	.31	015	.75	.0036	011	.210	.0010	83.42	7.96	.35	.006	.002						
27	.46606	12	126	4.91	35.08	105	.287	2.05	071	4.73	.30	012	.67	.0036	010	.195	.0010	34.72	2.105	.30	.0038	.0011	95.64	90.577	9.056	.358	.007	.002
			128	4.81	34.36	100	.302	2.16	077	4.68	.30	015	.75	.0040	011	.210	.0011	86.63	8.66	.34	.007	.002						
28	.44352	12	122	4.72	35.44	099	.271	2.03	067	4.39	.30	011	.62	.0035	010	.195	.0011	34.915	2.05	.295	.0036	.0011	95.89	90.845	8.795	.351	.006	.002
			123	4.58	34.39	092	.276	2.07	072	4.34	.29	013	.64	.0036	010	.190	.0011	87.11	8.43	.34	.006	.002						
29	.41401	12	123	4.77	38.37	097	.265	2.13	067	4.39	.32	011	.62	.0037	009	.180	.0011	37.605	2.165	.315	.0040	.0011	103.10	91.002	8.640	.349	.007	.002
			123	4.58	36.84	091	.273	2.20	070	4.22	.31	014	.69	.0042	010	.190	.0011	93.83	8.91	.36	.007	.002						
30	.38337	8.33	149	6.01	36.25	121	.332	2.00	083	6.06	.33	009	.50	.0033	009	.180	.0012	35.705	2.045	.315	.0036	.0012	97.87	91.027	8.597	.368	.006	.002
			150	5.83	35.16	113	.347	2.09	088	5.43	.30	012	.59	.0038	009	.175	.0011	89.08	8.41	.36	.006	.002						
31	.34515	8.33	140	5.56	37.25	117	.322	2.16	077	4.32	.26	010	.56	.0041	009	.180	.0013	36.58	2.22	.28	.0044	.0014	100.73	90.605	9.068	.318	.008	.002
			140	5.36	35.91	111	.341	2.28	081	4.93	.30	013	.64	.0046	010	.190	.0014	91.27	9.13	.32	.008	.002						

see next page

32	.29040	8.33	113	4.33	34.48	088	.240	1.91	065	4.22	.30	008	.44	.0038	007	.135	.0012	33.966	1.94	.296	.0041	.0012	93.07	91.052	8.576	.362	.008	.002
			114	4.20	33.45	083	.248	1.97	068	4.08	.29	010	.50	.0043	007	.135	.0012	84.74	7.98	.34	.007	.002						
33	.24731	6.5	119	4.60	33.55	092	.251	1.83	071	4.73	.31	008	.44	.0044	006	.115	.0012	32.895	1.865	.30	.0044	.0012	90.10	91.093	8.516	.380	.009	.002
			119	4.42	32.24	087	.261	1.90	074	4.48	.29	009	.44	.0044	006	.115	.0012	82.07	7.67	.34	.008	.002						
34	.18544	5.4	116	4.46	36.05	090	.246	1.99	065	4.22	.31	006	.33	.0044	004	.080	.0011	35.32	2.01	.305	.0045	.0012	96.75	91.082	8.548	.360	.008	.002
			116	4.28	34.59	084	.251	2.03	068	4.08	.30	007	.34	.0046	005	.095	.0013	88.12	8.27	.35	.008	.002						
35	.16235	4.33	125	4.86	35.99	097	.265	1.96	068	4.48	.30	006	.33	.0051	004	.080	.0012	35.47	2.00	.296	.0048	.0012	97.07	91.166	8.476	.347	.009	.002
			126	4.72	34.95	092	.276	2.04	073	4.41	.29	006	.39	.0045	004	.080	.0012	88.50	8.23	.34	.009	.002						
36	.11992	3.5	113	4.33	35.08	093	.253	2.05	063	4.07	.30	004	.22	.0046	003	.060	.0013	34.675	2.09	.295	.0043	.0015	95.46	90.628	9.008	.353	.008	.003
			115	4.23	34.27	088	.263	2.13	067	4.02	.29	004	.19	.0040	004	.080	.0017	86.51	8.60	.341	.008	.003						
38	.02172	o.s.	084	3.10	39.64	064	.172	2.20	044	2.79	.32	003	.17	.0196	0.5	.010	.0012	39.066	2.23	.315	.0185	.0015	107.04	91.058	8.572	.336	.031	.003
			085	3.01	38.49	060	.177	2.26	047	2.72	.31	003	.15	.0173	001	.020	.0023	97.47	9.18	.36	.033	.003						

EXPLANATION FOR TABLE D-8

A plate number
"1" designates oldest plate in series

B weight of plate (grams)
B' volume of original 25 ml solution added to 20 ml aliquot for calcium and magnesium determinations (ml)

C raw absorbance measurements of calcium in replicate (atomic absorbance units)
C' concentrations of Ca present in solution, converted from replicate readings (µg/ml)
C" weight percent Ca calculated for each replicate [note that volume of original solution added to 20 ml aliquots of distilled water for Ca analysis varied; hence dilution factor used in this calculation varied for each plate; see column B']

D raw absorbance measurements of magnesium in replicate (atomic absorbance units)
D' concentrations of Mg present in solution, converted from replicate readings (µg/ml)
D" weight percent Mg calculated for each replicate [measurements for Mg from solution used for Ca; see note regarding dilution factor for C"]

E raw absorbance measurements of strontium in replicate (atomic absorbance units)
E' concentrations of Sr present in solution, converted from replicate readings (µg/ml)
E" weight percent Sr calculated for each replicate (no dilution factor; original 25 ml solution used]

F mean weight percent Ca and corresponding mole fraction Ca x 100% for each plate
F' mean weight percent Mg and corresponding mole fraction Mg x 100% for each plate
F" mean weight percent Sr and corresponding mole fraction Sr x 100% for each plate

G total of mole fractions of all cations analyzed for each plate

H mole percent Ca for each plate
H' mole percent Mg for each plate
H" mole percent Sr for each plate

Table D-8: Chemical analyses of *S. droebachiensis*: interambulacral series. (data graphed in Figure 12)

A	B	B'	C	C'	C"	D	D'	D"	E	E'	E"	F	F'	F"	G	H	H'	H"
1/3	.01333	13	093	3.47	34.26	082	.223	2.20	049	3.03	.30	34.11	2.245	.30	94.68	89.88	9.76	.36
			096	3.44	33.96	078	.232	2.29	053	3.10	.30	85.10	9.24	.34				
2/4	.01656	17	094	3.51	36.31	079	.215	2.22	045	2.76	.28	36.15	2.26	.285	99.82	90.35	9.32	.33
			097	3.48	35.99	075	.222	2.30	049	2.84	.29	90.19	9.30	.33				
5	.01107	11	088	3.27	32.73	075	.204	2.04	044	2.79	.28	32.78	2.075	.275	90.64	90.24	9.42	.34
			092	3.28	32.83	071	.211	2.11	047	2.72	.27	81.79	8.54	.31				
6	.01245	12	093	3.47	33.65	080	.218	2.11	046	2.82	.27	33.89	2.155	.275	93.74	90.21	9.46	.33
			098	3.52	34.13	076	.227	2.20	050	2.91	.28	84.56	8.87	.31				
7	.01577	15	091	3.38	32.41	077	.209	2.00	048	2.97	.28	32.13	2.04	.29	88.88	90.19	9.44	.37
			093	3.32	31.83	073	.217	2.08	054	3.17	.30	80.16	8.39	.33				
8	.01817	18	088	3.27	32.66	074	.202	2.02	047	2.89	.29	32.46	2.05	.29	89.75	90.24	9.39	.37
			091	3.23	32.26	070	.208	2.08	051	2.97	.29	80.99	8.43	.33				
9	.01796	18	089	3.31	33.43	073	.198	2.00	047	2.89	.29	33.28	2.03	.295	91.72	90.53	9.10	.37
			092	3.28	33.13	069	.204	2.06	052	3.03	.30	83.03	8.35	.34				
10	.01963	20	087	3.23	33.29	075	.204	2.10	048	2.97	.30	33.135	2.135	.30	91.79	90.06	9.57	.37
			090	3.20	32.98	071	.211	2.17	051	2.97	.30	82.67	8.78	.34				
11	.02108	21	103	3.90	39.20	085	.232	2.33	050	3.11	.31	39.20	2.36	.31	107.86	90.67	9.00	.32
			107	3.90	39.20	080	.238	2.39	053	3.10	.31	97.80	9.71	.35				
12	.02661	26	093	3.47	34.26	076	.207	2.04	050	3.11	.30	34.31	2.09	.30	94.54	90.54	9.10	.36
			097	3.48	34.36	073	.217	2.14	053	3.10	.30	85.60	8.60	.34				
13	.02910	29	093	3.47	34.93	076	.207	2.08	049	3.03	.30	35.43	2.11	.30	97.42	90.74	8.91	.35
			099	3.57	35.93	072	.213	2.14	052	3.03	.30	88.40	8.68	.34				
14	.02908	29	091	3.38	34.02	073	.198	1.99	049	3.03	.30	34.12	2.02	.305	93.79	90.77	8.86	.37
			095	3.40	34.22	069	.204	2.05	053	3.10	.31	85.13	8.31	.35				
15	.03268	32	092	3.43	33.90	073	.198	1.96	048	2.97	.29	33.75	2.025	.295	92.88	90.67	8.97	.37
			095	3.40	33.60	071	.211	2.09	053	3.10	.30	84.21	8.33	.34				
16	.03424	34	094	3.51	35.24	081	.221	2.22	049	3.03	.30	34.89	2.26	.305	96.70	90.02	9.62	.36
			096	3.44	34.54	077	.229	2.30	053	3.10	.31	87.05	9.30	.35				
17	.04279	43	090	3.34	33.89	075	.204	2.07	048	2.97	.30	33.79	2.105	.30	93.31	90.35	9.28	.36
			093	3.32	33.69	071	.211	2.14	052	3.03	.30	84.31	8.66	.34				
18	.04397	44	084	3.10	31.31	066	.178	1.80	049	3.03	.30	31.21	1.84	.31	85.79	90.77	9.96	.41
			087	3.08	31.11	063	.186	1.88	054	3.17	.32	77.87	7.57	.35				
19	.04601	46	092	3.43	34.64	071	.192	1.94	050	3.11	.31	34.69	1.99	.315	95.10	91.01	8.61	.38
			096	3.44	34.74	068	.202	2.04	054	3.17	.32	86.55	8.19	.36				
20	.04714	47	093	3.47	34.97	073	.198	2.00	050	3.11	.31	35.475	2.05	.31	97.29	90.98	8.66	.36
			099	3.57	35.98	070	.208	2.10	053	3.10	.31	88.51	8.43	.35				
21	.04075	40	091	3.38	33.47	073	.198	1.96	051	3.17	.31	33.966	2.025	.31	93.42	90.71	8.92	.37
			097	3.48	34.46	071	.211	2.09	054	3.17	.31	84.74	8.33	.35				
22	.04138	41	094	3.51	35.11	074	.202	2.02	051	3.17	.31	35.16	2.05	.31	96.50	90.90	8.74	.36
			098	3.52	35.21	070	.208	2.08	054	3.17	.31	87.72	8.43	.35				

next page

23	.04239	42	093	3.47	34.72	072	.195	1.95	050	3.11	.31	34.57	1.995	.31	94.81	90.97	8.66	.37
			096	3.44	34.42	069	.204	2.04	053	3.10	.31	86.25	8.21	.35				
24	.04161	42	090	3.34	34.06	068	.183	1.87	049	3.03	.31	33.755	1.935	.315	92.54	91.01	8.60	.39
			092	3.28	33.45	066	.196	2.00	054	3.17	.32	84.22	7.96	.36				
25	.03688	37	098	3.68	37.27	074	.202	2.05	050	3.11	.31	37.32	2.08	.315	102.03	91.26	8.39	.35
			102	3.69	37.37	070	.208	2.11	054	3.17	.32	93.11	8.56	.36				
26	.03516	35	092	3.43	34.45	086	.234	2.35	049	3.03	.30	34.50	2.37	.31	96.18	89.50	10.14	.36
			096	3.44	34.55	080	.238	2.39	054	3.17	.32	86.08	9.75	.35				
27	.03389	34	091	3.38	34.24	071	.192	1.94	050	3.11	.31	34.14	1.966	.31	93.61	90.99	8.63	.37
			094	3.36	34.04	066	.196	1.99	053	3.10	.31	85.18	8.08	.35				
28	.03241	32	095	3.56	35.51	073	.198	1.98	051	3.17	.31	35.56	2.005	.31	97.32	91.16	8.48	.36
			099	3.57	35.61	069	.204	2.03	054	3.17	.31	88.72	8.25	.35				
29	.02907	29	090	3.34	33.62	071	.192	1.93	050	3.11	.31	33.72	1.98	.31	92.63	90.82	8.80	.38
			094	3.36	33.82	068	.202	2.03	053	3.10	.31	84.13	8.15	.35				
30	.02630	26	091	3.38	33.75	071	.192	1.92	049	3.03	.30	33.85	1.97	.30	92.91	90.91	8.73	.37
			095	3.40	33.95	068	.202	2.02	052	3.03	.30	84.46	8.11	.34				
31	.02199	22	088	3.27	33.03	068	.183	1.85	048	2.97	.30	33.28	1.925	.305	91.30	90.94	8.67	.38
			093	3.32	33.53	067	.198	2.00	053	3.10	.31	83.03	7.92	.35				
32	.02022	20	090	3.34	33.40	069	.186	1.86	047	2.89	.29	33.30	1.91	.29	91.27	91.03	8.61	.36
			093	3.32	33.20	066	.196	1.96	051	2.97	.29	83.08	7.86	.33				
33	.01629	16	092	3.43	34.01	069	.186	1.84	047	2.89	.28	33.86	1.87	.285	92.50	91.33	8.31	.36
			095	3.40	33.71	065	.192	1.90	051	2.97	.29	84.48	7.69	.33				
34	.01396	14	090	3.34	33.73	068	.183	1.85	046	2.82	.28	33.835	1.88	.28	92.48	91.28	8.37	.35
			094	3.36	33.94	064	.189	1.91	049	2.84	.28	84.42	7.74	.32				
35	.01104	11	087	3.23	32.62	064	.172	1.74	045	2.76	.28	32.47	1.765	.28	88.59	91.44	8.20	.36
			090	3.20	32.32	060	.177	1.79	049	2.84	.28	81.01	7.26	.32				
36	.00623	6	089	3.31	32.35	066	.178	1.74	045	2.76	.27	32.205	1.78	.27	87.98	91.33	8.32	.35
			092	3.28	32.06	063	.186	1.82	048	2.78	.27	80.35	7.32	.31				
37	.00231	3	071	2.57	33.86	052	.138	1.82	033	1.98	.26	33.595	1.89	.26	91.90	91.21	8.47	.33
			073	2.53	33.33	051	.149	1.96	035	1.97	.26	83.82	7.78	.30				

EXPLANATION FOR TABLE D-9

A plate number
"1" designates oldest plate in series

B weight of plate (grams)
B' volume of original 25 ml solution added to 20 ml aliquot for calcium and magnesium determinations (ml)

C raw absorbance measurements of calcium in replicate (atomic absorbance units)
C' concentrations of Ca present in solution, converted from replicate readings (µg/ml)
C" weight percent Ca calculated for each replicate [note that volume of original solution added to 20 ml aliquots of distilled water for Ca analysis varied; hence dilution factor used in this calculation varied for each plate; see column B']

D raw absorbance measurements of magnesium in replicate (atomic absorbance units)
D' concentrations of Mg present in solution, converted from replicate readings (µg/ml)
D" weight percent Mg calculated for each replicate [measurements for Mg from solution used for Ca; see note regarding dilution factor for C"]

E raw absorbance measurements of strontium in replicate (atomic absorbance units)
E' concentrations of Sr present in solution, converted from replicate readings (µg/ml)
E" weight percent Sr calculated for each replicate (no dilution factor; original 25 ml solution used]

F mean weight percent Ca and corresponding mole fraction Ca x 100% for each plate
F' mean weight percent Mg and corresponding mole fraction Mg x 100% for each plate
F" mean weight percent Sr and corresponding mole fraction Sr x 100% for each plate

G total of mole fractions of all cations analyzed for each plate

H mole percent Ca for each plate
H' mole percent Mg for each plate
H" mole percent Sr for each plate

Table D-9: Chemical analyses of *S. droebachiensis*: interambulacral series. (data not graphed)

A	B	B'	C	C'	C"	D	D'	D"	E	E'	E"	F	F'	F"	G	H	H'	H"
1/3	.00572	1.2	118	4.26	33.01	089	.246	1.91	006	.32	.13	32.895	1.89	.145	90.02	91.17	8.64	.19
			122	4.23	32.78	089	.241	1.87	006	.38	.16	82.07	7.78	.17				
2	.00410	1.8	120	4.34	32.05	096	.267	1.97	003	.16	.10	32.57	1.945	.14	89.41	90.87	8.95	.18
			128	4.48	33.08	096	.260	1.92	003	.28	.18	81.25	8.00	.16				
4	.00543	1.4	133	4.88	34.53	103	.286	2.02	006	.32	.16	34.00	2.01	.16	93.28	90.94	8.87	.19
			134	4.73	33.47	104	.282	2.00	005	.32	.16	84.83	8.27	.18				
5	.00324	2.3	117	4.22	31.97	096	.267	2.02	002	.11	.09	31.435	2.025	.095	86.87	90.28	9.59	.13
			118	4.08	30.90	099	.268	2.03	002	.12	.10	78.43	8.33	.11				
6	.00835	.9	134	4.92	34.00	102	.284	1.96	010	.54	.17	33.485	1.935	.185	91.72	91.09	8.68	.23
			135	4.77	32.97	102	.277	1.91	010	.65	.20	83.55	7.96	.21				
7	.00990	.7	127	4.64	34.71	094	.262	1.96	013	.71	.18	34.23	1.95	.20	93.65	91.19	8.56	.25
			129	4.52	33.75	096	.260	1.94	013	.86	.22	85.40	8.02	.23				
8	.01108	.7	140	5.19	34.57	105	.293	1.95	023	1.32	.30	34.00	1.915	.39	93.16	91.06	8.46	.48
			141	5.02	33.43	104	.282	1.88	028	2.12	.48	84.83	7.88	.45				
9	.01243	.6	140	5.19	35.93	103	.286	1.98	059	3.66	.76	35.06	1.965	.975	96.67	90.49	8.36	1.15
			139	4.94	34.19	104	.282	1.95	068	5.72	1.19	87.48	8.08	1.11				
10	.01428	.5	136	5.02	35.98	100	.278	1.99	021	1.20	.21	35.265	1.975	.24	96.39	91.29	8.43	.28
			136	4.82	34.55	101	.274	1.96	021	1.51	.27	87.99	8.13	.27				
11	.01742	.4	135	4.98	36.49	099	.275	2.02	27.5	1.62	.24	36.05	1.99	.265	98.44	91.38	8.32	.30
			137	4.86	35.61	099	.268	1.96	026	1.94	.29	89.95	8.19	.30				
12	.02063	.4	155	5.85	36.21	114	.318	1.97	32.5	1.93	.23	36.086	1.965	.26	98.41	91.48	8.21	.30
			159	5.81	35.96	116	.316	1.96	31.5	2.42	.29	90.03	8.08	.30				
13	.02042	.4	145	5.42	33.88	108	.302	1.89	038	2.29	.29	34.535	1.87	.335	94.24	91.44	8.16	.40
			155	5.63	35.19	109	.296	1.85	039	3.06	.38	86.17	7.69	.38				
14	.02316	.3	124	4.52	32.96	086	.239	1.74	36.5	2.18	.24	32.56	1.725	.265	88.64	91.65	8.01	.34
			126	4.41	32.16	087	.235	1.71	035	2.71	.29	81.24	7.10	.30				
15	.02497	.3	148	5.53	37.42	102	.284	1.92	041	2.48	.25	36.88	1.905	.28	100.18	91.85	7.83	.32
			149	5.37	36.34	103	.279	1.89	039	3.07	.31	92.02	7.84	.32				
16	.03104	.2	125	4.56	37.14	082	.228	1.86	052	3.19	.26	36.325	1.82	.29	98.45	92.06	7.61	.34
			125	4.36	35.51	081	.219	1.78	49.5	4.00	.32	90.63	7.49	.33				
17	.03115	.2	125	4.56	36.90	081	.226	1.83	051	3.12	.25	36.295	1.80	.28	98.29	92.14	7.54	.33
			126	4.41	35.69	081	.219	1.77	048	3.86	.31	90.56	7.41	.32				
18	.03134	.2	133	4.88	39.37	085	.237	1.91	054	3.32	.27	38.48	1.87	.305	104.05	92.27	7.39	.34
			132	4.66	37.59	084	.227	1.83	052	4.20	.34	96.01	7.69	.35				
21	.03287	.2	123	4.42	33.92	077	.213	1.63	058	3.59	.27	33.19	1.63	.30	89.86	92.15	7.47	.38
			122	4.23	32.46	078	.212	1.63	054	4.39	.33	82.81	6.71	.34				
22	.03750	.2	146	5.45	36.70	095	.264	1.78	064	4.00	.26	35.99	1.76	.295	97.38	92.22	7.43	.35
			146	5.24	35.28	095	.258	1.74	60.5	5.09	.33	89.80	7.24	.34				

23	.03722	.2	138	5.11	34.68	091	.253	1.72	63.5	3.96	.27	34.24	1.685	.30	92.70	92.16	7.48	.37
			140	4.98	33.80	090	.243	1.65	59.5	4.90	.33	85.43	6.93	.34				
24	.03252	.2	132	4.84	37.60	089	.246	1.91	055	3.39	.26	37.525	1.88	.295	101.71	92.06	7.61	.33
			136	4.82	37.45	088	.238	1.85	053	4.30	.33	93.63	7.74	.34				
25	.03329	.2	103	3.63	27.74	068	.187	1.43	55.5	3.42	.26	27.935	1.425	.29	75.86	91.88	7.72	.40
			108	3.68	28.13	069	.186	1.42	052	4.20	.32	69.70	5.86	.30				
26	.03204	.2	128	4.68	37.22	080	.223	1.76	057	3.52	.28	36.01	1.75	.315	97.41	92.24	7.39	.37
			126	4.41	34.80	082	.221	1.74	054	4.39	.35	89.85	7.20	.36				
27	.02813	.3	155	5.87	35.34	100	.278	1.67	047	2.87	.26	34.495	1.67	.295	93.28	92.27	7.36	.36
			154	5.59	33.65	102	.277	1.67	46.5	3.72	.33	86.07	6.87	.34				
28	.02711	.3	157	5.95	37.74	103	.286	1.81	78.5	4.99	.47	37.135	1.795	.565	100.68	92.02	7.34	.64
			158	5.76	36.53	103	.280	1.78	080	7.02	.66	92.65	7.39	.64				
29	.02434	.3	137	5.06	35.23	086	.239	1.66	040	2.41	.25	34.67	1.67	.285	93.70	92.32	7.33	.35
			138	4.90	34.11	089	.241	1.68	39.5	3.11	.32	86.50	6.87	.33				
30	.02155	.3	134	4.92	38.53	085	.237	1.86	036	2.16	.25	37.945	1.85	.285	102.61	92.26	7.42	.32
			135	4.77	37.36	087	.235	1.84	036	2.80	.32	94.67	7.61	.33				
31	.01879	.4	146	5.45	36.96	098	.273	1.85	29.5	1.74	.23	36.69	1.825	.265	99.35	92.14	7.56	.30
			149	5.37	36.42	098	.266	1.80	030	2.29	.30	91.54	7.51	.30				
32	.01580	.4	120	4.34	35.02	078	.217	1.75	024	1.39	.22	34.94	1.735	.25	94.61	92.15	7.55	.31
			124	4.32	34.86	079	.213	1.72	24.5	1.82	.28	87.18	7.14	.29				
33	.01267	.5	113	4.06	32.77	074	.204	1.65	018	1.00	.19	32.85	1.64	.215	88.96	92.13	7.59	.28
			118	4.08	32.93	075	.202	1.63	018	1.27	.24	81.96	6.75	.25				
34	.00953	.7	117	4.22	32.84	084	.233	1.81	012	.65	.16	32.76	1.80	.19	89.37	91.46	8.29	.25
			121	4.20	32.68	085	.230	1.79	013	.86	.22	81.74	7.41	.22				
35	.00719	1.5	184	7.26	36.27	120	.335	1.67	008	.43	.15	35.75	1.66	.18	96.24	92.68	7.10	.22
			185	7.05	35.23	121	.330	1.65	009	.58	.21	89.20	6.83	.21				
36	.00453	1.5	121	4.38	34.88	077	.213	1.70	006	.32	.16	34.16	1.695	.19	92.42	92.22	7.54	.24
			121	4.20	33.44	078	.212	1.69	007	.44	.22	85.23	6.97	.22				
37	.00180	4	114	4.09	34.08	082	.228	1.90	002	.11	.14	33.54	1.895	.135	91.63	91.32	8.51	.16
			115	3.96	33.00	084	.227	1.89	1.5	.10	.13	83.68	7.80	.15				
38	.00046	14	083	2.83	34.36	090	.250	3.04	-	-	-	34.12	3.215	-	97.53	87.29	12.71	-
			085	2.79	33.88	091	.246	2.99				85.13	12.40	-				

EXPLANATION FOR TABLE D-10

A plate number
"1" designates oldest plate in series

B weight of plate (grams)
B' volume of original 25 ml solution added to 20 ml aliquot for calcium and magnesium determinations (ml)

C raw absorbance measurements of calcium in replicate (atomic absorbance units)
C' concentrations of Ca present in solution, converted from replicate readings (µg/ml)
C" weight percent Ca calculated for each replicate [note that volume of original solution added to 20 ml aliquots of distilled water for Ca analysis varied; hence dilution factor used in this calculation varied for each plate; see column B']

D raw absorbance measurements of magnesium in replicate (atomic absorbance units)
D' concentrations of Mg present in solution, converted from replicate readings (µg/ml)
D" weight percent Mg calculated for each replicate [measurements for Mg from solution used for Ca; see note regarding dilution factor for C"]

E raw absorbance measurements of strontium in replicate (atomic absorbance units)
E' concentrations of Sr present in solution, converted from replicate readings (µg/ml)
E" weight percent Sr calculated for each replicate (no dilution factor; original 25 ml solution used]

F mean weight percent Ca and corresponding mole fraction Ca x 100% for each plate
F' mean weight percent Mg and corresponding mole fraction Mg x 100% for each plate
F" mean weight percent Sr and corresponding mole fraction Sr x 100% for each plate

G total of mole fractions of all cations analyzed for each plate

H mole percent Ca for each plate
H' mole percent Mg for each plate
H" mole percent Sr for each plate

Table D-10: Chemical analyses of *S. purpuratus*: interambulacral series.
(data graphed in Figure 13)

A	B	B'	C	C'	C"	D	D'	D"	E	E'	E"	F	F'	F"	G	H	H'	H"
1	.00455	5	071	2.57	31.01	058	.156	1.88	033	1.98	.25	30.77	1.935	.25	84.98	90.34	9.37	.29
			073	2.53	30.53	056	.165	1.99	036	2.03	.25	76.77	7.96	.29				
2	.00504	5	083	3.06	33.97	070	.189	2.10	045	2.76	.28	33.80	2.15	.28	93.50	90.19	9.47	.34
			086	3.03	33.63	067	.198	2.20	049	2.84	.28	84.33	8.85	.32				
3	.00573	6	082	3.02	35.29	075	.204	2.38	047	2.89	.30	35.345	2.425	.30	98.51	89.52	10.13	.35
			086	3.03	35.40	071	.211	2.47	049	2.84	.30	88.19	9.98	.34				
4	.00913	9	091	3.38	37.11	081	.221	2.43	050	3.11	.31	37.22	2.47	.30	103.36	89.84	9.83	.33
			095	3.40	37.33	077	.229	2.51	051	2.97	.29	92.86	10.16	.34				
5	.00540	5	096	3.61	37.10	083	.226	2.32	050	3.11	.29	36.64	2.35	.285	101.42	90.14	9.53	.33
			098	3.52	36.18	078	.232	2.38	052	3.03	.28	91.42	9.67	.33				
6	.00866	9	095	3.56	40.88	087	.237	2.72	044	2.79	.29	40.65	2.75	.285	113.06	89.70	10.00	.29
			098	3.52	40.42	081	.242	2.78	046	2.66	.28	101.42	11.31	.33				
7	.01102	11	088	3.27	36.30	077	.209	2.32	049	3.03	.30	35.91	2.34	.30	99.57	89.99	9.67	.34
			090	3.20	35.52	072	.213	2.36	051	2.97	.30	89.60	9.63	.34				
8	.01149	11	081	2.98	31.64	075	.204	2.17	046	2.82	.27	31.375	2.19	.27	87.60	89.36	10.29	.35
			083	2.93	31.11	070	.208	2.21	049	2.84	.27	78.28	9.01	.31				
9	.00968	10	083	3.06	35.02	070	.189	2.16	046	2.82	.29	34.845	2.215	.29	96.38	90.21	9.45	.34
			086	3.03	34.67	067	.198	2.27	049	2.84	.29	86.94	9.11	.33				
10	.01181	12	086	3.18	35.90	073	.198	2.24	047	2.89	.29	35.56	2.295	.295	98.50	90.07	9.58	.35
			088	3.12	35.22	070	.208	2.35	050	2.91	.30	88.72	9.44	.34				
11	.00969	10	085	3.14	35.93	071	.192	2.20	045	2.76	.28	35.815	2.265	.285	99.01	90.25	9.41	.33
			088	3.12	35.70	069	.204	2.33	048	2.78	.29	89.36	9.32	.33				
12	.01736	17	088	3.27	35.46	075	.204	2.21	047	2.89	.28	35.73	2.26	.28	98.77	90.26	9.42	.32
			093	3.32	36.00	072	.213	2.31	049	2.84	.28	89.15	9.30	.32				
13	.01280	13	087	3.23	36.41	071	.192	2.16	047	2.89	.29	36.245	2.22	.285	99.89	90.53	9.14	.33
			090	3.20	36.08	068	.202	2.28	047	2.72	.28	90.43	9.13	.33				
14	.02294	23	086	3.18	35.45	070	.189	2.11	047	2.89	.29	35.115	2.16	.29	96.83	90.48	9.18	.34
			088	3.12	34.78	067	.198	2.21	049	2.84	.29	87.61	8.89	.33				
15	.02780	28	086	3.18	35.55	071	.192	2.15	047	2.89	.29	35.44	2.215	.29	97.86	90.35	9.31	.34
			089	3.16	35.33	069	.204	2.28	050	2.91	.29	88.42	9.11	.33				
16	.03258	33	091	3.38	37.98	075	.204	2.29	047	2.89	.29	37.64	2.33	.29	103.83	90.45	9.24	.32
			093	3.32	37.30	071	.211	2.37	050	2.91	.29	93.91	9.59	.33				
17	.03410	34	092	3.42	37.85	077	.209	2.31	047	2.89	.29	37.295	2.385	.295	103.20	90.16	9.51	.33
			093	3.32	36.74	075	.222	2.46	051	2.97	.30	93.05	9.81	.34				
18	.03844	38	090	3.34	36.69	072	.195	2.14	048	2.97	.29	36.36	2.21	.295	100.15	90.58	9.08	.34
			092	3.28	36.03	070	.208	2.28	052	3.03	.30	90.72	9.09	.34				
19	.04886	50	090	3.34	37.91	077	.209	2.37	046	2.82	.29	37.795	2.435	.29	104.65	90.11	9.57	.32
			093	3.32	37.68	074	.220	2.50	049	2.84	.29	94.30	10.02	.33				

next page

20	.05221	52	089 092	3.31 3.28	36.60 36.27	072 069	.195 .204	2.16 2.26	049 051	3.03 2.97	.30 .30	36.435 90.91	2.21 9.09	.30 .34	100.34	90.60	9.06	.34
21	.04911	50	105 110	3.99 4.03	45.10 45.55	087 083	.237 .248	2.68 2.80	047 050	2.89 2.91	.29 .30	45.325 113.09	2.74 11.27	.295 .34	124.70	90.69	9.04	.27
22	.05386	54	090 095	3.34 3.40	37.14 37.81	075 073	.204 .213	2.27 2.37	048 051	2.97 2.97	.30 .30	37.475 93.50	2.32 9.55	.30 .34	103.39	90.43	9.24	.33
23	.06817	68	086 091	3.18 3.23	35.19 35.75	072 071	.195 .211	2.16 2.34	043 051	2.63 2.97	.26 .30	35.47 88.50	2.25 9.26	.28 .32	98.08	90.23	9.44	.33
24	.06881	68	091 093	3.38 3.32	37.08 36.42	074 071	.202 .211	2.22 2.31	049 052	3.03 3.03	.30 .30	36.75 91.69	2.265 9.32	.30 .34	101.34	90.48	9.20	.34
25	.06119	60	094 095	3.52 3.40	38.31 37.00	078 075	.213 .222	2.32 2.42	049 052	3.03 3.03	.30 .30	37.655 93.95	2.37 9.75	.30 .34	104.04	90.30	9.37	.33
26	.06098	60	091 093	3.38 3.32	36.90 36.25	077 074	.209 .220	2.28 2.40	050 052	3.11 3.03	.31 .30	36.575 91.25	2.34 9.63	.305 .35	101.23	90.14	9.51	.35
27	.07213	72	088 091	3.27 3.23	36.25 35.80	071 067	.192 .198	2.13 2.19	050 053	3.11 3.10	.31 .31	36.025 89.88	2.16 8.89	.31 .35	99.12	90.68	8.97	.35
28	.06268	62	090 091	3.34 3.23	36.66 35.45	070 068	.189 .202	2.07 2.22	050 052	3.11 3.03	.31 .30	36.055 89.96	2.145 8.83	.305 .35	99.14	90.74	8.91	.35
29	.06146	62	090 092	3.34 3.28	37.38 36.70	072 068	.195 .202	2.18 2.26	050 051	3.11 2.97	.31 .30	37.04 92.42	2.22 9.13	.305 .35	101.90	90.70	8.96	.34
30	.06799	68	091 092	3.38 3.28	37.52 36.41	069 066	.186 .196	2.06 2.18	049 052	3.03 3.03	.30 .30	36.965 92.23	2.12 8.72	.30 .34	101.29	91.06	8.61	.34
31	.06169	62	085 086	3.14 3.03	35.02 33.80	065 062	.175 .183	1.95 2.04	048 051	2.97 2.97	.30 .30	34.41 85.85	1.995 8.21	.30 .34	94.40	90.94	8.70	.36
32	.05714	56	098 099	3.68 3.57	40.06 38.86	075 072	.204 .213	2.22 2.32	054 057	3.38 3.36	.33 .33	39.46 98.45	2.27 9.34	.33 .38	108.17	91.01	8.63	.35
33	.05538	55	088 089	3.27 3.16	36.03 34.83	067 065	.181 .192	1.99 2.12	048 053	2.97 3.10	.29 .31	35.43 88.40	2.065 8.46	.30 .34	97.20	90.95	8.70	.35
34	.05415	54	084 085	3.10 3.01	34.28 33.29	065 062	.175 .183	1.94 2.02	047 050	2.89 2.91	.29 .29	33.785 84.29	1.98 8.15	.29 .33	92.77	90.86	8.79	.36
35	.04994	50	085 088	3.14 3.12	34.92 34.70	064 062	.172 .183	1.91 2.04	049 052	3.03 3.03	.30 .30	34.81 86.85	1.975 8.13	.30 .34	95.32	91.11	8.53	.36
36	.04518	45	089 091	3.31 3.23	36.58 35.69	071 068	.192 .202	2.12 2.23	048 051	2.97 2.97	.30 .30	36.135 90.16	2.165 8.91	.30 .34	99.41	90.70	8.96	.34
37	.04611	46	085 087	3.14 3.08	34.78 34.11	065 062	.175 .183	1.94 2.03	049 052	3.03 3.03	.30 .30	34.445 85.94	1.985 8.17	.30 .34	94.45	90.99	8.65	.36
38	.03522	35	090 091	3.34 3.23	36.86 35.65	073 070	.198 .208	2.19 2.30	046 049	2.82 2.84	.28 .28	36.255 90.46	2.245 9.24	.28 .32	100.02	90.44	9.24	.32
39	.03281	33	087 088	3.23 3.12	36.07 34.84	070 067	.189 .198	2.11 2.21	047 051	2.89 2.97	.29 .30	35.455 88.46	2.16 8.89	.295 .34	97.69	90.55	9.10	.35
40	.02575	26	085 086	3.14 3.03	35.12 33.89	065 062	.175 .183	1.96 2.05	047 051	2.89 2.97	.29 .30	34.505 86.09	2.005 8.25	.295 .34	94.68	90.93	8.71	.36

next page

41	.02264	23	088	3.27	36.94	065	.175	2.02	046	2.82	.29	36.32	2.045	.295	99.37	91.19	8.46	.34
			089	3.16	35.70	062	.183	2.07	050	2.91	.30	90.62	8.41	.34				
42	.01754	18	080	2.94	33.57	057	.152	1.74	047	2.89	.30	33.225	1.795	.305	90.64	91.46	8.15	.39
			082	2.88	32.88	055	.162	1.85	051	2.97	.31	82.90	7.39	.35				
43	.01621	16	092	3.42	37.49	068	.183	2.01	049	3.03	.30	37.165	2.04	.30	101.46	91.40	8.27	.34
			094	3.36	36.84	064	.189	2.07	052	3.03	.30	92.73	8.39	.34				
44	.01005	10	091	3.38	37.15	063	.169	1.86	047	2.89	.29	36.82	1.915	.285	100.08	91.80	7.87	.33
			093	3.32	36.49	061	.179	1.97	049	2.84	.28	91.87	7.88	.33				
45	.00564	6	084	3.10	36.87	064	.172	2.05	046	2.82	.30	36.455	2.115	.30	100.00	90.96	8.70	.34
			086	3.03	36.04	062	.183	2.18	048	2.78	.30	90.96	8.70	.34				
46	.00228	2	089	3.31	31.95	069	.186	1.80	054	3.38	.29	31.42	1.825	.295	86.24	90.90	8.71	.39
			090	3.20	30.89	065	.192	1.85	059	3.49	.30	78.39	7.51	.34				

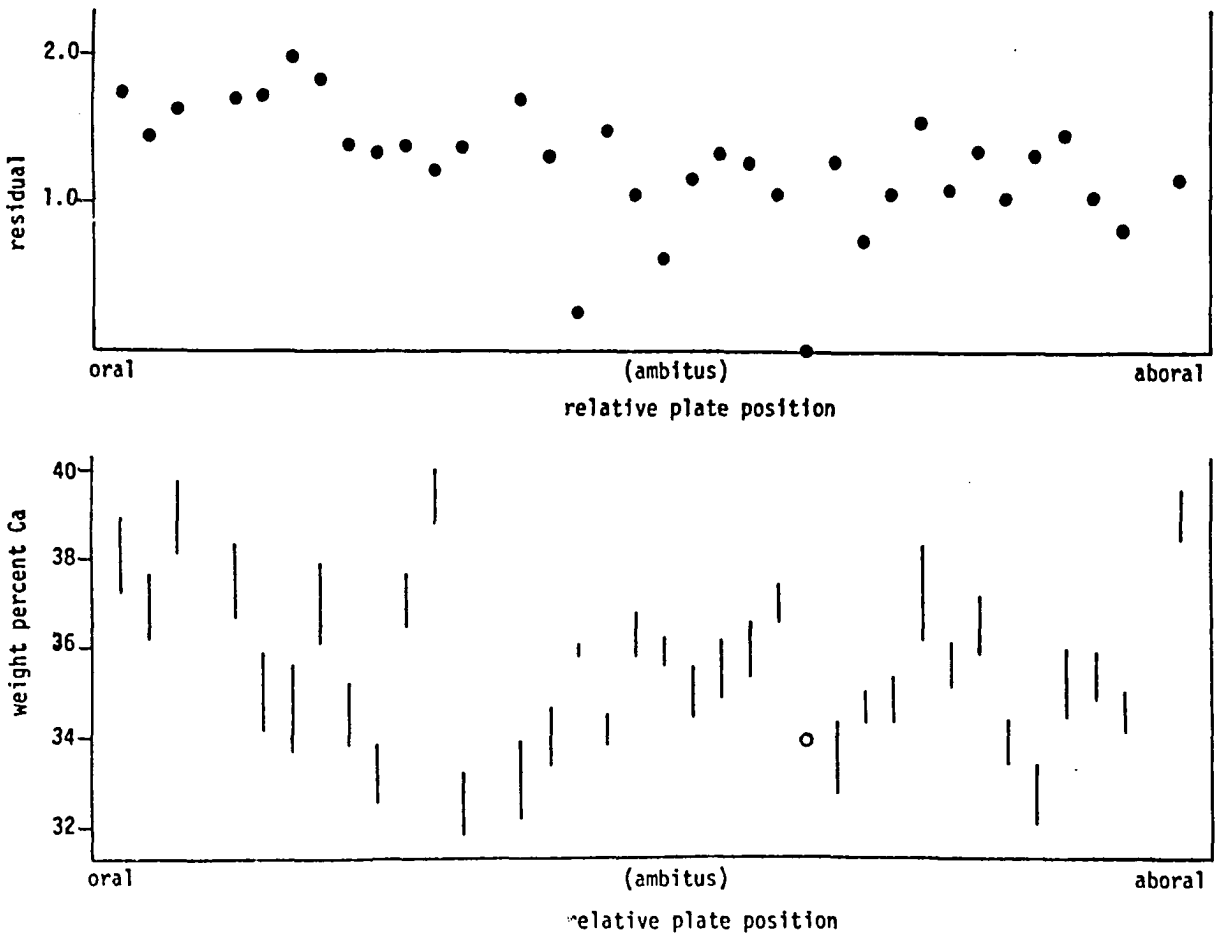

Figure D-11. (A) $CaCO_3$ composition (weight percent) of an interambulacral series: *S. franciscanus*, with (B) corresponding residual values.

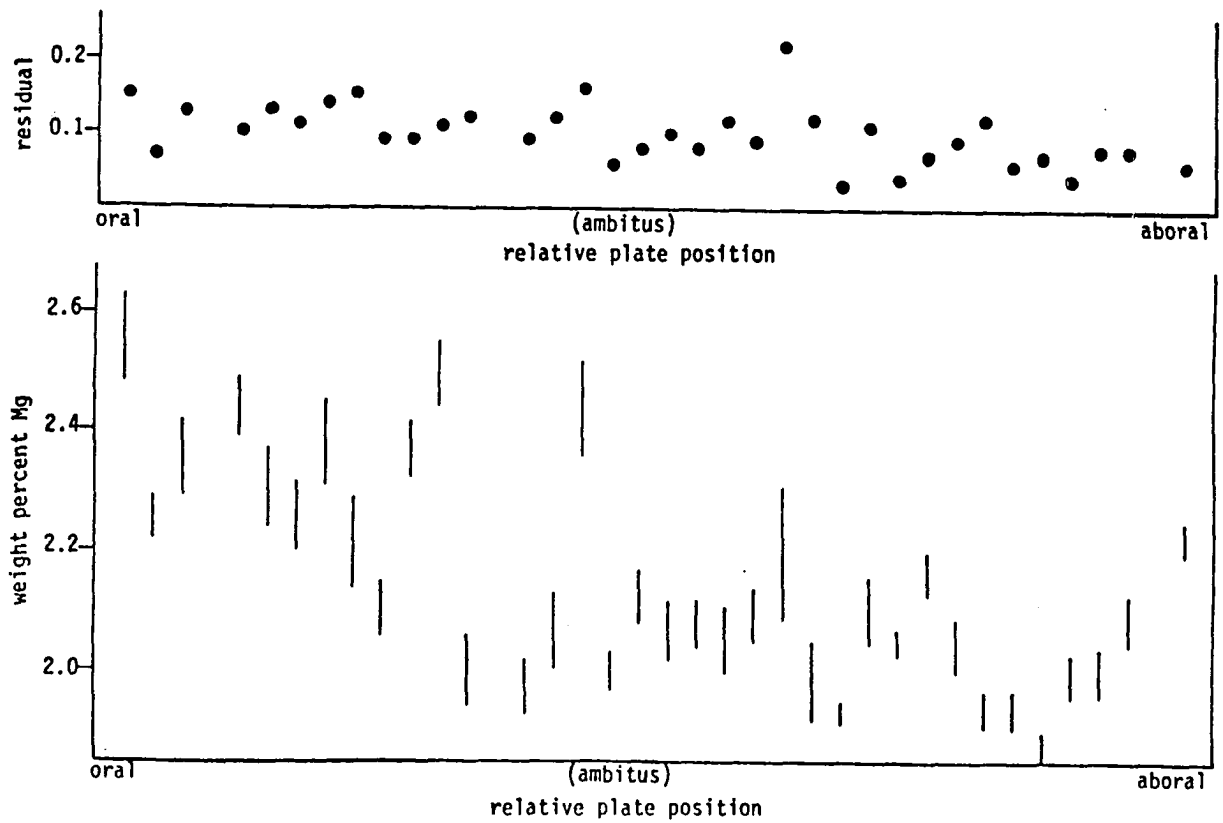

Figure D-12. (A) $MgCO_3$ composition (weight percent) of an interambulacral series: *S. franciscanus*, with (B) corresponding residual values.

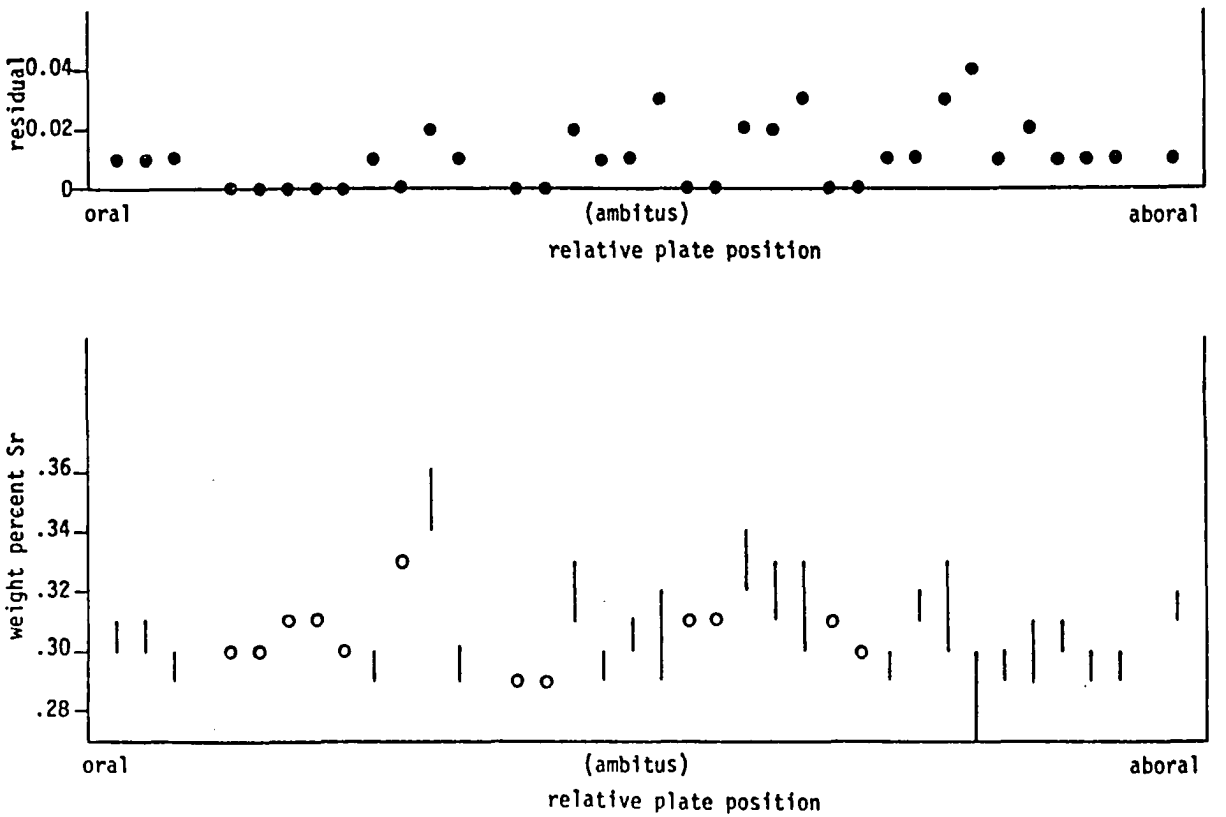

Figure D-13. (A) $SrCO_3$ composition (weight percent) of an interambulacral series: *S. franciscanus*, with (B) corresponding residual values.

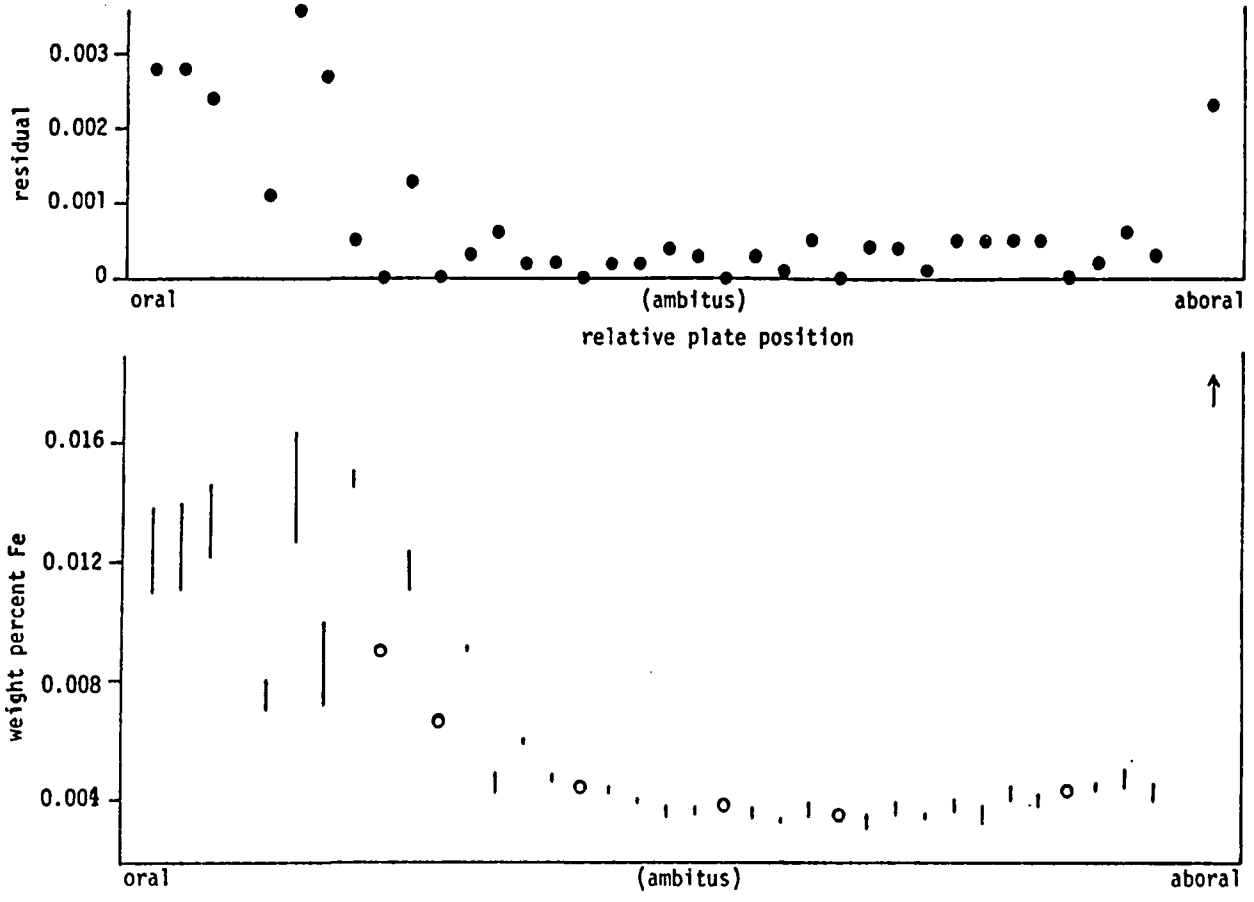

Figure D-14. (A) $FeCO_3$ composition (weight percent) of an interambulacral series: *S. franciscanus*, with (B) corresponding residual values.

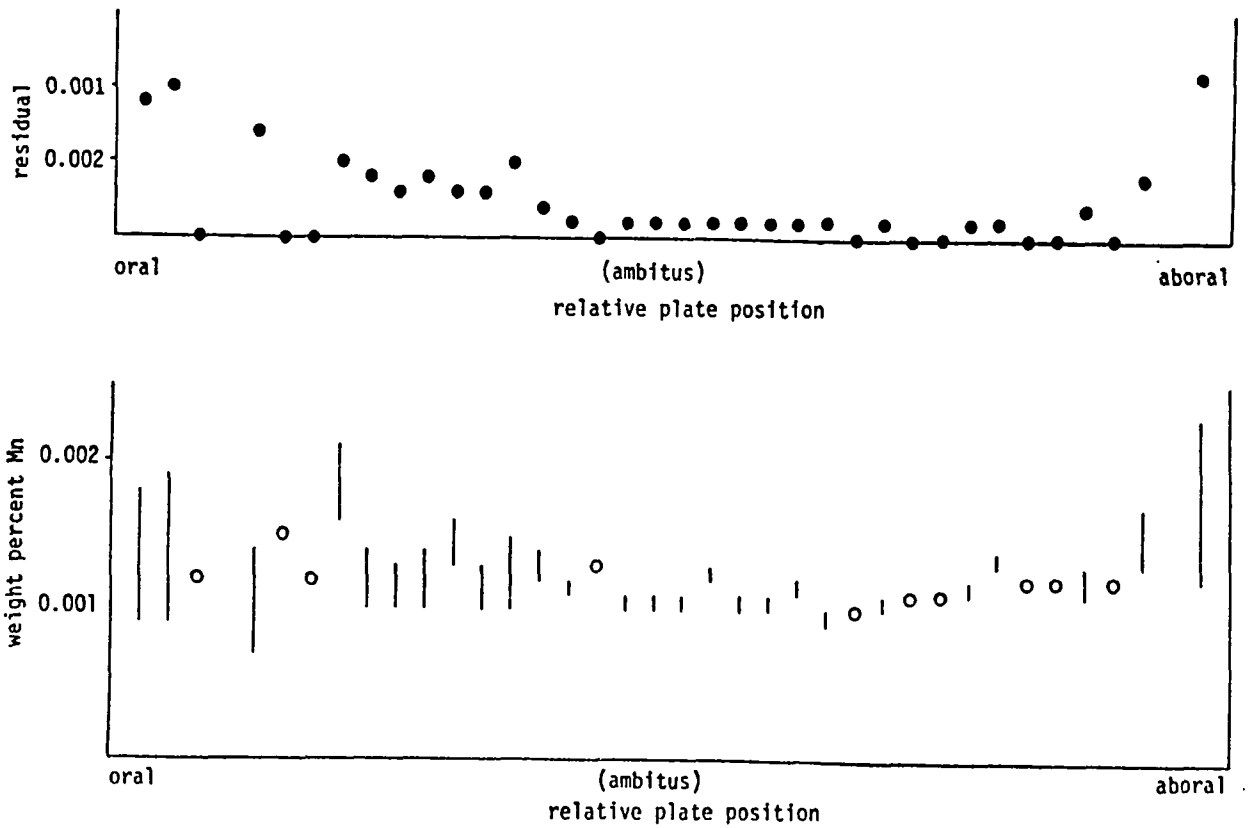

Figure D-15. (A) $MnCO_3$ composition (weight percent) of an interambulacral series: *S. franciscanus*, with (B) corresponding residual values.

Table D-16: Mg:Ca ratios of *Strongylocentrotus* species (interambulacrals)

A	B	C	D
1	10.86	11.06	10.37
2	10.32	10.08	10.50
3	10.86	9.97	11.32
4	10.32	10.10	10.94
5	10.44	10.71	10.57
6	10.49	10.86	11.15
7	10.47	10.72	10.75
8	10.41	10.61	11.52
9	10.05	10.57	10.48
10	10.63	10.45	10.64
11	9.93	10.52	10.43
12	10.05	10.44	10.44
13	9.82	10.13	10.10
14	9.76	–	10.15
15	9.89	9.84	10.30
16	10.69	10.03	10.22
17	10.27	11.17	10.55
18	10.97	9.67	10.02
19	9.46	9.67	10.62
20	9.52	9.49	9.78
21	9.83	9.78	9.97
22	9.61	9.52	10.22
23	9.52	9.60	10.46
24	9.45	9.78	10.17
25	9.19	9.61	10.38
26	11.33	9.54	10.55
27	9.48	10.00	9.89
28	9.30	9.68	9.82
29	9.69	9.49	9.88
30	9.60	9.44	9.46
31	9.53	10.01	9.57
32	9.46	9.42	9.48
33	9.10	9.35	9.57
34	9.17	9.38	9.67
35	8.97	9.30	9.36
36	9.11	9.94	9.88
37	9.29	–	9.51
38	–	9.41	10.22
39	–	–	10.05
40	–	–	9.58
41	–	–	9.28
42	–	–	8.91
43	–	–	9.05
44	–	–	8.57
45	–	–	9.56
46	–	–	9.58

Explanation:

A: plate number ("1" is always oldest plate)
B: ratios for *S. droebachiensis* (mole percents in Table D-8)
C: ratios for *S. franciscanus* (mole percents in Table D-7)
D: ratios for *S. purpuratus* (mole percents in Table D-10)

Table D-17: Mg:Sr ratios of *Strongylocentrotus* species (interambulacrals)

A	B	C	D
1	2.71	3.03	3.23
2	2.82	2.67	2.79
3	2.71	2.88	2.89
4	2.82	3.67	2.98
5	2.77	2.93	2.89
6	2.87	2.77	3.45
7	2.55	2.62	2.84
8	2.53	2.77	2.94
9	2.46	2.67	2.78
10	2.59	2.57	2.74
11	2.81	2.58	2.85
12	2.53	2.57	2.94
13	2.55	2.44	2.77
14	2.40	-	2.70
15	2.42	2.45	2.74
16	2.67	2.57	2.89
17	2.58	2.75	2.88
18	2.43	2.44	2.67
19	2.27	2.52	2.99
20	2.41	2.45	2.67
21	2.41	2.50	3.35
22	2.43	2.39	2.80
23	2.34	2.56	2.86
24	2.21	2.48	2.71
25	2.40	2.26	2.84
26	2.82	2.25	2.72
27	2.33	2.53	2.56
28	2.36	2.51	2.55
29	2.32	2.48	2.64
30	2.36	2.34	2.53
31	2.28	2.85	2.42
32	2.39	2.37	2.47
33	2.31	2.24	2.49
34	2.39	2.37	2.44
35	2.28	2.44	2.37
36	2.37	2.55	2.64
37	2.57	-	2.40
38	-	2.55	2.89
39	-	-	2.60
40	-	-	2.42
41	-	-	2.49
42	-	-	2.09
43	-	-	2.43
44	-	-	2.39
45	-	-	2.56
46	-	-	2.23

Explanation:

A: plate number ("1" is always oldest plate)
B: ratios for *S. droebachiensis* (mole percents in Table D-8)
C: ratios for *S. franciscanus* (mole percents in Table D-7)
D: ratios for *S. purpuratus* (mole percents in Table D-10)